

STUDIES OF THE DONOR PROPERTIES OF NEW  
POLYANIONIC CHELATING LIGANDS THROUGH THE  
SYNTHESIS AND CHARACTERIZATION OF OSMIUM COMPLEXES

Thesis by  
Geoffrey Tower Peake

In Partial Fulfillment of the Requirements  
for the Degree of  
Doctor of Philosophy

California Institute of Technology  
Pasadena, California

1987

(Submitted November 24, 1986)

## Acknowledgment

While I have been at Caltech working at learning and doing chemistry I have been given encouragement, guidance, support, and assistance from many people, in many ways. I certainly have neither the space nor the memory to thank all of these people individually, but I think it my duty to express my gratitude to some of the deserving people.

My adviser Terry Collins has been everything from coworker to guide to resource to critic. His honesty and great enthusiasm are exemplary. The rest of the Kiwi group, past and present, must be thanked for contributing to intelligent discussions and an enjoyable environment, both in and out of lab.

Certain results in this thesis are the work of others. The discussion would not be complete without including a good deal of related work done John Keech. Crystal structures reported here were done by Bob Coots, Ting Lai, Sonny Lee, and Bernie Santarsiero. A few of the early electrochemical experiments were done by Steve Gipson, and the kinetic results reported for the ligand exchange reaction were obtained by Sonny Lee. Doug Meinhart assisted in the 2D-COSY NMR spectrum and the difference NOE spectra. Tom Richmond was a big help in getting me started with many new instruments and techniques. I thank you all for kind assistance.

Bernie Santarsiero has been a tremendous help downstairs in the X-tal department. I could always count on his help down there, wheth-

er it be for crystallography or psychology. I have made many good friends here. Dean, George, Leigh, and of course the Hog Heaven squad have helped to make life here its best.

Janet, you have been so good to have around, and can certainly brighten the smoggiest day. Thank you for being such fun to be with.

Finally, I must thank my parents for teaching me of the value of a good education, without ever pressuring my decisions. I know I can always count on their support in whatever I do.

iv

*to Janet*

### Abstract

The synthesis, characterization, physical and chemical properties of osmium complexes containing highly donating polyanionic chelating (PAC) ligands are discussed.

The tetradentate tetraanionic ligand HBA-B ( $H_4HBA-B \equiv 1,2$ -bis(2-hydroxybenzamido)benzene) coordinates to osmium to form a variety of complexes. Reaction of  $H_4HBA-B$  with  $K_2[Os(OH)_4(O)_2]$  gives an osmium(VI) trans-dioxo complex coordinating the PAC ligand through two deprotonated phenol groups and two deprotonated amide groups. Reduction of the dioxo species with triphenylphosphine gives the neutral osmium(IV) species *trans*- $Os(\eta^4-HBA-B)(PPh_3)_2$  (3). This complex is an excellent starting material to make a series of osmium(IV) complexes because of the lability of the phosphine ligands. Ligand exchange reactions with nitrogen-base ligands, anionic two-electron donor ligands, mono- and bidentate phosphines,  $\pi$ -acid ligands, and bipyridines are observed. Most of the osmium(IV) PAC ligand complexes prepared are paramagnetic with  $\mu_{eff} \sim 1$  BM. The paramagnetic osmium(IV) species all exhibit well-resolved, paramagnetically shifted NMR spectra. The complex *trans*- $Os(\eta^4-HBA-B)(PPh_3)(py)$  (5) has twelve inequivalent sets of protons, all of which are on aromatic rings. The twelve resonances are observed in the  $^1H$  NMR spectrum in the range +11 to -5 ppm. The results of 2D-COSY and difference NOE experiments allow the complete assignment of the  $^1H$  NMR spectrum.

Electrochemical studies of these osmium(IV) complexes, and the

coordination chemistry observed indicate that these PAC ligands are very good electron donors to osmium. The Os(IV/III) reversible couples for the neutral osmium(IV) species have potentials in the range  $-0.9$  to  $-0.7$  V vs.  $\text{Fc}^+/\text{Fc}$ . The cation/neutral reversible couples have potentials in the range  $+0.2$  to  $+0.35$  V vs.  $\text{Fc}^+/\text{Fc}$ , but probably cannot be called Os(V/IV) couples. Reaction of **3** with carbon monoxide produces a rare osmium(IV) carbonyl complex, *cis*- $\alpha$ -Os( $\eta^4$ -HBA-B)-(PPh<sub>3</sub>)(CO) (**10**). Reaction of *t*-butylisocyanide with **3** gives the analogous mono-phosphine mono-isocyanide. The stability of these complexes is an indication of the strong donating nature of the PAC ligand.

A crystal structure of **10** shows it to have a *cis*- $\alpha$  coordination geometry. Complexes with *cis* geometries can also be made by reacting **3** with bidentate ligands, such as dppe. *Cis*- $\alpha$  and *cis*- $\beta$  osmium complexes of the HBA-B PAC ligand, and other PAC ligand complexes, contain the first nonplanar amide ligands. We have defined three causes for the formation of nonplanar amide ligands: (1) structural requirements of the metal center (for instance coordination of a bidentate dppe ligand forcing a *cis* geometry), (2) depletion of electron density from the metal center (either by oxidation or coordination of an electron withdrawing ligand), causing the amide ligands to adopt the more highly donating nonplanar structure and offset the depletion of electron density at the metal, (3) steric interactions forcing deformation of the amide ligand to a nonplanar state.

The syntheses of osmium complexes containing the CHBA ligand ( $\text{H}_2\text{CHBA} \equiv 3,5\text{-dichloro-2-hydroxybenzamide}$ ) are discussed. Several complexes, including *trans*-Os( $\eta^2$ -CHBA)<sub>2</sub>(PBu<sub>3</sub>)<sub>2</sub> (**26**) and *trans*-Os( $\eta^2$ -

CHBA)<sub>2</sub>(OPBu<sub>3</sub>)<sub>2</sub> (27), have been prepared in attempts to make a long-lived catalyst for the electrochemical oxidation of alcohols. The cyclic voltammetric experiments with 26 and 27 in the presence of alcohol are discussed. It appears that 27 exhibits catalytic behavior and 26 does not. A detailed study probing the catalysis has not been done.

The results of reactions between K<sub>2</sub>[Os(OH)<sub>4</sub>(O)<sub>2</sub>] and ligands similar to 2-(2-hydroxyphenyl)imidazole are reported. The reactions give neutral osmium(VI) trans-dioxo complexes containing two 2-(2-phenoxy)imidazole ligands coordinated as bidentate monoanions through a phenoxy ligand and an imidazole ligand. This coordination mode contrasts with that observed for osmium complexes of 2-(3,5-dichloro-2-hydroxyphenyl)-5,6-dichlorobenzimidazole, which coordinates as a dianion.

## Table of Contents

	<b>Page</b>
Acknowledgment	ii
Abstract	v
List of Figures	x
List of Tables	xii
List of Schemes	xiv
Abbreviations	xvi
Chapter 1. Introduction	1
References	19
Chapter 2. Synthesis, Characterization, and Physical Properties of Osmium Complexes of the Polyanionic Chelating Ligand 1,2-bis(2-hydroxybenzamido)benzene, (H <sub>4</sub> HBA-B)	22
Introduction	23
Results and Discussion	25
Conclusions	98
Experimental	101
References	114
Chapter 3. Nonplanar Amide Ligands	118
Introduction	119
Results and Discussion	121
Conclusions	168



	Experimental	170
	References	171
Chapter 4.	Synthesis and Characterization of Osmium Complexes of 3,5-dichloro-2-hydroxy- benzamide, (H <sub>2</sub> CHBA)	177
	Introduction	178
	Results and Discussion	185
	Conclusions	198
	Experimental	199
	References	206
Chapter 5.	Synthesis of Osmium Complexes Containing 2-(2-hydroxyphenyl)imidazole Ligands	208
	Introduction	209
	Results and Discussion	217
	Conclusions	225
	Experimental	229
	References	234

## List of Figures

Figure	Page
1.1 Commonly used polyanionic chelating (PAC) ligands.	4
1.2 The desired mode of coordination of a PAC ligand.	6
1.3 ORTEP view of $[\text{Cr}((\text{H})\text{CHBA-Et})(\text{py})_2]_2$	9
1.4 Structure of $\text{Co}(\eta^4\text{-CHBA-DCB})(t\text{-Bupy})$	14
2.1 Nomenclature for the possible diastereomers of a tetradentate ligand in an octahedral complex.	31
2.2 400 MHz $^1\text{H}$ NMR spectrum of <i>trans</i> - $\text{Os}(\eta^4\text{-HBA-B})(\text{PPh}_3)(\text{py})$ (5)	43
2.3 2D-( $^1\text{H}$ - $^1\text{H}$ ) COSY spectrum of <i>trans</i> - $\text{Os}(\eta^4\text{-HBA-B})(\text{PPh}_3)(\text{py})$ (5).	45
2.4 A set of $^1\text{H}$ difference NOE spectra of <i>trans</i> - $\text{Os}(\eta^4\text{-HBA-B})(\text{PPh}_3)(\text{py})$ (5).	48
2.5 Assignment of the resonances of the 400 MHz $^1\text{H}$ NMR spectrum of <i>trans</i> - $\text{Os}(\eta^4\text{-HBA-B})(\text{PPh}_3)(\text{py})$ (5).	51
2.6 ORTEP view of <i>cis</i> - $\alpha$ - $\text{Os}(\eta^4\text{-HBA-B})(\text{PPh}_3)(\text{CO})$ (10).	70
2.7 Representative bond distances for some metal-ligand fragments.	76
2.8 ORTEP view of $\text{Os}(\eta^3\text{-(H)HBA-B})(\text{PPh}_3)(\text{phen})$ (15).	87
3.1 ORTEP view of <i>cis</i> - $\alpha$ - $\text{Os}(\eta^4\text{-HBA-B})(\text{PPh}_3)(\text{CO})$ (10) showing nonplanar amide groups.	122
3.2 Organic molecules containing nonplanar amide groups.	127
3.3 Projection down the amide C-N bond of a coordinated	

	amide showing the derivation of the angular parameters.	130
3.4	Plots of angular parameters for all structurally characterized $\text{RC}(\text{O})\text{NR}'\text{M}$ and $\text{RC}(\text{OM}')\text{NR}'\text{M}$ fragments.	133
3.5	Cyclic voltammograms of $\text{Os}(\eta^4\text{-CHBA-DCB})(t\text{-Bupy})_2$ .	156
3.6	ORTEP view of $\text{Os}(\eta^3\text{-(H)HBA-B})(\text{PPh}_3)(\text{phen})$ ( <b>15</b> ) showing the angular parameters for the two amide ligands.	165
4.1	Structure of <i>cis</i> - $\alpha\text{-Os}(\eta^2\text{-CHBA})_2(\text{py})_2$ ( <b>21</b> ).	179
4.2	Structure of $[\text{Os}(\text{dppe})(\eta^2\text{-CHBA})(\eta^1\text{-CHBN})]_2(\text{dppe})$ ( <b>28</b> ).	189
4.3	Cyclic voltammograms of <i>trans</i> - $\text{Os}(\eta^2\text{-CHBA})_2(\text{PBu}_3)_2$ ( <b>26</b> ).	193
4.4	Cyclic voltammograms of <i>trans</i> - $\text{Os}(\eta^2\text{-CHBA})_2(\text{OPBu}_3)_2$ ( <b>27</b> ).	195
5.1	The PAC ligand $\text{H}_4\text{HBA-DMB}$ .	211
5.2	Structure of $\text{OsCl}_2(\eta^2\text{-2-(2-phenoxy)-4,4,5,5-tetramethylimidazoline})$ .	213
5.3	The two ligands: 2-(5- <i>t</i> -butyl-2-hydroxyphenyl)imidazoline ( <b>32</b> ), and 2-(2-hydroxyphenyl)-5,6-dimethylbenzimidazole ( <b>33</b> ).	221

## List of Tables

Table	Page
2.1 Solid-state, room temperature effective magnetic moments of osmium complexes of HBA-B.	40
2.2 $^1\text{H}$ NMR data for osmium complexes of HBA-B.	53
2.3 Electrochemical data for osmium complexes of HBA-B.	56
2.4 Comparison of electrochemical data of osmium(IV) complexes.	58
2.5 Experimental data and cell parameters for the crystal structure determination of <i>cis</i> - $\alpha$ -Os( $\eta^4$ -HBA-B)(PPh <sub>3</sub> )(CO) (10).	68
2.6 Bond angles and distances in <i>cis</i> - $\alpha$ -Os( $\eta^4$ -HBA-B)(PPh <sub>3</sub> )(CO) (10).	72
2.7 Experimental data and cell parameters for the crystal structure determination of Os( $\eta^3$ -(H)HBA-B)(PPh <sub>3</sub> )(phen) (15).	85
2.8 Bond distances (Å) and angles (°) for Os( $\eta^3$ -(H)HBA-B)(PPh <sub>3</sub> )(phen) (15).	89
3.1 Angular parameters for RC(O)NR'M and RC(OM')NR'M fragments with $ \bar{\tau}  > 25^\circ$ .	139
3.2 Formal potentials of the three isomers of Os( $\eta^4$ -CHBA)-( <i>p</i> -chloro-py) <sub>2</sub> .	147
3.3 Electrochemical data for the trans and <i>cis</i> - $\alpha$ isomers of Os( $\eta^2$ -CHBA) <sub>2</sub> (py) <sub>2</sub> .	150

3.4	Electrochemical and IR data for isomers of Os( $\eta^4$ -CHBA-Pr)- (py) <sub>2</sub> .	153
3.5	Angular parameters for the two amide ligands of <i>cis</i> - $\alpha$ -Os( $\eta^4$ -HBA-B)(PPh <sub>3</sub> )(CO) ( <b>10</b> ).	162
4.1	Collection data and cell constants for the crystal structure determination of <b>28</b> .	202

## List of Schemes

Scheme	Page
1.1 Oxidative and hydrolytic decomposition of <i>trans</i> -Os( $\eta^4$ -CHBA-Et)(py) <sub>2</sub> .	11
1.2 Catalytic oxidation of styrene by iodosobenzene and [Co(HMPA-B)] <sup>-</sup> .	16
2.1 Synthesis of H <sub>4</sub> HBA-B (1).	26
2.2 Synthesis of K <sub>2</sub> [ <i>trans</i> -Os( $\eta^4$ -HBA-B)(O) <sub>2</sub> ] (2).	28
2.3 Synthesis of <i>trans</i> -Os( $\eta^4$ -HBA-B)(PPh <sub>3</sub> ) <sub>2</sub> (3).	33
2.4 Reactions of <i>trans</i> -Os( $\eta^4$ -HBA-B)(PPh <sub>3</sub> ) <sub>2</sub> (3) with neutral two-electron donor ligands.	36
2.5 Resonance structures of a coordinated HBA-B ligand.	61
2.6 Reaction of <i>trans</i> -Os( $\eta^4$ -HBA-B)(PPh <sub>3</sub> ) <sub>2</sub> (3) with chloride.	65
2.7 Reaction of <i>trans</i> -Os( $\eta^4$ -HBA-B)(PPh <sub>3</sub> ) <sub>2</sub> (3) with $\pi$ -acid ligands.	80
2.8 Reaction of <i>trans</i> -Os( $\eta^4$ -HBA-B)(PPh <sub>3</sub> ) <sub>2</sub> (3) with dppe.	82
2.9 Acetylation of Os( $\eta^3$ -(H)HBA-B)(PPh <sub>3</sub> )(phen) (15).	96
3.1 Organic amide resonance.	125
3.2 Resonance in a coordinated amide.	144
3.3 Thermodynamic relationships between <i>cis</i> - $\alpha$ and <i>trans</i> isomers of the different oxidation states of Os( $\eta^4$ -CHBA-DCB)( <i>t</i> -Bupy) <sub>2</sub> .	159
4.1 Synthesis of Os( $\eta^2$ -CHBA) <sub>2</sub> (L) <sub>2</sub> complexes.	182

5.1	Resonance of coordinated phenoxide-imidazole ligands.	215
5.2	Synthesis of 2-(2-hydroxyphenyl)imidazole (31).	219
5.3	Synthesis of osmium complexes of 2-(2-hydroxyphenyl)- imidazole ligands.	223
5.4	Osmium complexes with 2-(3,5-dichloro-2-hydroxyphenyl)- 5,6-dichlorobenzimidazole ligands.	227

## Abbreviations

Å	angstroms
as	asymmetric
bipy	2,2'-bipyridine
BM	Bohr magneton
b.p.	boiling point
BPG	basal plane pyrolytic graphite
Bu	butyl
H <sub>2</sub> CHBA	3,5-dichloro-2-hydroxybenzamide
H <sub>4</sub> CHBA-Et	1,2-bis(3,5-dichloro-2-hydroxybenzamido)ethane
H <sub>4</sub> CHBA-DCB	1,2-bis(3,5-dichloro-2-hydroxybenzamido)-4,5-dichlorobenzene
CHBA	3,5-dichloro-2-hydroxybenzotrile
CV	cyclic voltammogram
d	doublet
DMBP	4,4'-dimethylbipyridine
dppe	1,2-bis(diphenylphosphino)ethane
E	electrochemical potential
Et	ethyl
eu	entropy units
Fc	ferrocene
G	Gibbs free energy
h	hour
H <sub>4</sub> HBA-B	1,2-bis(2-hydroxybenzamido)benzene



H <sub>4</sub> HMPA-DMP	2,4-bis(2-hydroxy-2-methylpropanamido)-2,4-dimethylpentan-3-one
Hz	hertz
ImH	imidazole
IR	infrared
K	equilibrium constant
L	ligand
m	multiplet(NMR), moderate(IR)
<i>m</i>	meta
M	moles liter <sup>-1</sup>
Me	methyl
MHz	megahertz
min	minutes
mol	moles
m.p.	melting point
μ	magnetic moment
NHE	normal hydrogen electrode
NMR	nuclear magnetic resonance
<i>o</i>	ortho
ORTEP	Oak Ridge Thermal Elipsoid Program
<i>p</i>	para
PAC	polyanionic chelating
Ph	phenyl
phen	1,10-phenanthroline
4-pic	4-picoline
ppm	parts per million

py	pyridine
q	quartet
R	alkyl
s	second, singlet(NMR), strong(IR)
S	entropy
SCE	saturated calomel electrode
SSCE	saturated sodium chloride electrode
t	triplet
<i>t</i>	tert
TBAP	tetrabutylammonium perchlorate
THF	tetrahydrofuran
TLC	thin-layer chromatography
V	volts
vs	very strong
$\nu$	stretching frequency
w	weak
$\omega$	dihedral angle

## **Chapter 1**

### **Introduction**

Oxidation chemistry, an important field of inorganic chemistry, encompasses a wide range of topics from electrochemical redox reactions of metal ions to oxidation of hydrocarbons by transition metal catalysts.<sup>1</sup> Oxidation reactions are used in many important areas including large-scale industrial processes, drug syntheses, and laboratory-scale organic syntheses.<sup>1 a</sup> When a specific oxidation of an organic functional group is the goal, one can find a specific oxidation technology, including oxidizing agent and reaction conditions, that will effect the desired oxidation. The problem with the available oxidation technology is limited selectivity. In oxidation chemistry, all areas of selectivity, including chemoselectivity, regioselectivity, and product selectivity, need improvement.<sup>1</sup> Many inorganic oxidizing agents react with organic functional groups to give a mixture of products. In some cases, a distribution of products can be explained by the presence of several oxidizing species in solution,<sup>1 c, f</sup> for example, an oxidation using a chromium(VI) or manganese(VII) reagent involves a three- or four-electron reduction of the metal, while the organic substrate usually undergoes a two-electron oxidation. This results in intermediate inorganic species that also oxidize the organic substrate. Thus, several oxidizing species, each with its own reactivity and selectivity, are present during the reaction. The consequence of several oxidants reacting with one substrate is poor selectivity. The goal of improving selectivity in the oxidation of organic substrates by transition metal compounds provides the overall motivation for research in our group.

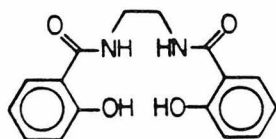
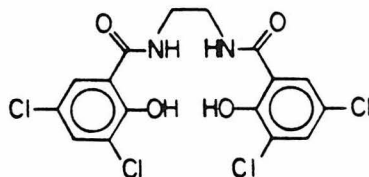
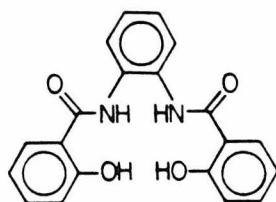
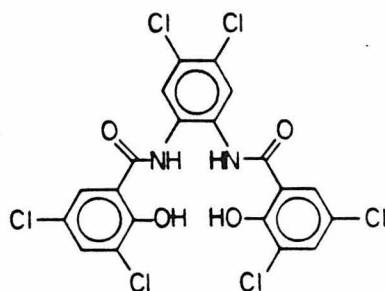
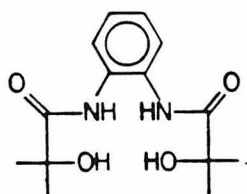
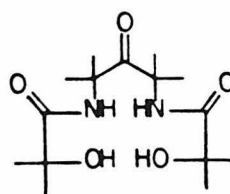
An approach to achieving the goal of improved selectivity with

inorganic oxidizing agents is to insure that there is a single two-electron oxidizing agent present during the reaction. The approach we have taken to work toward this goal is to design and synthesize chelating ligands to stabilize high oxidation state transition metals. An inorganic complex containing such a chelate ligand, after oxidizing an organic substrate, should be stable to further reduction, and a clean two-electron oxidation would be the result. The chelating ligand is present only to stabilize the metal center and should not be involved in the chemistry. This approach seems to be effective, and has produced catalysts for olefin epoxidation that could be cycling between cobalt(V) and cobalt(III) species.<sup>2</sup>

Some examples of ligands designed to stabilize high oxidation state metal centers are shown in Figure 1.1. A deprotonated ligand can coordinate to a single metal center as a tetradentate tetraanion through five- and six-membered chelate rings. (Figure 1.2.) The figures serve to demonstrate the features of the ligands deemed necessary to stabilize highly oxidized metal centers. Coordination is through four anionic groups that are known to be very good  $\sigma$ -donors.<sup>3</sup> The strong  $\sigma$ -donation serves to stabilize a high formal positive charge on the metal center. The five- and six-membered chelate rings encourage monomer formation, and the chelating nature of the ligand will keep the ligand coordinated to the metal throughout chemical reactions. Another feature that is important for the chelating ligand to have is inertness towards oxidation. The ligand should not participate in any redox chemistry.

The major achievements of the overall project are briefly summar-

**Figure 1.1.** Commonly used polyanionic chelating (PAC) ligands.

H<sub>4</sub>HBA-EtH<sub>4</sub>CHBA-EtH<sub>4</sub>HBA-BH<sub>4</sub>CHBA-DCBH<sub>4</sub>HMPA-BH<sub>4</sub>HMPA-DMP

H<sub>4</sub>HBA-Et ≡ 1,2-bis(2-hydroxybenzamido)ethane

H<sub>4</sub>CHBA-Et ≡ 1,2-bis(3,5-dichloro-2-hydroxybenzamido)ethane

H<sub>4</sub>HBA-B ≡ 1,2-bis(2-hydroxybenzamido)benzene

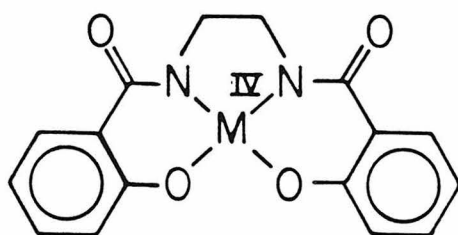
H<sub>4</sub>CHBA-DCB ≡ 1,2-bis(3,5-dichloro-2-hydroxybenzamido)-  
4,5-dichlorobenzene

H<sub>4</sub>HMPA-B ≡ 1,2-bis(2-hydroxy-2-methylpropanamido)benzene

H<sub>4</sub>HMPA-DMP ≡ 2,4-bis(2-hydroxy-2-methylpropanamido)-  
2,4-dimethylpentan-3-one

**Figure 1.2.** The desired mode of coordination of a PAC ligand.

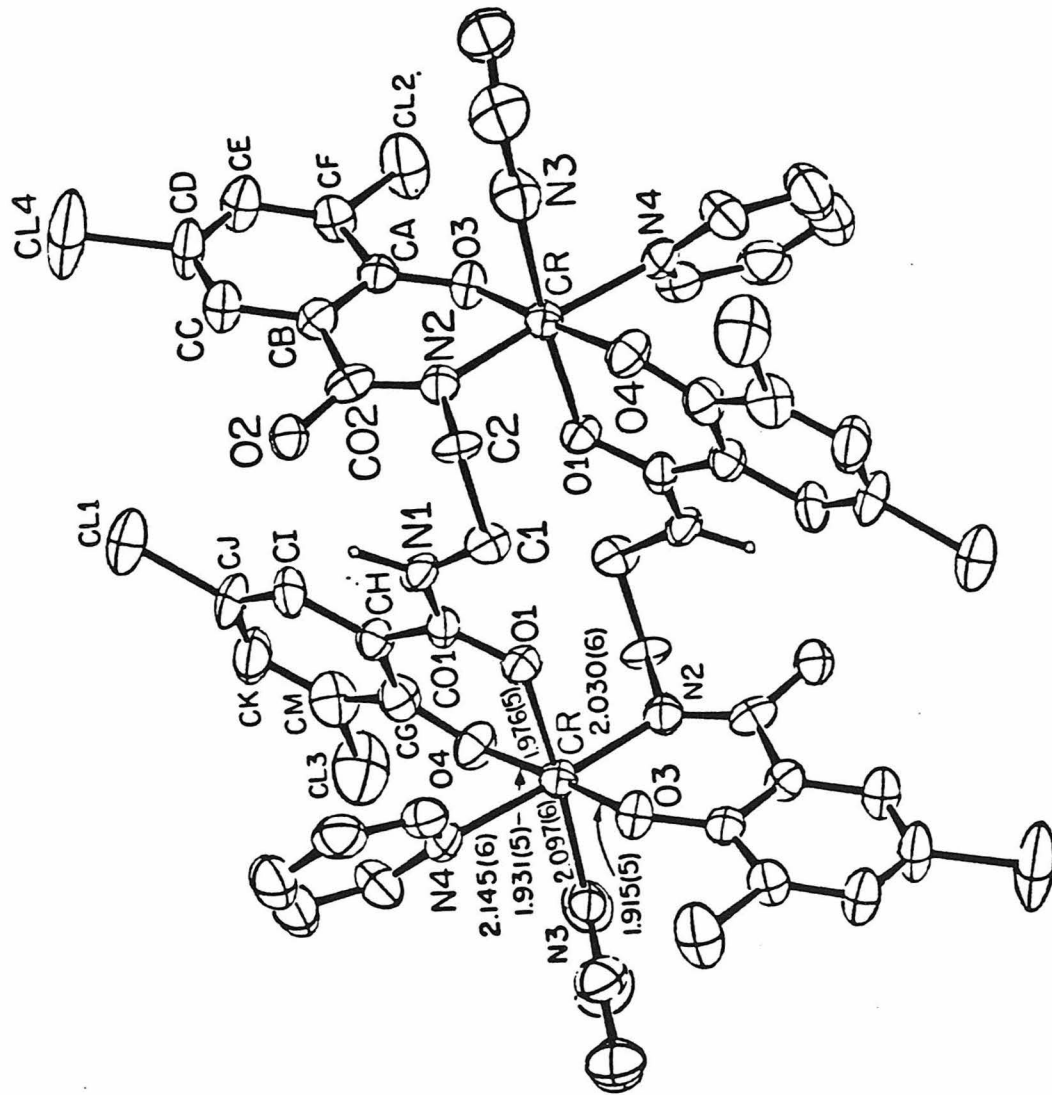




ized below. This is a convenient way of putting the work discussed in the body of the thesis in the context of the overall PAC ligand project and its progress.

Early work with these polyanionic chelating (PAC) ligands involved developing methods for coordinating them to transition metals. Once proper coordination was achieved, high oxidation state chemistry and any oxidative activity would be explored. The ligand 1,2-bis(3,5-dichloro-2-hydroxybenzamido)ethane,  $H_4CHBA-Et$  (see Figure 1.1), was that most investigated in early coordination studies. Reacting  $CrCl_3 \cdot 6H_2O$  with one equivalent of  $H_4CHBA-Et$  in pyridine gave a dinuclear complex that was characterized by an X-ray crystal structure.<sup>4</sup> The ORTEP of the complex,  $[Cr((H)CHBA-Et)(py)_2]_2$ , is shown in Figure 1.3. An interesting aspect of this complex is that it contains coordinated amides in both possible coordination modes: through the amide oxygen, and through the deprotonated nitrogen. Osmium(VI) oxo complexes containing the CHBA-Et ligand were easily obtained,<sup>5</sup> and could then be reduced to neutral osmium(IV) complexes such as  $Os(\eta^4-CHBA-Et)(py)_2$ .<sup>5 a</sup> Electro-oxidation of this compound in the presence of alcohol led to a remarkable CHBA-Et ligand decomposition sequence involving oxidation and hydrolysis of the ethylene bridge of the PAC ligand, that produced fifteen characterized species en route to a complex that was a catalyst for the electrochemical oxidation of alcohols.<sup>5 c,6</sup> (Scheme 1.1.) Besides producing interesting catalytic species, the decomposition sequence demonstrated that the CHBA-Et ligand did not meet one of the criteria required of the PAC ligands; it was sensitive to oxidation. This problem can be avoided by replacing the

**Figure 1.3.** ORTEP view of  $[\text{Cr}((\text{H})\text{CHBA-Et})(\text{py})_2]_2$ . Bond distances are in angstroms, and bond angles in degrees.



**Scheme 1.1.** Oxidative and hydrolytic decomposition of *trans*-Os( $\eta^4$ -CHBA-Et)(py)<sub>2</sub>.



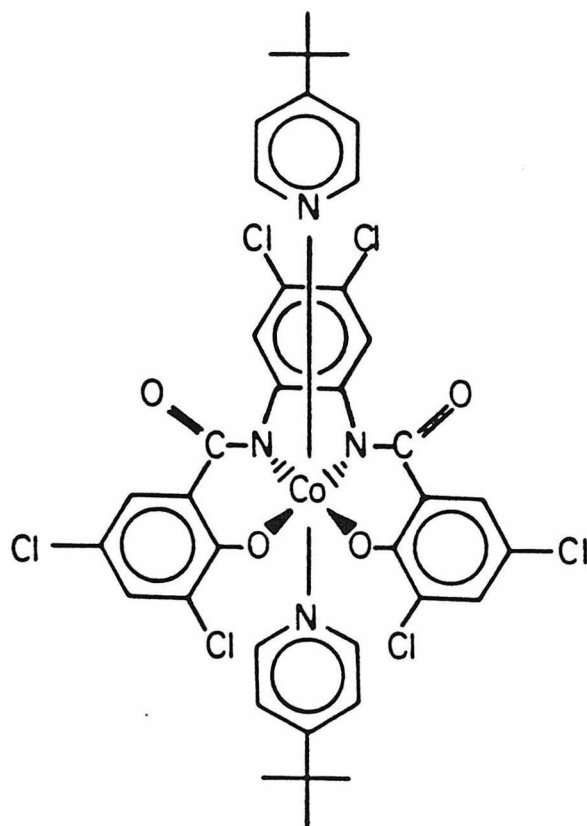
ethylene bridge unit with a phenylene bridge as in  $H_4CHBA-DCB$ . Electrochemical experiments with  $Os(\eta^4-CHBA-DCB)(py)_2$  show that solution-stable oxidants with formal potentials in the region of 2 volts vs. NHE can be produced.<sup>7</sup>

Along with the studies pursued with  $Os(CHBA-DCB)$  complexes, the coordination chemistry of PAC ligands to cobalt was investigated. The complex  $Co(\eta^4-CHBA-DCB)(t-Bupy)_2$  (Figure 1.4) was prepared and shown to be a stable cobalt(IV) complex,<sup>8</sup> demonstrating the highly donating nature of the PAC ligand. Other PAC ligands coordinated to form rare square-planar cobalt(III) complexes.<sup>9</sup> Many of these cobalt(III) species were catalysts for olefin epoxidation using iodosobenzene (Scheme 1.2) and may lead to the first cobalt(V) terminal oxo complexes<sup>2</sup> (isoelectronic with iron(IV) oxo's). Additionally, PAC ligand coordination to copper produced highly stabilized copper(III) complexes.<sup>10</sup> Complexes with III/II couples as low as -0.65 volts vs. SCE were prepared. There is currently a debate about the participation of copper(III) complexes in certain enzymatic oxidations.<sup>11</sup> Studies with the copper(III) PAC ligand complexes could provide valuable information regarding this topic.

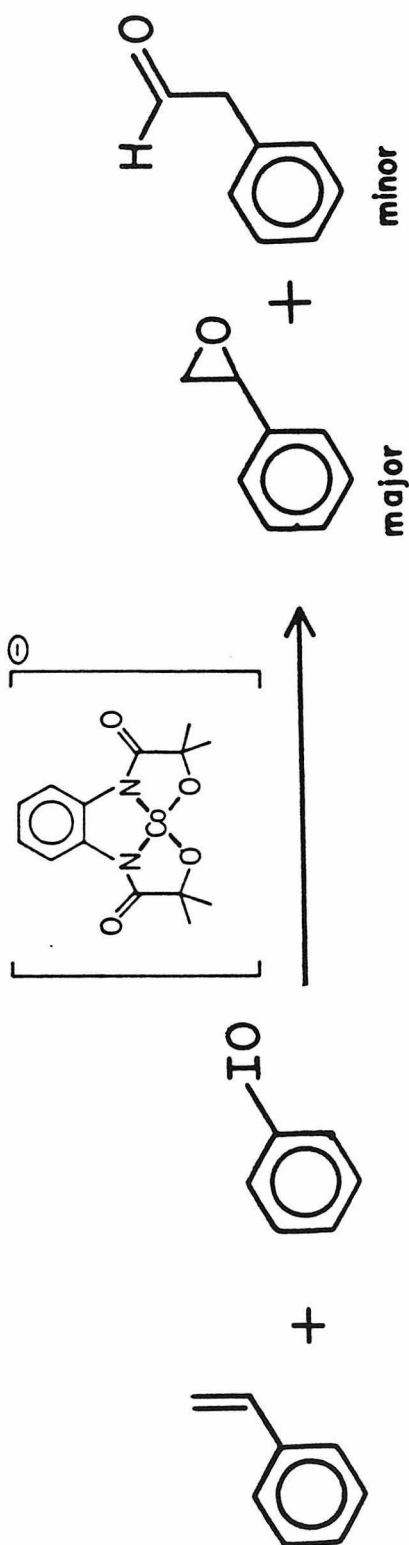
A remarkable level of understanding has been achieved regarding the electron-donating properties of these new ligands. Isomerization reactions have been discovered that involve a change in the coordination geometry of the PAC ligand, producing the first nonplanar amide ligands.<sup>12</sup> The nonplanar amide groups are much better donors than the planar amides,<sup>13</sup> so their formation greatly affects the donor properties of the PAC ligand and thus the nature of the inorganic complex.

**Figure 1.4.** Structure of  $\text{Co}(\eta^4\text{-CHBA-DCB})(t\text{-Bupy})_2$ .





**Scheme 1.2.** Catalytic oxidation of styrene by iodosobenzene and  $[\text{Co}(\eta^4\text{-HMPA-B})]^-$ .



These nonplanar amide ligands can be caused by structural constraints of the metal's coordination sphere, electronic demands of the metal center, or deformation of the PAC ligand due to steric interactions.

This thesis reports on three different projects, each involving a different PAC ligand. Although the specific goals of the projects are not related, the three types of ligands are similar, and the projects are results of the group's research efforts with transition metal PAC ligand complexes. The one theme that ties the projects together is the search for new and interesting properties demonstrated by complexes of PAC ligands and a clearer understanding of the unique properties of this new type of ligand. Chapters 2 and 3 cover studies of the chemistry of complexes of osmium with the tetradentate, tetraanionic ligand HBA-B (Figure 1.1.) Some unusual coordination chemistry and an interesting isomerization feature of the HBA-B ligand, forming nonplanar amides, alluded to above, are discussed. Chapter 4 reports on the chemistry of osmium complexes with two bidentate dianionic ligands as part of an attempt to make improved catalysts for the electrochemical oxidation of alcohols. Chapter 5 discusses the results of coordination chemistry between osmium and bidentate ligands containing imidazole and imidazoline groups.

References

1. (a) Sheldon, R.A.; Kochi, J.K. "Metal-Catalyzed Oxidations of Organic Compounds"; Academic Press, Inc.: New York, 1981. (b) "Report of the International Workshop on Activation of Dioxygen Species and Homogeneous Catalytic Oxidations", Collins, T.J., Ed.; Galzignano, Italy, June 28–29, 1984. (c) Wiberg, K.W., Ed. "Oxidation in Organic Chemistry, Part A"; Academic Press, Inc.: New York, 1973. (d) Trahanovsky, W.S., Ed. "Oxidation in Organic Chemistry, Part B"; Academic Press, Inc.: New York, 1973. (e) Trahanovsky, W.S., Ed. "Oxidation in Organic Chemistry, Part C"; Academic Press, Inc.: New York, 1978. (f) Benson, D. "Mechanisms of Oxidation by Metal Ions"; Elsevier: New York, 1976.
2. Brewer, J.; Collins, T.J.; Ozaki, S.; Richmond, T.G. unpublished results.
3. (a) Sigel, H.; Martin, R.B. *Chem. Rev.* **1982**, *82*, 385–426. (b) Margerum, D.W.; Wong, L.F.; Bossu, F.P.; Chellappa, K.L.; Czarnicki, J.J.; Kirksey, S.T., Jr.; Neubecker, T.A. *Adv. Chem. Ser.* **1977**, *162*, 281–303.
4. (a) Spies, G.H. Ph.D. Dissertation, California Institute of Technology, Pasadena, California, 1985. (b) Collins, T.J.; Santarsiero, B.D.; Spies, G.H. *J. Chem. Soc., Chem. Commun.* **1983**, 681–2.

5. (a) Anson, F.C.; Christie, J.A.; Collins, T.J.; Coots, R.J.; Furutani, T.T.; Gipson, S.L.; Keech, J.T.; Krafft, T.E.; Santarsiero, B.D.; Spies, G.H. *J. Am. Chem. Soc.* **1984**, *106*, 4460-72. (b) Christie, J.A.; Collins, T.J.; Krafft, T.E.; Santarsiero, B.D.; Spies, G.H. *J. Chem. Soc., Chem. Commun.* **1984**, 198-9. (c) Gipson, S.L.; Krafft, T.E. Ph.D. Dissertations, California Institute of Technology, Pasadena, California, 1985.
6. Anson, F.C.; Collins, T.J.; Coots, R.J.; Gipson, S.L.; Krafft, T.E. *Inorg. Chem.* submitted.
7. Keech, J.T. Ph.D. Dissertation, California Institute of Technology, Pasadena, California, 1987.
8. Anson, F.C.; Collins, T.J.; Coots, R.J.; Gipson, S.L.; Richmond, T.G. *J. Am. Chem. Soc.* **1984**, *106*, 5037-8.
9. Collins, T.J.; Richmond, T.G.; Santarsiero, B.D.; Treco, B.G.R.T. *J. Am. Chem. Soc.* **1986**, *108*, 2088-90.
10. Anson, F.C.; Collins, T.J.; Richmond, T.G.; Toth, J.E.; Treco, B.G.R.T. *J. Am. Chem. Soc.* submitted.
11. (a) Johnson, J.M.; Halshall, H.B.; Heineman, W.R. *Biochemistry* **1985**, *24*, 1579-85. (b) Kwiatkowski, L.D.; Adelman, M.; Pennelly, R.; Kosman, D.J. *J. Inorg. Biochem.* **1981**, *14*, 209-22. (c) Winkler, M.E.; Bereman, R.D. *J. Am. Chem. Soc.* **1980**, *102*, 6244-7. (d) Hamilton, G.A.; Adolf, P.K.; de Jersey, J.; DuBois, G.C.; Dyrkacz, G.R.; Libby, R.D. *J. Am. Chem. Soc.* **1978**, *100*, 1899-1912.
12. Collins, T.J.; Coots, R.J.; Furutani, T.T.; Keech, J.T.; Peake,

- G.T.; Santarsiero, B.D. *J. Am. Chem. Soc.* **1986**, *108*, 5333–9.
13. Anson, F.C.; Collins, T.J.; Gipson, S.L.; Keech, J.T.; Krafft, T.E.; Peake, G.T. *J. Am. Chem. Soc.* **1986**, *108*, 6593–605.

## Chapter 2

Synthesis, Characterization, and Physical Properties of  
Osmium Complexes of the Polyanionic Chelating Ligand  
1,2-bis(2-hydroxybenzamido)benzene ( $H_4HBA-B$ )



## Introduction

As our research with PAC ligands progressed, we learned a great deal about the design features of the ligands that created problems. Increased understanding of the PAC ligands led us to make design changes in the ligands to overcome these problems. For example, discovery of the oxidative decomposition of the ethane bridge in osmium-(CHBA-Et) complexes initiated work with the more robust phenylene-bridged ligands.<sup>1</sup> A problem with the phenylene-bridged ligands was that a resonance form that reduces the metal's formal oxidation state existed, so new PAC ligands with aliphatic bridges were designed and synthesized.<sup>2</sup> Work in our group soon included a wide range of PAC ligands. We found that slight differences between PAC ligands could result in significant differences in the properties and reactivity of the complexes of these ligands. A detailed understanding of the binding and donating properties of these new PAC ligands was necessary in order to explain, and perhaps predict, differences between complexes of different ligands.

The need for a complete understanding of the behavior of the tetradentate, tetraanionic chelating ligands was the motivation for the study of osmium complexes of the HBA-B ligand shown in Figure 1.1. The choice to study the HBA-B ligand and its complexes might not seem logical. Focusing on the ultimate goals of making high oxidation state complexes and highly oxidizing complexes, the HBA-B ligand is not a good choice. The ligand contains unprotected aromatic rings

that are susceptible to oxidation. Additionally, the ligand has a phenylene bridge, so complexes of this ligand would have the problems associated with the diimine resonance form that formally reduces the oxidation state of the metal by two units.

Osmium complexes of HBA-B were selected for study for several reasons. Unlike some of the more robust PAC ligands, large quantities of  $H_4HBA-B$  were easy to obtain. A well-developed technology for coordinating the PAC ligands to osmium existed.<sup>1,3</sup> This seemed a good place to begin to explore general coordination features of PAC ligands. We quickly found that the HBA-B ligand easily formed complexes with osmium, and the reaction chemistry of these complexes was very clean and produced beautiful materials. This was an ideal system to study the donor properties of the PAC ligand, the coordination chemistry of the complexes, and the shortcomings of the particular ligand design.

The study of the osmium HBA-B system produced a wide range of reaction chemistry, and a great deal was discovered about osmium complexes of PAC ligands. Much of what was discovered was unique to this system. The results were a detailed understanding of osmium-PAC ligand coordination chemistry and the introduction of some new concepts useful in interpreting the chemistry. This helped in continuing the ever-changing ligand design that focuses on the ultimate goals of the PAC ligand project.

## Results and Discussion

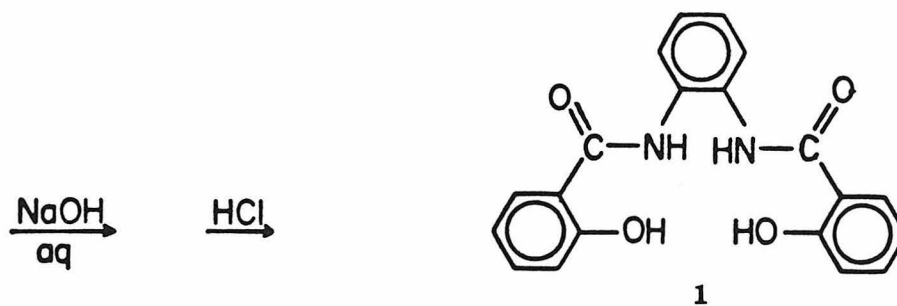
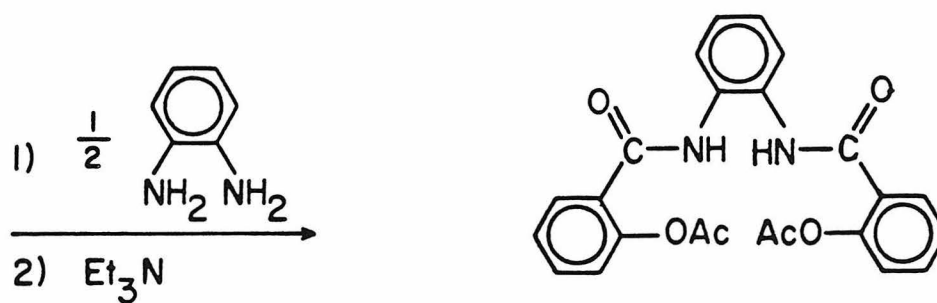
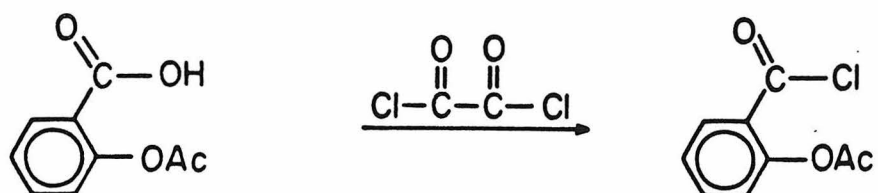
An important feature of the PAC ligands is that they are easy to synthesize. The synthesis of 1,2-bis(2-hydroxybenzamido)benzene, H<sub>4</sub>HBA-B (1) is shown in Scheme 2.1.<sup>4</sup> Acetylsalicylic acid reacts with excess oxalyl chloride to give the acid chloride. Two equivalents of acid chloride then react with one equivalent of phenylenediamine, and the ester groups are hydrolyzed by aqueous base to give 1 in 80% yield. The molecule is characterized by <sup>1</sup>H NMR, IR and elemental analysis. The <sup>1</sup>H NMR data are recorded in Table 2.2.

Coordination of the HBA-B ligand to osmium is achieved by reacting one equivalent of 1 with K<sub>2</sub>[Os(OH)<sub>4</sub>(O)<sub>2</sub>]. The osmium(VI) starting material is an excellent one to use to coordinate the PAC ligands. K<sub>2</sub>[Os(OH)<sub>4</sub>(O)<sub>2</sub>] contains four equivalents of base that react with the protons released from the ligand; the reaction is rapid to give K<sub>2</sub>[Os(HBA-B)(O)<sub>2</sub>] (2) in quantitative yield. (Scheme 2.2.)

The infrared spectrum of 2 has one amide CO stretch at 1600 cm<sup>-1</sup>. Another band at 822 cm<sup>-1</sup> is in the region indicative of a trans-osmium-dioxo asymmetric stretch.<sup>5</sup> Labeling both oxo groups with <sup>18</sup>O shifts this band down 40 cm<sup>-1</sup>, which agrees with the shift calculated for a trans-dioxo fragment. The presence of trans-dioxo groups in 2 indicates that the tetradentate ligand is coordinated in a planar fashion occupying the four equatorial sites with oxo groups occupying the axial positions, as shown in Scheme 2.2.

K<sub>2</sub>[Os(HBA-B)(O)<sub>2</sub>] is diamagnetic and gives a normal diamagnetic

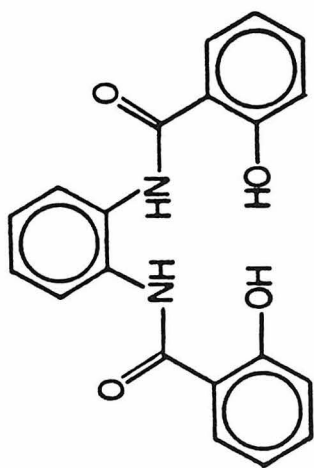
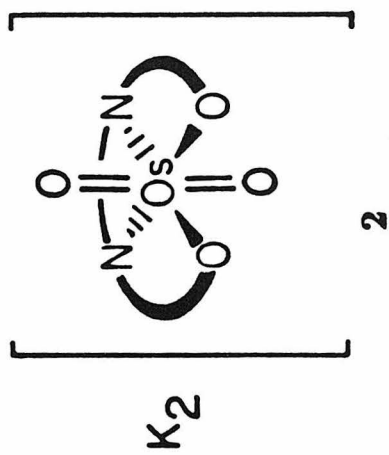
**Scheme 2.1.** Synthesis of H<sub>4</sub>HBA-B (1).



1

$\text{H}_4\text{HBA-B} \equiv 1,2\text{-bis(2-hydroxybenzamido)benzene}$

**Scheme 2.2.** Synthesis of  $K_2[trans-Os(\eta^4-HBA-B)(O)_2]$  (**2**).



1

$^1\text{H}$  NMR spectrum. All the protons are on aromatic rings, so the NMR spectrum shows all the signals between 6.5 and 9.1 ppm. The  $^1\text{H}$  NMR data, together with other spectroscopic data, are similar to those found for other trans-dioxo osmium(VI) PAC ligand complexes,<sup>1</sup> supporting the structure shown in Scheme 2.2.

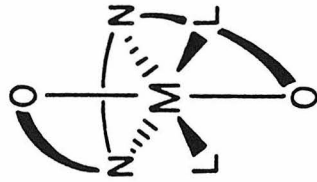
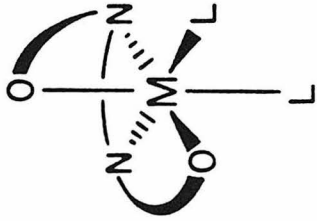
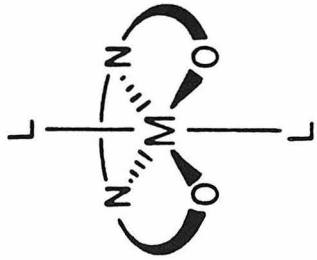
Three possible coordination geometries of a PAC ligand such as 1 can be imagined for a metal with an octahedral coordination sphere. The terminology for these isomers was introduced by Sargeson<sup>6</sup> and is given in Figure 2.1. The trans isomer coordinates the tetradentate ligand in a planar geometry with the two auxiliary ligands occupying equatorial positions. If one arm of the tetradentate ligand is twisted out of its equatorial position to an axial position, the result is the *cis*- $\beta$  isomer. If both arms of the tetradentate ligand are twisted into axial positions, the *cis*- $\alpha$  isomer is formed. Compound 2 contains a planar HBA-B ligand, so it is referred to as  $\text{K}_2[\text{trans-Os}(\eta^4\text{-HBA-B})(\text{O})_2]$ . The results below show that osmium coordinates HBA-B to make complexes of all three isomers.

The reactivity of 2 is limited. Reaction with acid gives a blue insoluble solid that has not been characterized. Reduction of 2 can be achieved with excess triphenylphosphine in the presence of trifluoroacetic acid to produce a dark green compound 3. (Scheme 2.3.)

Compound 3 analyses as  $\text{Os}(\text{HBA-B})(\text{PPh}_3)_2$ . A magnetic study shows that 3 is paramagnetic with a room temperature magnetic moment of 1.0 BM. Compound 3 exhibits a well-resolved, paramagnetically-shifted  $^1\text{H}$  NMR spectrum that indicates there are two triphenylphosphines per

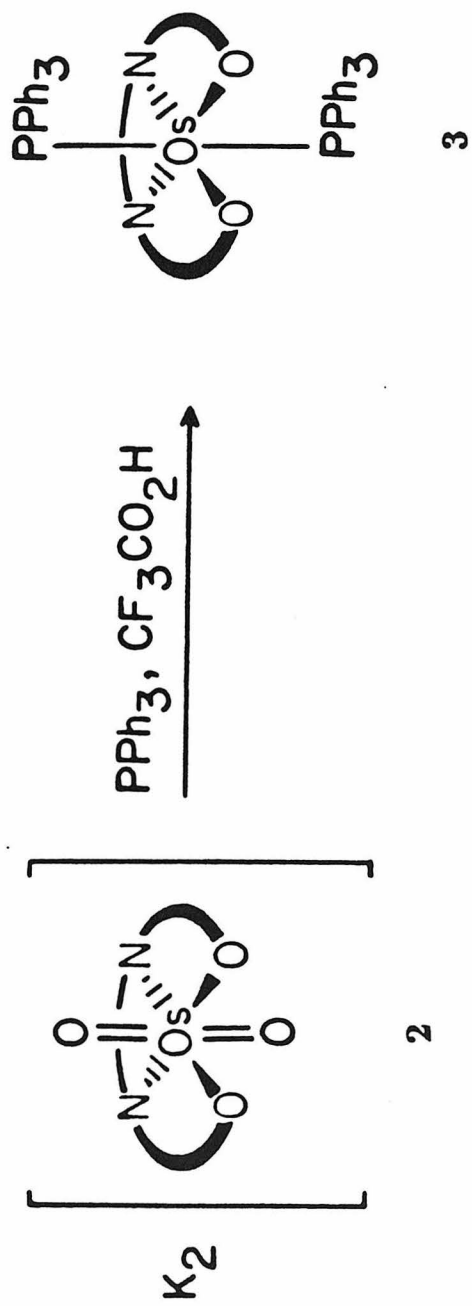


**Figure 2.1.** Nomenclature for the possible diastereomers of a tetradentate ligand in an octahedral complex. (Ref. 6.)

cis- $\alpha$ cis- $\beta$ 

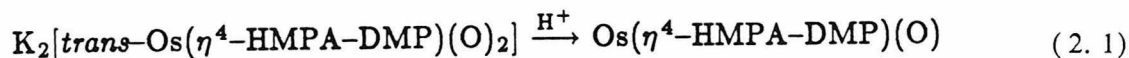
trans

**Scheme 2.3.** Synthesis of *trans*-Os( $\eta^4$ -HBA-B)(PPh<sub>3</sub>)<sub>2</sub> (3).

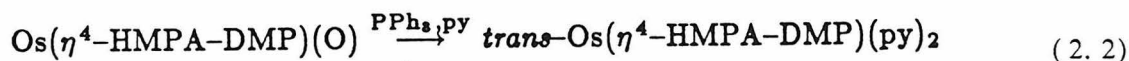


HBA-B ligand, and that there is a plane or axis of symmetry in the molecule. The infrared spectrum of **3** has HBA-B ligand bands in the same position as in the IR spectrum of **2**, implying the same ligand geometry. These data lead to the formulation of **3** as *trans*-Os( $\eta^4$ -HBA-B)(PPh<sub>3</sub>)<sub>2</sub>.

The mechanism of the reduction shown in Scheme 2.3 is not known, but the reactivity of a related system gives evidence of a possible pathway. The *trans*-dioxo compound K<sub>2</sub>[*trans*-Os( $\eta^4$ -HMPA-DMP)(O)<sub>2</sub>] reacts with acid to give the neutral osmium(VI) mono-oxo compound.<sup>7</sup> (Equation 2.1.)



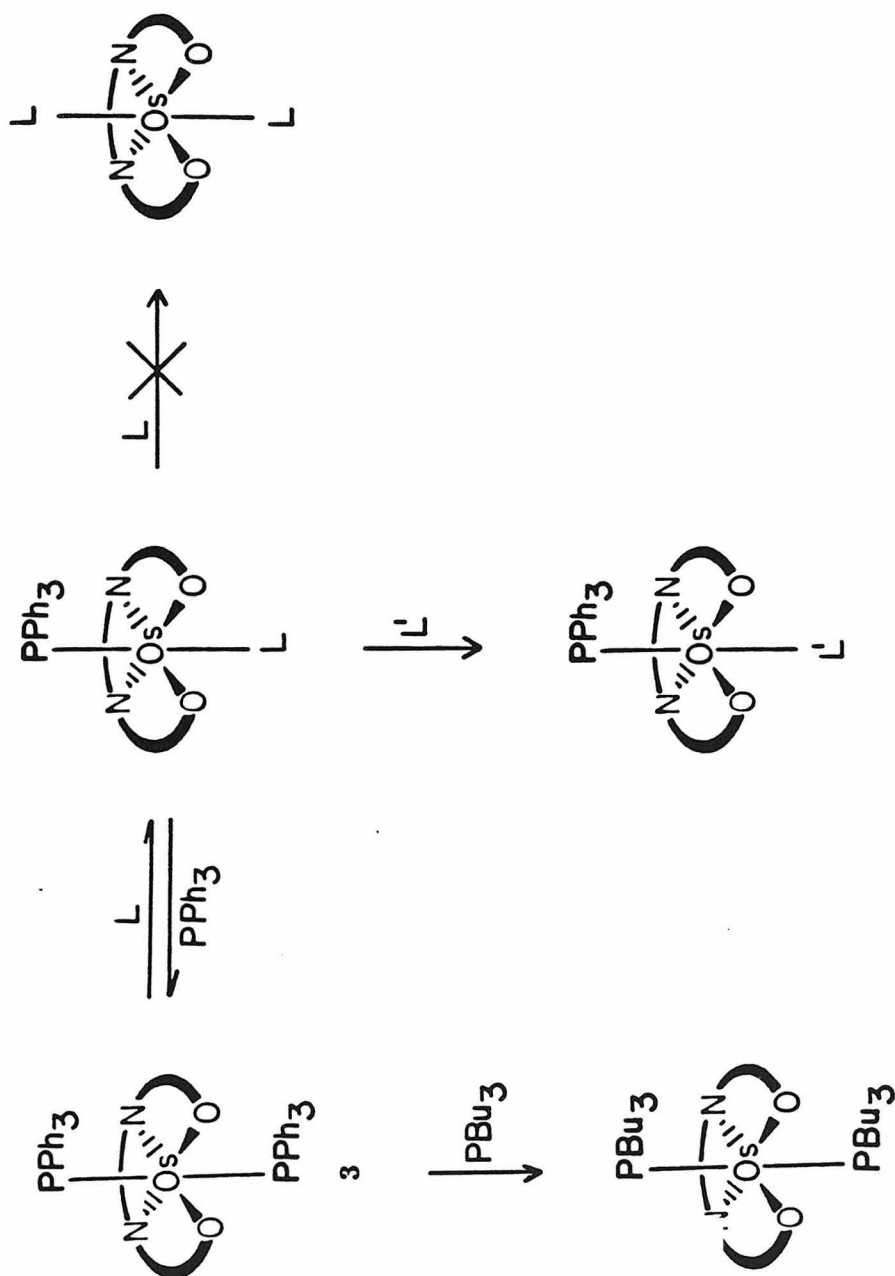
The mono-oxo compound reacts with excess triphenylphosphine in pyridine to give the bis-pyridine complex.<sup>7</sup>



This suggests that the reduction of **2** to give **3** in the presence of acid and triphenylphosphine could be going through an osmium(VI) mono-oxo intermediate. The oxo group is then removed as triphenylphosphine oxide.<sup>8</sup>

Compound **3**, *trans*-Os( $\eta^4$ -HBA-B)(PPh<sub>3</sub>)<sub>2</sub>, is an important compound because the phosphine ligands are labile and **3** demonstrates a rich ligand substitution chemistry. The reaction of **3** with excess tri-*n*-butylphosphine produces the bis-substituted product *trans*-Os( $\eta^4$ -HBA-B)(PBu<sub>3</sub>)<sub>2</sub> (**4**). (Scheme 2.4.) Reaction of **3** with nitrogen

**Scheme 2.4.** Reactions of *trans*-Os( $\eta^4$ -HBA-B)(PPh<sub>3</sub>)<sub>2</sub> (3) with neutral two-electron donor ligands.



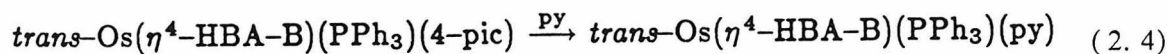
(L, L' = py, 4-t-Bupy, 4-pic, imidazole)

base ligands results in mono-substitution giving a mono-phosphine, mono-L (L = py, *t*-Bupy, 4-pic, ImH) complex. Substitution of both phosphines by two pyridine type ligands has never been observed, even under forcing conditions.<sup>9</sup> A mono-phosphine, mono-pyridine compound will, however, exchange pyridine ligands quite readily as shown in Scheme 2.4. A mono-phosphine, mono-pyridine compound will also react with excess phosphine to reproduce the bis-phosphine compound.

The neutral osmium(IV) compound *trans*-Os( $\eta^4$ -HBA-B)(PPh<sub>3</sub>)<sub>2</sub> is a sixteen-electron compound, so both associative and dissociative ligand exchange pathways are possible. A kinetic study of reaction 2.3<sup>10</sup>



demonstrates that the reaction is first order in osmium complex concentration and zeroth order in *t*-Bupy concentration implying a dissociative pathway. The Arrhenius parameters of  $\Delta H^\ddagger = 23.8 \pm 0.8$  kcal mol<sup>-1</sup> and  $\Delta S^\ddagger = 12 \pm 3$  eu are consistent with such a mechanism. Initial kinetic results of the ligand exchange reaction 2.4



indicate the reaction might be proceeding through two distinct steps. The lack of a spectroscopic means to monitor the course of the reaction over a wide range of 4-pic concentration prohibits a detailed study.

It is interesting that while both triphenylphosphine ligands in 3 will be replaced by other phosphines, only one phosphine will be re-



placed with pyridine, but the mono-phosphine, mono-pyridine, **5**, will freely exchange pyridine. One explanation is that a kinetic trans effect is responsible for the result. Phosphine is a much better trans-labilizer than pyridine,<sup>11</sup> so **3** would be expected to lose phosphine more rapidly than **5**. Complex **5** does exchange pyridine readily indicating the ligand trans to phosphine is still labile.

Several physical techniques have been used to characterize these osmium(IV) species and to study their physical properties. One of the properties studied is the magnetics. All the trans-osmium(IV) compounds prepared are paramagnetic, demonstrating temperature independent paramagnetism, with room temperature effective magnetic moments near 1 BM. (See Table 2.1.) These values are well below the spin-only values for octahedral low-spin-d<sup>4</sup> configurations, but are common for octahedral osmium(IV) species.<sup>12</sup>

NMR spectroscopy is the most useful tool for characterizing the osmium(IV) species. Most of the osmium(IV) complexes are paramagnetic, but all exhibit well-resolved, narrow-lined, paramagnetically-shifted NMR spectra. Paramagnetic NMR spectra for octahedral low-spin-d<sup>4</sup> systems are commonly observed.<sup>13</sup> The paramagnetic shifting results in a wide chemical shift range for Os(IV)(HBA-B) complexes, but line widths are comparable to those in spectra of diamagnetic complexes. Reliable integrations are obtained, indicating that relaxation times of different protons in the complexes are quite uniform.

It is often assumed that because a molecule is paramagnetic, NMR spectroscopy is not only difficult to perform, but also that the spectra obtained are not very useful. The osmium(IV) PAC ligand compounds

**Table 2.1.** Solid-state, room temperature effective magnetic moments of osmium complexes of HBA-B.

<u>Compound</u>	<u><math>\mu_{\text{eff}}</math></u>
$\text{K}_2[\text{trans-Os}(\eta^4\text{-HBA-B})(\text{O})_2]$ ( <b>2</b> )	d
$\text{trans-Os}(\eta^4\text{-HBA-B})(\text{PPh}_3)_2$ ( <b>3</b> )	1.0
$\text{trans-Os}(\eta^4\text{-HBA-B})(\text{PBu}_3)_2$ ( <b>4</b> )	1.0
$\text{trans-Os}(\eta^4\text{-HBA-B})(\text{PPh}_3)(\text{py})$ ( <b>5</b> )	1.0
$\text{trans-Os}(\eta^4\text{-HBA-B})(\text{PPh}_3)(t\text{-Bupy})$ ( <b>6</b> )	1.1
$\text{trans-Os}(\eta^4\text{-HBA-B})(\text{PPh}_3)(4\text{-pic})$ ( <b>7</b> )	1.0
$\text{trans-Os}(\eta^4\text{-HBA-B})(\text{PPh}_3)(\text{ImH})$ ( <b>8</b> )	1.1
$(\text{NBu}_4)[\text{trans-Os}(\eta^4\text{-HBA-B})(\text{PPh}_3)\text{Cl}]$ ( <b>9</b> )	0.8
$\text{cis-}\alpha\text{-Os}(\eta^4\text{-HBA-B})(\text{PPh}_3)(\text{CO})$ ( <b>10</b> )	d
$\text{cis-}\alpha\text{-Os}(\eta^4\text{-HBA-B})(\text{PPh}_3)(t\text{-BuNC})$ ( <b>11</b> )	d
$\text{cis-}\beta\text{-Os}(\eta^4\text{-HBA-B})(\text{dppe})$ ( <b>12</b> )	d
$\text{Os}(\eta^3\text{-(H)HBA-B})(\text{PPh}_3)(\text{bipy})$ ( <b>13</b> )	1.5
$\text{Os}(\eta^3\text{-(H)HBA-B})(\text{PPh}_3)(\text{DMBP})$ ( <b>14</b> )	1.5
$\text{Os}(\eta^3\text{-(H)HBA-B})(\text{PPh}_3)(\text{phen})$ ( <b>15</b> )	1.4

---

d  $\equiv$  diamagnetic

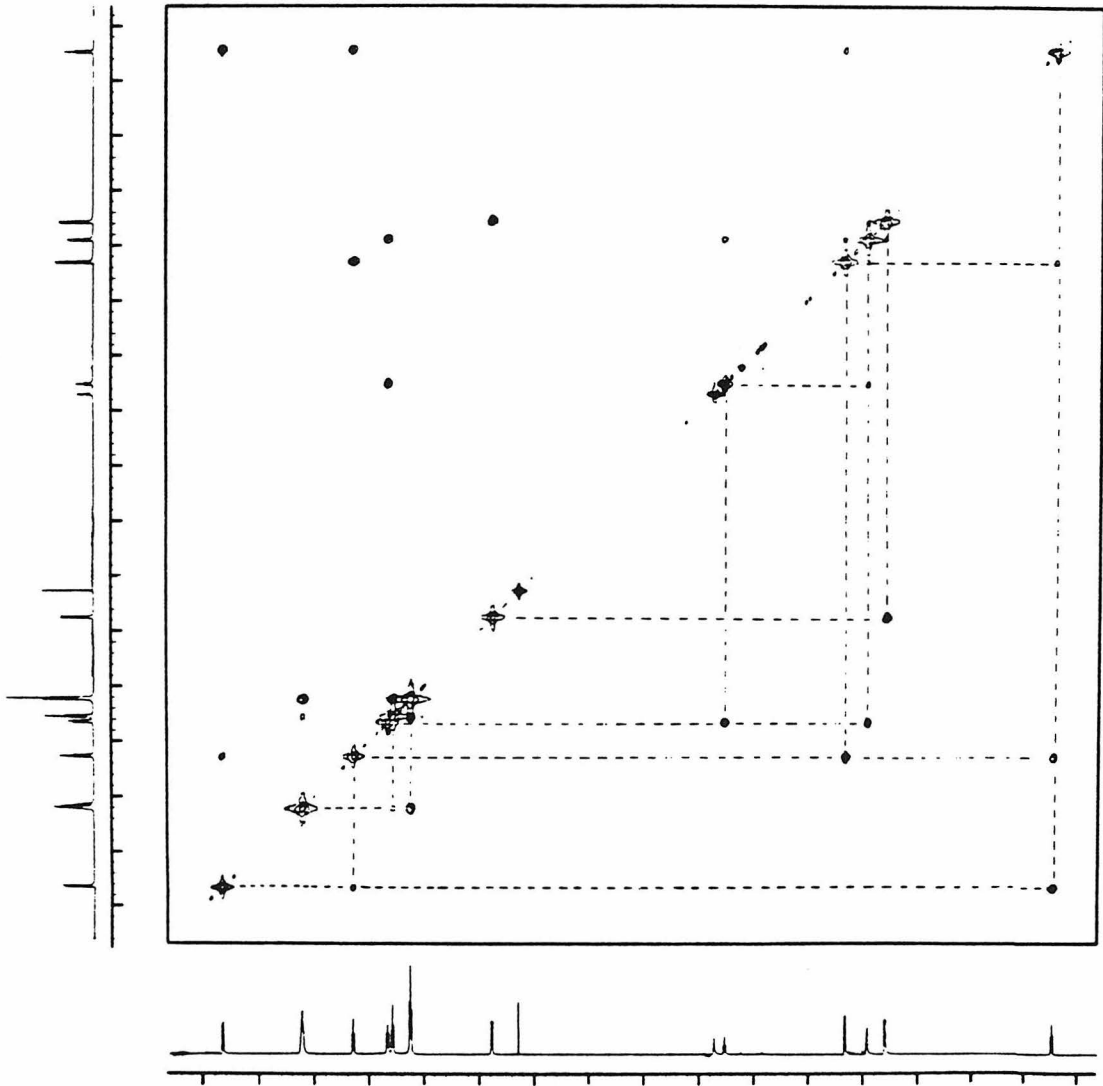
give very useful NMR spectra which are in some cases easier to assign than if they were spectra of diamagnetic compounds. As an example, consider the  $^1\text{H}$  NMR spectrum of *trans*-Os( $\eta^4$ -HBA-B)(PPh<sub>3</sub>)(py) (**5**). The compound is paramagnetic with a room temperature effective magnetic moment of 1.0 BM. The 400 MHz  $^1\text{H}$  NMR spectrum of this compound is shown in Figure 2.2. Compound **5** has twelve inequivalent protons and so should give twelve resonances in the  $^1\text{H}$  NMR spectrum. All the protons in the molecule are on aromatic rings, and for a diamagnetic complex, would be expected to have chemical shifts between 7 and 9 ppm. A spectrum with twelve resonances in that small range of chemical shifts would be quite complicated. However, paramagnetic shifting in the  $^1\text{H}$  NMR spectrum of **5** leads to twelve well-resolved resonances spread over the range +11 to -5 ppm. In this case the paramagnetism of the complex serves as an internal shift reagent and makes the NMR spectrum easier to assign.

A complete assignment of the resonances in the  $^1\text{H}$  NMR spectrum of **5** (Figure 2.2) can be made employing a variety of NMR experiments. From the simple one-dimensional proton spectrum shown in Figure 2.2, the three triphenylphosphine resonances (B, E, F), the three pyridine resonances (D, H, J), and the six HBA-B ligand resonances (A, C, G, I, K, L), can be identified on the basis of integration and coupling constants. The two-dimensional ( $^1\text{H}$ - $^1\text{H}$ ) COSY spectrum of **5**<sup>14</sup> is shown in Figure 2.3. In the two-dimensional plot the presence of an off-diagonal peak indicates J-coupling between the two protons whose resonance frequencies intersect at the peak. The COSY spectrum confirms the identifications made from the one-dimensional spectrum. In addition,

**Figure 2.2.** 400 MHz  $^1\text{H}$  NMR spectrum of *trans*-Os( $\eta^4$ -HBA-B)(PPh<sub>3</sub>)-(py) (5). Obtained in CDCl<sub>3</sub> containing Me<sub>4</sub>Si.



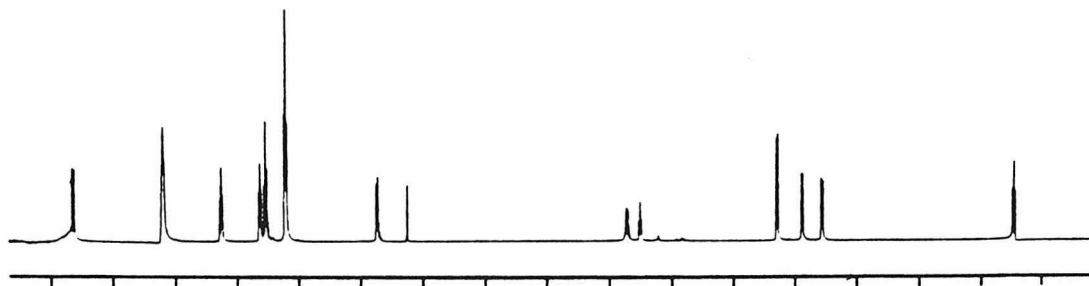
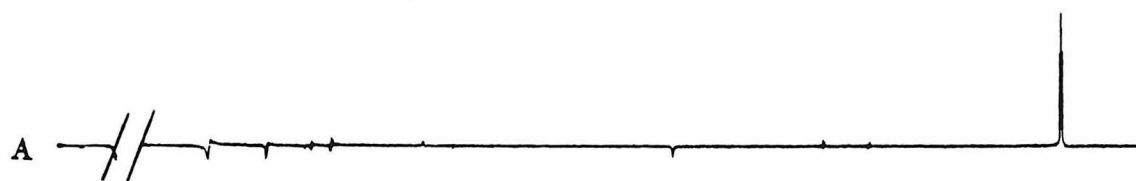
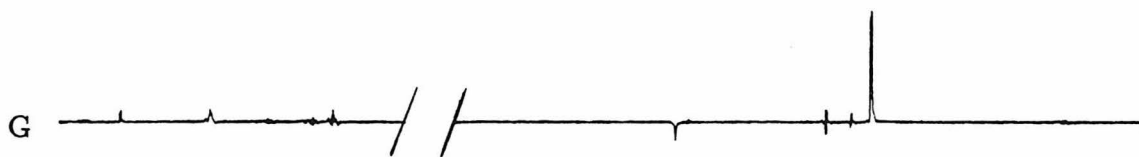
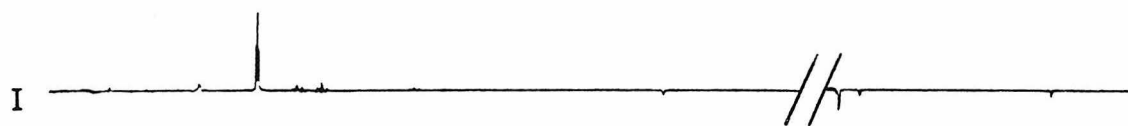
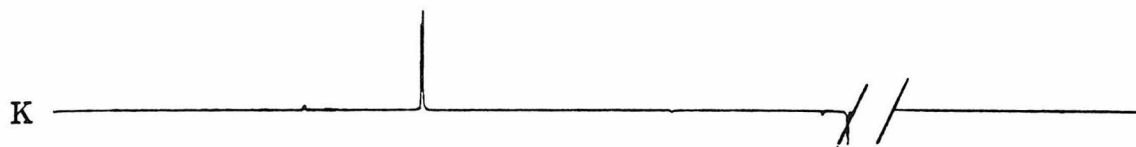
**Figure 2.3.** 2D-( $^1\text{H}$ - $^1\text{H}$ ) COSY spectrum of *trans*-Os( $\eta^4$ -HBA-B)(PPh<sub>3</sub>)-(py) (5). Obtained at 400 MHz in CDCl<sub>3</sub> solvent.





it indicates which protons are coupled to each other, making a more detailed assignment possible. The 2D-spectrum shows that the triphenylphosphine resonance B is coupled to F, E is coupled to F, and F is coupled to both B and E. Thus resonance B corresponds to the triphenylphosphine ortho protons, E represents the para protons, and F represents the meta protons. Likewise, pyridine resonance D is coupled to H and J. This information, plus the integration, assigns D to the pyridine meta proton, H to the para proton, and J to the ortho proton. The HBA-B ligand resonance G is strongly coupled to resonance K. This is the only coupling of these two resonances, assigning them to the two inequivalent phenylene bridge protons. Resonances A, C, I, and L must correspond to the four protons on the phenol ring. The coupling from the 2D-spectrum indicates the four protons are arranged around the ring in the order A-L-C-I. We have assigned the pyridine and phosphine resonances, and the HBA-B ligand bridge and phenol arm resonances, but we still cannot completely assign the HBA-B ligand resonances. That is, we know that G and K are the bridge resonances, but we do not know which corresponds to which proton. We also know the ordering of the phenol arm resonances around the ring, but we cannot say whether A is ortho to the phenol oxygen and I is ortho to the amide, or vice versa. A set of Nuclear Overhauser Effect (NOE) experiments<sup>14</sup> answers these questions. A set of difference NOE spectra is shown in Figure 2.4. The top four spectra are difference spectra recorded after irradiation at signals K, I, G, and A, respectively, with the negative signals of the irradiated resonances omitted for clarity. The bottom spectrum is the "normal" spectrum. Irradiation of reso-

**Figure 2.4.** A set of  $^1\text{H}$  difference NOE spectra of *trans*-Os( $\eta^4$ -HBA-B)(PPh<sub>3</sub>)(py) (5). Obtained at 400 MHz in CDCl<sub>3</sub> solvent.



nance K shows an in-phase signal at resonance G indicating a strong positive NOE enhancement of G. This is expected, as protons G and K are bound to adjacent carbon atoms. Irradiation of resonance I shows a positive NOE enhancement of C, which in turn causes the small negative effect observable for L.<sup>15</sup> Irradiation of G gives the strong positive enhancement of K expected and a weak positive NOE enhancement of signal A, also. Irradiation of signal A leads to a strong enhancement of L, with the accompanying small negative enhancement of C, and also a weak enhancement of G. The observation that irradiation of A or G leads to a weak enhancement of the other suggests that hydrogen atoms A and G are nearby in the same molecule. Since irradiation of K and I give no such enhancements the conclusion is that A is ortho to the amide group, and G is also ortho to the amide group, which allows a through-space interaction resulting in the NOE enhancement. This gives the assignment of the spectrum shown in Figure 2.5.

All of the paramagnetic osmium(IV) species give <sup>1</sup>H NMR spectra with a similar arrangement of HBA-B ligand resonances. A complete assignment of the resonances as discussed above was done only for 5, but assignment of resonances of other molecules can be made relying on the similarity of the spectra. A complete listing of the <sup>1</sup>H NMR data of all the complexes discussed in Chapter 2 is given in Table 2.2.

Cyclic voltammetric experiments with the osmium PAC ligand complexes have proven useful in obtaining information about the electron density of the osmium center and the donating properties of the HBA-B ligand. In general, a cyclic voltammogram of one of the osmium(IV) PAC ligand species shows reversible electrochemistry. A typical CV

**Figure 2.5.** Assignment of the resonances of the 400 MHz  $^1\text{H}$  NMR spectrum of *trans*-Os( $\eta^4$ -HBA-B)(PPh<sub>3</sub>)(py) (**5**).

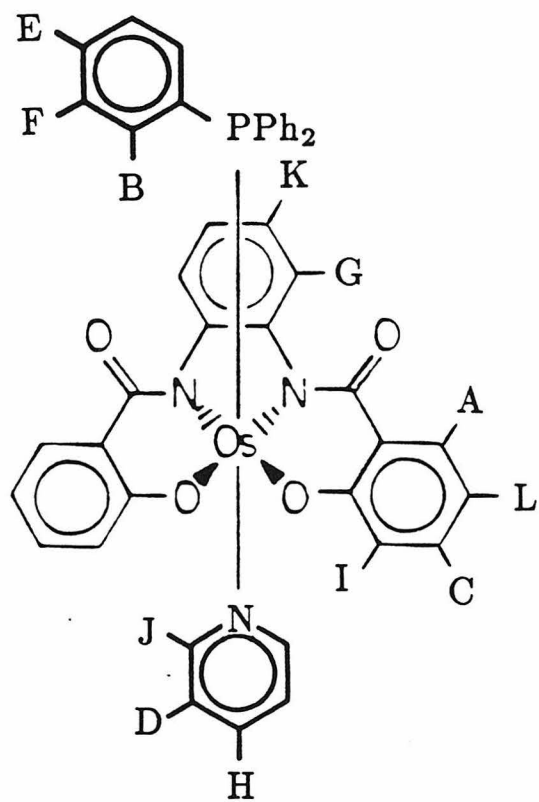


**Table 2.2.**  $^1\text{H}$  NMR data for osmium complexes of HBA-B.

<sup>1</sup>H NMR DATA FOR ALL COMPOUNDS OF PAC LIGAND [(P<sup>t</sup>-HBA-B)]<sup>4+</sup>, 1<sup>a</sup>

Compound	Chelate Ligand		Phosphine Aromatic		Other
	HBA <sup>a</sup>	-B	H <sub>a</sub>	H <sub>b</sub>	
H <sub>4</sub> -1 <sup>d</sup>	6.7-7.0 4H	7.2-7.5 2H 7.6-8.1 2H			10.1 (-OH) broad <sup>e</sup>
K <sub>2</sub> [trans-Os(η <sup>4</sup> -1)(O) <sub>2</sub> ](2) <sup>4+</sup>	6.4-6.9 m 6H	8.3 dd 2H (6, 3)	9.1 dd 2H (7, 3)		
trans-Os(η <sup>4</sup> -1)(PPh <sub>3</sub> ) <sub>2</sub> (3) <sup>4+</sup>	-4.33 2H (7)	1.33 2H (6)	0.90 2H (6, 3)	8.28 12H (7)	0.90 12H (7)
trans-Os(η <sup>4</sup> -1)(PPh <sub>3</sub> ) <sub>2</sub> (4) <sup>4+</sup>	-3.73 2H (6)	3.07 2H (6)	7.97 2H (6, 3)	9.48 2H (6, 3)	0.66 12H (6)
trans-Os(η <sup>4</sup> -1)(PPh <sub>3</sub> ) <sub>2</sub> (5) <sup>4+</sup>	-4.53 2H (6, 1)	-0.69 2H (6, 1)	8.37 2H (6, 1)	10.65 2H (6, 2)	7.55 6H (7)
trans-Os(η <sup>4</sup> -1)(PPh <sub>3</sub> ) <sub>2</sub> (6) <sup>4+</sup>	-4.61 2H (6)	-0.26 2H (6)	8.52 2H (6)	10.80 2H (6, 3)	7.56 6H (6)
trans-Os(η <sup>4</sup> -1)(PPh <sub>3</sub> ) <sub>2</sub> (7) <sup>4+</sup>	-4.61 2H (7)	-0.73 2H (7)	8.44 2H (7)	10.96 2H (7)	7.58 6H (6)
trans-Os(η <sup>4</sup> -1)(PPh <sub>3</sub> ) <sub>2</sub> (8) <sup>4+</sup>	-5.04 2H (7)	-1.42 2H (7)	9.35 2H (7)	12.26 2H (7)	7.46 6H (7)
(NBu <sub>2</sub> )[trans-Os(η <sup>4</sup> -1)(PPh <sub>3</sub> )Cl](9) <sup>4+</sup>	-5.09 2H (6)	-1.50 2H (6)	9.55 2H (6)	12.95 2H (6, 3)	7.53 6H (6)
cis-β-Os(η <sup>4</sup> -1)(PPh <sub>3</sub> ) <sub>2</sub> (CO)(10) <sup>4+</sup>	5.40 1H (6)	0.67 1H (6)	6.74 1H (6)	7.04 1H (6)	7.40 13H (6)
cis-β-Os(η <sup>4</sup> -1)(PPh <sub>3</sub> ) <sub>2</sub> (C <sup>t</sup> BuNC)(11) <sup>4+</sup>	5.66 1H (6)	0.81 1H (6)	6.90 1H (6)	7.30 1H (6)	7.2-7.4 15H (6)
cis-β-Os(η <sup>4</sup> -1)(dpppe) <sub>2</sub> (12) <sup>4+</sup>	5.32 1H (6)	5.46 1H (6)	5.56 1H (6)	5.97 1H (6)	7.03 7.1-7.33 4H (7)
					7.93 4H (9)

<sup>a</sup> The chemical shifts of paramagnetic osmium(IV) species are somewhat concentration dependent. Coupling constants given in parentheses.  
<sup>b</sup> Assignments for fragments of HBA-B ligand hold for complexes 3-9. <sup>c</sup> Measured at 90 MHz. <sup>d</sup> Measured at 400 MHz. <sup>e</sup> Measured at 500 MHz. <sup>f</sup> δ in (CD<sub>3</sub>)<sub>2</sub>CO. <sup>g</sup> δ in CDCl<sub>3</sub>. <sup>h</sup> Hidden by phosphine H<sub>a</sub> signal. <sup>i</sup> H<sub>2</sub> and H<sub>3</sub>. <sup>j</sup> Includes 1H of HBA-B ligand. <sup>k</sup> Hidden by phosphine signal.



consists of two reversible one-electron reductions, one reversible one-electron oxidation, and one irreversible oxidation. The formal potentials of the reversible couples give an indication of how electron-rich or electron-poor the osmium center is. A listing of the potentials of these couples for the  $\text{Os}(\eta^4\text{-HBA-B})$  complexes is given in Table 2.3.<sup>16</sup> The formal potentials vary as the auxiliary ligands are changed, reflecting the relative donating abilities of the auxiliary ligands; lower potentials indicate a more electron-rich osmium center. Presumably the two one-electron reductions correspond to the  $\text{Os(IV/III)}$  and  $\text{Os(III/II)}$  couples. It is tempting to assume that the reversible oxidation is osmium centered and corresponds to an  $\text{Os(V/IV)}$  couple, but as we will see below, comparison of these potentials to those of osmium complexes with other PAC ligands suggests that the reversible oxidation is not simply an oxidation to osmium(V).

Table 2.4 repeats some redox potentials for osmium(HBA-B) complexes, along with some potentials for osmium complexes of other PAC ligands, and one other osmium complex. Several conclusions can be drawn by comparing these potentials. The IV/III couple of *trans*- $\text{Os}(\eta^4\text{-HBA-B})(\text{PPh}_3)_2$  is over half a volt lower than the IV/III couple of *trans*- $\text{OsCl}_4(\text{PPh}_3)_2$ . This demonstrates just how donating the HBA-B ligand is compared to four chloride donor ligands. We can see that all the PAC ligands are *very* good donors. Also notice that the HBA-B ligand is a good deal more donating than the CHBA-DCB ligand. A direct comparison of the potentials for *trans*- $\text{Os}(\eta^4\text{-HBA-B})(\text{PPh}_3)(t\text{-Bupy})$  and *trans*- $\text{Os}(\eta^4\text{-CHBA-DCB})(\text{PPh}_3)(t\text{-Bupy})$  shows that the better donation of the HBA-B ligand results in a lowering by about 300 mV of the

**Table 2.3.** Electrochemical data for osmium complexes of HBA-B.  
Cyclic voltammograms were measured in  $\text{CH}_2\text{Cl}_2/0.1 \text{ M TBAP}$  with  
a BPG working electrode ( $0.17 \text{ cm}^2$ ). Scan rate =  $200 \text{ mV s}^{-1}$ .

<u>Compound</u>	<u>III/II<sup>a</sup></u>	<u>IV/III</u>	<u>V/IV<sup>b</sup></u>	<u>VI/V</u>
<i>trans</i> -Os( $\eta^4$ -HBA-B)(PPh <sub>3</sub> ) <sub>2</sub> ( <b>3</b> )	(-1.73, -1.91) <sup>c</sup>	-0.79	+0.21	-
<i>trans</i> -Os( $\eta^4$ -HBA-B)(PBU <sub>3</sub> ) <sub>2</sub> ( <b>4</b> )	-	-0.88	+0.22	-
<i>trans</i> -Os( $\eta^4$ -HBA-B)(PPh <sub>3</sub> )(py) ( <b>5</b> )	(-1.94)	-0.73	+0.34	(+1.07)
<i>trans</i> -Os( $\eta^4$ -HBA-B)(PPh <sub>3</sub> )( <i>t</i> -Bupy) ( <b>6</b> )	(-1.93)	-0.73	+0.33	(+1.08)
<i>trans</i> -Os( $\eta^4$ -HBA-B)(PPh <sub>3</sub> )(4-pic) ( <b>7</b> )	(-1.90)	-0.74	+0.34	(+1.01)
<i>trans</i> -Os( $\eta^4$ -HBA-B)(PPh <sub>3</sub> )(ImH) ( <b>8</b> )	-	-0.75	+0.25	-
(NBu <sub>4</sub> )[ <i>trans</i> -Os( $\eta^4$ -HBA-B)(PPh <sub>3</sub> )Cl] ( <b>9</b> )	(-1.68)	(-0.98)	-0.04	(+0.76)
<i>cis</i> - $\alpha$ -Os( $\eta^4$ -HBA-B)(PPh <sub>3</sub> )(CO) ( <b>10</b> )	-1.17	-0.63	+0.90	-
<i>cis</i> - $\alpha$ -Os( $\eta^4$ -HBA-B)(PPh <sub>3</sub> )( <i>t</i> -BuNC) ( <b>11</b> )	-	(-0.86)	+0.46	-
<i>cis</i> - $\beta$ -Os( $\eta^4$ -HBA-B)(dppe) ( <b>12</b> )	-1.47	-0.68	+0.25	-
Os( $\eta^3$ -(H)HBA-B)(PPh <sub>3</sub> )(bipy) ( <b>13</b> )	-1.09	-0.29	+0.70	-
Os( $\eta^3$ -(H)HBA-B)(PPh <sub>3</sub> )(DMBP) ( <b>14</b> )	-1.29	-0.33	+0.66	-
Os( $\eta^3$ -(H)HBA-B)(PPh <sub>3</sub> )(phen) ( <b>15</b> )	-1.12	-0.31	+0.72	-
Os( $\eta^3$ -(CH <sub>3</sub> CO)HBA-B)(PPh <sub>3</sub> )(phen) ( <b>16</b> )	-1.11	-0.28	(+0.68)	-

<sup>a</sup>All potentials listed vs. the Fc<sup>+</sup>/Fc couple.

<sup>b</sup>As discussed in the text, the “V/IV” and “VI/V” couples are not necessarily metal based.

<sup>c</sup>Parentheses indicate an irreversible couple.

**Table 2.4.** Comparison of electrochemical data for osmium(IV) compounds.

<u>Compound</u>	<u>III/II<sup>a</sup></u>	<u>IV/III</u>	<u>V/IV</u>
<i>trans</i> -Os( $\eta^4$ -HBA-B)(PPh <sub>3</sub> ) <sub>2</sub> ( <b>3</b> )	(-1.73, -1.91) <sup>b</sup>	-0.79	+0.21
<i>trans</i> -Os( $\eta^4$ -HBA-B)(PPh <sub>3</sub> )(py) ( <b>5</b> )	(-1.94)	-0.73	+0.34
<i>trans</i> -Os( $\eta^4$ -HBA-B)(PPh <sub>3</sub> )( <i>t</i> -Bupy) ( <b>6</b> )	(-1.93)	-0.73	+0.33
<i>trans</i> -Os( $\eta^4$ -CHBA-DCB)(PPh <sub>3</sub> ) <sub>2</sub> <sup>c</sup>	(-1.72)	-0.46	+0.59
<i>trans</i> -Os( $\eta^4$ -CHBA-DCB)(PPh <sub>3</sub> )( <i>t</i> -Bupy)	-1.63	-0.44	+0.69
<i>trans</i> -Os( $\eta^4$ -CHBA-DCB)( <i>t</i> -Bupy) <sub>2</sub>	-1.77	-0.51	+0.70
<i>trans</i> -Os( $\eta^4$ -CHBA-DCB)(py) <sub>2</sub>	-1.68	-0.44	+0.72
<i>trans</i> -Os( $\eta^4$ -HMPA-DMP)(py) <sub>2</sub> <sup>d</sup>	-	-1.31	+0.35
<i>trans</i> -Os( $\eta^4$ -HMPA-DMP)( <i>t</i> -Bupy) <sub>2</sub>	-	-1.36	+0.30
<i>trans</i> -OsCl <sub>4</sub> (PPh <sub>3</sub> ) <sub>2</sub> <sup>e,f</sup>	-	-0.12	+1.34

<sup>a</sup>All potentials listed in volts vs. the Fc<sup>+</sup>/Fc couple.

<sup>b</sup>Parentheses indicate an irreversible couple.

<sup>c</sup>CHBA-DCB complexes prepared by John Keech.<sup>17</sup>

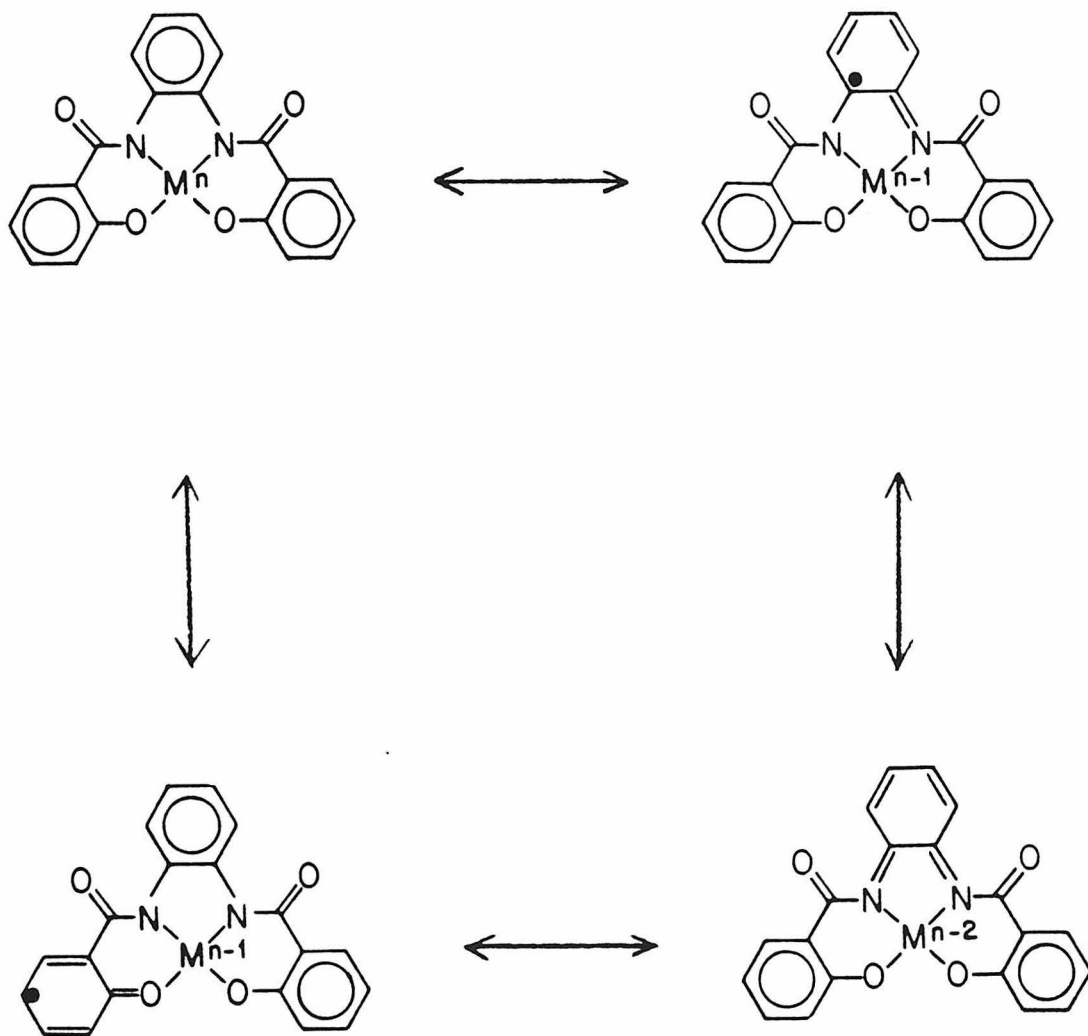
<sup>d</sup>HMPA-DMP complexes prepared by Brian Treco.<sup>18</sup>

<sup>e</sup>See reference 19.

<sup>f</sup>Tetra-*n*-butylammonium hexafluorophosphate supporting electrolyte.

formal potentials. This reflects the reduction in donating ability from the addition of six electron-withdrawing chlorine atoms to the PAC ligand framework. A comparison of the potentials for the Os(HBA-B) complexes to those for the Os(HMPA-DMP) complexes is also interesting. The HMPA-DMP ligand with an all aliphatic backbone, including tertiary alcohol donors is expected to be an extremely good donating ligand; it should be much more donating than HBA-B. Comparing the IV/III couples of  $\text{Os}(\eta^4\text{-HMPA-DMP})(\text{py})_2$  and  $\text{Os}(\eta^4\text{-HBA-B})(\text{PPh}_3)(\text{py})$ , it is clear that HMPA-DMP is indeed the much better donor. What is surprising is that the V/IV couple for *trans*- $\text{Os}(\eta^4\text{-HBA-B})(\text{PPh}_3)(\text{py})$  is at about the same potential as the V/IV couple for *trans*- $\text{Os}(\eta^4\text{-HMPA-DMP})(\text{py})_2$ . This indicates that there is some stabilization of the oxidized form of *trans*- $\text{Os}(\eta^4\text{-HBA-B})(\text{PPh}_3)(\text{py})$  that is not present in the oxidized form of *trans*- $\text{Os}(\eta^4\text{-HMPA-DMP})(\text{py})_2$ . As pointed out in Chapter 1, since the HBA-B ligand has aromatic rings, resonance forms exist that shift electron density onto the osmium center, as shown in Scheme 2.5. If the one-electron oxidation of *trans*- $\text{Os}(\eta^4\text{-HBA-B})(\text{PPh}_3)(\text{py})$  were osmium centered, an electron-poor osmium(V) would be the result. Since these resonance forms donate more electron density to the osmium center, the oxidized species is probably not truly osmium(V), but has some contribution from these resonance forms which stabilizes the oxidized species and thus lowers the potential of the cation/neutral redox couple. In *trans*- $\text{Os}(\eta^4\text{-HMPA-DMP})(\text{py})_2$ , the aliphatic ligand has no such resonance mechanism to donate electron density to the osmium center, and the oxidation is to a true osmium(V) species, which is why its Os(V/IV) potential is higher than that for

**Scheme 2.5.** Resonance structures of a coordinated HBA-B ligand.





*trans*-Os( $\eta^4$ -HBA-B)(PPh<sub>3</sub>)(py). It is difficult to estimate the extent of the contributions of the resonance forms in Scheme 2.5 in the oxidized form of *trans*-Os( $\eta^4$ -HBA-B)(PPh<sub>3</sub>)(py), but there can be no doubt that there is some contribution, and the reversible oxidation cannot be called an Os(V/IV) couple.

We conclude from the electrochemical data presented here that the HBA-B ligand, and all of our group's PAC ligands are very good donors, and so are good at stabilizing higher-valent metal centers. We can also conclude that at least in the HBA-B ligand, non-innocence of the aromatic rings is possible. That is, resonance can and does exist in certain cases to donate electron density to the metal, reducing its formal oxidation state. For the osmium PAC ligand species electrochemistry is a useful way to obtain valuable information about the electron density of the metal, and the donating properties of the ligands. A change in the donating properties of the ligands leads to a change in the potentials of the redox couples. We will use the redox potentials as a measure of the electron density of the osmium center.

The substitution chemistry of *trans*-Os( $\eta^4$ -HBA-B)(PPh<sub>3</sub>)<sub>2</sub> that has been discussed to this point has been with neutral two-electron donor ligands. Other ligands will also react with *trans*-Os( $\eta^4$ -HBA-B)-(PPh<sub>3</sub>)<sub>2</sub>. This substitution chemistry is discussed below.

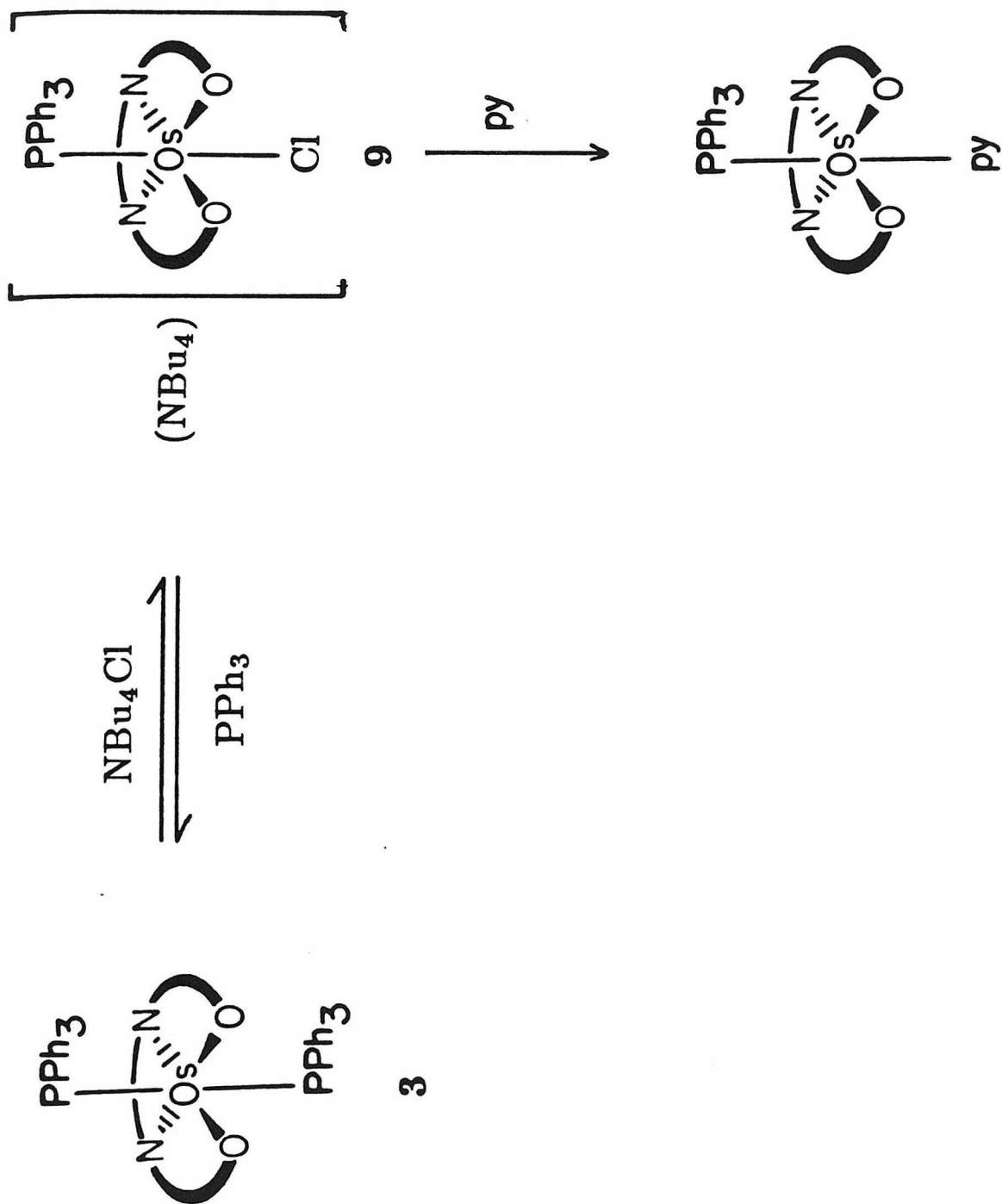
An interesting ligand substitution reaction is the substitution of a phosphine ligand with chloride. Reaction of *trans*-Os( $\eta^4$ -HBA-B)-(PPh<sub>3</sub>)<sub>2</sub> (3) with excess tetrabutylammonium chloride causes substitution of one phosphine ligand by chloride to give (NBu<sub>4</sub>)[*trans*-Os( $\eta^4$ -

$\text{HBA-B}(\text{PPh}_3)\text{Cl}]$  (**9**) in high yield, as shown in Scheme 2.6. Complex **9** is paramagnetic with a room temperature effective magnetic moment of 0.84 BM, and exhibits a well-resolved, paramagnetically-shifted  $^1\text{H}$  NMR spectrum. The  $^1\text{H}$  NMR data are given in Table 2.2. The spectrum indicates the presence of one HBA-B ligand, one triphenylphosphine ligand, and one tetrabutylammonium ion. There are six HBA-B ligand resonances, implying a trans geometry, and the resonances are very similar in chemical shift to the other *trans*-osmium(IV) complexes of HBA-B. The formulation of **9** as  $(\text{NBu}_4)[\text{trans-Os}(\eta^4\text{-HBA-B})(\text{PPh}_3)\text{Cl}]$  also agrees with the elemental analysis. The chloride ligand of **9** is replaced with triphenylphosphine or pyridine by reacting **9** with excess phosphine or pyridine.

The cyclic voltammogram of **9** consists of two irreversible one-electron reduction waves, one reversible one-electron oxidation wave, and one irreversible one-electron oxidation wave. (See Table 2.3.) The potential of the reversible one-electron oxidation of  $-0.04$  V vs.  $\text{Fc}^+/\text{Fc}$  is quite low. This reflects the fact that a phosphine ligand has been replaced by a chloride ligand to give an anionic complex. Attempts to chemically oxidize **9** to a neutral species do not give any characterizable product.<sup>20</sup>

$\text{trans-Os}(\eta^4\text{-HBA-B})(\text{PPh}_3)_2$  (**3**) also reacts with  $\pi$ -acid ligands to give some interesting osmium(IV) complexes. Bubbling carbon monoxide through a solution of **3** gives a violet complex, **10**, which can be isolated in moderate yield. The complex analyses as  $\text{Os}(\text{HBA-B})(\text{PPh}_3)(\text{CO})$ . It is diamagnetic and gives an NMR spectrum with normal chemical shifts. The  $^1\text{H}$  NMR spectrum of **10** shows three triphenylphosphine res-

**Scheme 2.6.** Reaction of *trans*-Os( $\eta^4$ -HBA-B)(PPh<sub>3</sub>)<sub>2</sub> (**3**) with chloride.



onances and twelve HBA-B ligand resonances. The IR spectrum shows a strong band at  $1985\text{ cm}^{-1}$  characteristic of a carbonyl ligand, and also two bands in the amide carbonyl region at  $1695$  and  $1640\text{ cm}^{-1}$  corresponding to the amides of the HBA-B ligand. These data indicate that the osmium is complexed to an HBA-B ligand, a triphenylphosphine ligand, and a carbon monoxide ligand. The twelve HBA-B ligand resonances in the  $^1\text{H}$  NMR spectrum, and the two amide stretches in the IR spectrum indicate there is no symmetry in the molecule, so the molecule must have a *cis- $\alpha$*  or *cis- $\beta$*  coordination geometry.

Structural quality single crystals of **10** were obtained and an X-ray diffraction study was carried out.<sup>21</sup> Complex **10**, *cis- $\alpha$* -Os( $\eta^4$ -HBA-B)(PPh<sub>3</sub>)(CO), forms monoclinic crystals in the space group *P2<sub>1</sub>/c*. The crystallographic details are listed in Table 2.5, and the full details of the data collection and refinement can be found in the experimental section of this chapter. Figure 2.6 shows an ORTEP view of **10**. A few bond distances and angles are shown on the ORTEP, and a full listing of bond distances and angles is given in Table 2.6. Figure 2.6 shows that the preliminary formulation of **10** is correct and that **10** is the neutral species *cis- $\alpha$* -Os( $\eta^4$ -HBA-B)(PPh<sub>3</sub>)(CO), with the osmium center coordinating the HBA-B ligand in the *cis- $\alpha$*  geometry with *cis* PPh<sub>3</sub> and CO ligands. Two important features of this molecule are apparent. First, a ligand isomerization has taken place; the ligand is now coordinated in the *cis- $\alpha$*  geometry, rather than the *trans* geometry. This is the first evidence that the HBA-B ligand would coordinate in such a geometry.<sup>22</sup> The second important result is that complex **10** is an osmium(IV)-carbonyl compound. Oxidation state IV car-

**Table 2.5.** Experimental data and cell parameters for the crystal structure determination of *cis*- $\alpha$ -Os( $\eta^4$ -HBA-B)(PPh<sub>3</sub>)(CO) (**10**).

Formula	OsC <sub>39</sub> H <sub>27</sub> N <sub>2</sub> O <sub>5</sub> P
Formula weight	824.83
Space group	P2 <sub>1</sub> /c
<i>a</i>	18.007(5) Å
<i>b</i>	10.848(9) Å
<i>c</i>	17.848(6) Å
$\alpha$	90°
$\beta$	106.85(3)°
$\gamma$	90°
<i>V</i>	3337(1) Å <sup>3</sup>
<i>Z</i>	4
$\lambda$	0.7107 Å
$\mu$	2.389 mm <sup>-1</sup>
<i>D</i> <sub>calc</sub>	1.642 g/ml
Scans	$\theta$ -2 $\theta$ ; 2.0° plus dispersion
Reflections	4 < 2 $\theta$ < 50°, +h, ±k, ± $\ell$
Background time/scan time	0.5
Collected	11518 reflections
Averaged	2146 reflections
Final no. of parameters	203
Final cycle:	
R	0.059(1868*)
R <sub>3<math>\sigma</math></sub>	0.044(1512)
S	2.62(2146)

\* The number of reflections contributing to sums in parentheses.

**Figure 2.6.** ORTEP view of *cis*- $\alpha$ -Os( $\eta^4$ -HBA-B)(PPh<sub>3</sub>)(CO) (10).

Bond distances shown are in angstroms.



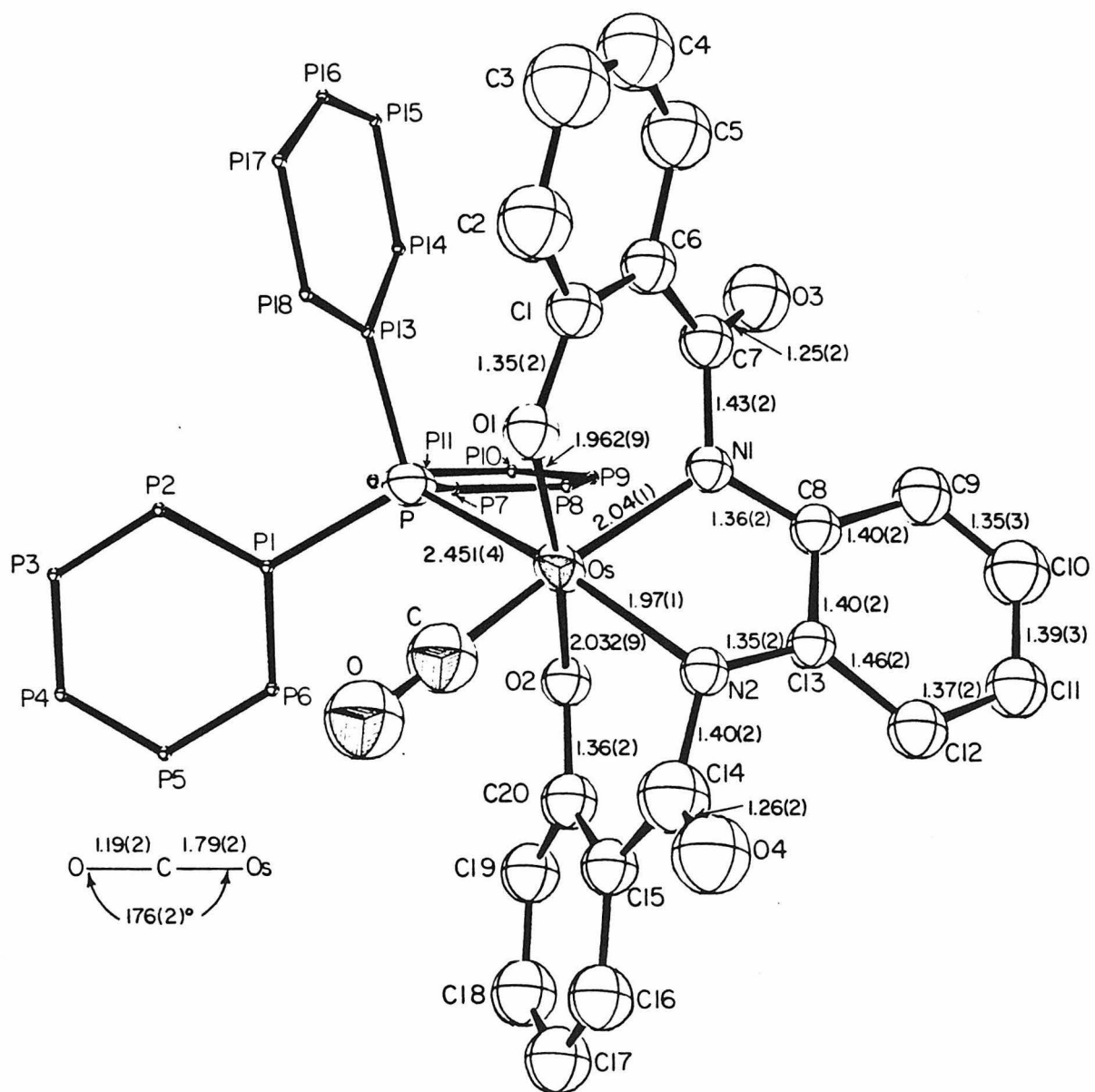


**Table 2.6.** Bond angles and distances in *cis*- $\alpha$ -Os( $\eta^4$ -HBA-B)-  
(PPh<sub>3</sub>)(CO) (**10**).

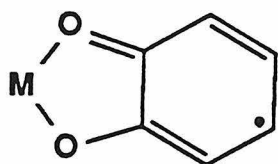
Atom	Atom	Dist(Å)	Atom	Atom	Dist(Å)	Atom	Atom	Dist(Å)
O <sub>s</sub>	C	1.79(2)	C1	C6	1.38(2)	P1	P2	1.36(2)
O <sub>s</sub>	P	2.451(4)	C2	C3	1.42(3)	P1	P6	1.39(2)
O <sub>s</sub>	O1	1.962(9)	C3	C4	1.35(3)	P2	P3	1.40(2)
O <sub>s</sub>	O2	2.032(9)	C4	C5	1.36(3)	P3	P4	1.36(3)
O <sub>s</sub>	N1	2.040(12)	C5	C6	1.44(3)	P4	P5	1.34(3)
O <sub>s</sub>	N2	1.973(12)	C6	C7	1.44(2)	P5	P6	1.41(3)
P	P1	1.85(2)	C8	C9	1.40(2)	P7	P8	1.39(2)
P	P7	1.79(2)	C8	C13	1.40(2)	P7	P12	1.38(3)
P	P13	1.81(2)	C9	C10	1.35(3)	P8	P9	1.39(2)
C	O	1.19(2)	C10	C11	1.39(3)	P9	P10	1.38(2)
O1	C1	1.35(2)	C11	C12	1.37(2)	P10	P11	1.36(3)
O2	C20	1.36(2)	C12	C13	1.46(2)	P11	P12	1.43(3)
O3	C7	1.25(2)	C14	C15	1.47(2)	P13	P14	1.40(3)
O4	C14	1.26(2)	C15	C16	1.40(2)	P13	P18	1.38(3)
N1	C7	1.43(2)	C15	C20	1.42(2)	P14	P15	1.48(3)
N1	C8	1.36(2)	C16	C17	1.37(2)	P15	P16	1.30(4)
N2	C13	1.35(2)	C17	C18	1.39(3)	P16	P17	1.30(3)
N2	C14	1.40(2)	C18	C19	1.37(2)	P17	P18	1.46(3)
C1	C2	1.42(2)	C19	C20	1.43(2)			

Atoms	Angle(°)	Atoms	Angle(°)	Atoms	Angle(°)	Atoms	Angle(°)
C-O <sub>s</sub> -P	90.9(6)	C8-N1-O <sub>s</sub>	117(1)	C11-C10-C9	122(2)	P3-P2-P1	120(2)
O1-O <sub>s</sub> -P	92.2(3)	C8-N1-C7	119(1)	C12-C11-C10	121(2)	P4-P3-P2	119(2)
O2-O <sub>s</sub> -P	78.0(3)	C13-N2-O <sub>s</sub>	116(1)	C13-C12-C11	117(2)	P5-P4-P3	123(2)
N1-O <sub>s</sub> -P	100.5(3)	C14-N2-O <sub>s</sub>	114(1)	C8-C13-N2	116(1)	P6-P5-P4	119(2)
N2-O <sub>s</sub> -P	157.9(4)	C14-N2-C13	121(1)	C12-C13-N2	123(1)	P5-P6-P1	119(2)
O1-O <sub>s</sub> -C	87.3(7)	C2-C1-O1	114(1)	C12-C13-C8	121(1)	P8-P7-P	122(1)
O2-O <sub>s</sub> -C	93.2(6)	C6-C1-O1	127(2)	N2-C14-O4	122(2)	P12-P7-P	119(1)
N1-O <sub>s</sub> -C	167.0(7)	C6-C1-C2	120(2)	C15-C14-O4	121(2)	P12-P7-P8	119(2)
N2-O <sub>s</sub> -C	95.8(7)	C3-C2-C1	120(2)	C15-C14-N2	118(2)	P9-P8-P7	121(2)
O2-O <sub>s</sub> -O1	170.2(7)	C4-C3-C2	119(2)	C16-C15-C14	120(2)	P10-P9-P8	120(2)
N1-O <sub>s</sub> -O1	86.0(4)	C5-C4-C3	124(2)	C20-C15-C14	119(1)	P11-P10-P9	121(2)
N2-O <sub>s</sub> -O1	109.0(4)	C6-C5-C4	119(2)	C20-C15-C16	122(2)	P12-P11-P10	120(2)
N1-O <sub>s</sub> -O2	95.2(4)	C5-C6-C1	119(2)	C17-C16-C15	121(2)	P11-P12-P7	120(2)
N2-O <sub>s</sub> -O2	80.7(4)	C7-C6-C1	126(2)	C18-C17-C16	118(2)	P14-P13-P	118(1)
N2-O <sub>s</sub> -N1	75.8(5)	C7-C6-C5	115(2)	C19-C18-C17	123(2)	P18-P13-P	122(1)
P7-P-P1	104.5(7)	N1-C7-O3	122(1)	C20-C19-C18	122(2)	P18-P13-P14	120(2)
P13-P-P1	104.6(7)	C6-C7-O3	123(2)	C15-C20-O2	127(1)	P15-P14-P13	122(2)
P13-P-P	107.1(8)	C6-C7-N1	115(1)	C19-C20-O2	118(1)	P16-P15-P14	109(2)
O-C-O <sub>s</sub>	175(2)	C9-C8-N1	131(2)	C19-C20-C15	115(1)	P17-P16-P15	136(2)
C1-O1-O <sub>s</sub>	126.6(9)	C13-C8-N1	111(1)	P2-P1-P	122(1)	P18-P17-P16	114(2)
C20-O2-O <sub>s</sub>	119(1)	C13-C8-C9	119(2)	P6-P1-P	118(1)	P17-P18-P13	119(2)
C7-N1-O <sub>s</sub>	123(1)	C10-C9-C8	120(2)	P6-P1-P2	120(1)		

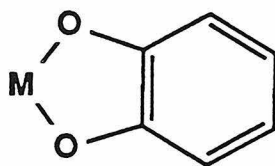
bonyl compounds are rare.<sup>2,3</sup> Carbon monoxide is a ligand that requires  $\pi$ -donation from the metal center for bonding, so it is usually found with low-valent metal centers. In compound 10 the carbonyl C-O distance of 1.19(2) Å, and the C-O stretching frequency of 1985 cm<sup>-1</sup> indicate that there is some  $\pi$ -donation from the metal to the CO  $\pi^*$ -orbital,<sup>2,4</sup> and that the metal center is not very electron deficient. The existence of an osmium(IV)-carbonyl complex is another demonstration of the powerful donating nature of the HBA-B ligand.

The question of phenylene bridge resonance is raised again here. Referring to 10 as an osmium(IV) carbonyl complex suggests there is no contribution from the diimine resonance form possible with the phenylene bridge of the HBA-B ligand. (Scheme 2.5.) Examination of certain bond lengths in the crystal structure of 10 should provide information about this resonance question. The bond lengths in the ligand bridge of complex 10, and other representative bond lengths are listed in Figure 2.7. If a diimine resonance form reducing the oxidation state of the metal by two units were dominant, we would expect C-N double bond distances on the order of 1.28–1.35 Å, and shortening of the C9-C10 and C11-C12 carbon-carbon bonds in the benzene ring. For a purely aromatic ring and carbon-nitrogen single bonds, we expect C-N bond distances of 1.45–1.51 Å and uniform C-C distances of ~1.40 Å around the benzene ring. The structure has C-N distances between the two extreme cases and a slight shortening of the C9-C10 and C11-C12 bonds. The relatively high sigma values on the bond distances and the lack of a large amount of structural data for similar complexes makes it difficult to draw conclusions from the available data. It does

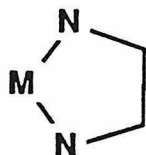
**Figure 2.7.** Representative bond distances for some metal-ligand fragments. Distances are in angstroms.



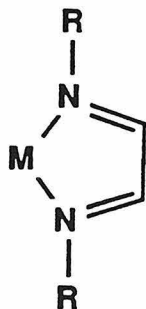
C=O 1.28-1.30<sup>25a</sup>  
 C-C 1.43-1.45<sup>25a</sup>



C-O 1.34-1.36<sup>25a,b</sup>  
 C-C 1.38-1.41<sup>25a,b</sup>



C-N 1.45-1.51<sup>25c,d</sup>



C=N 1.28-1.35<sup>25e,f</sup>

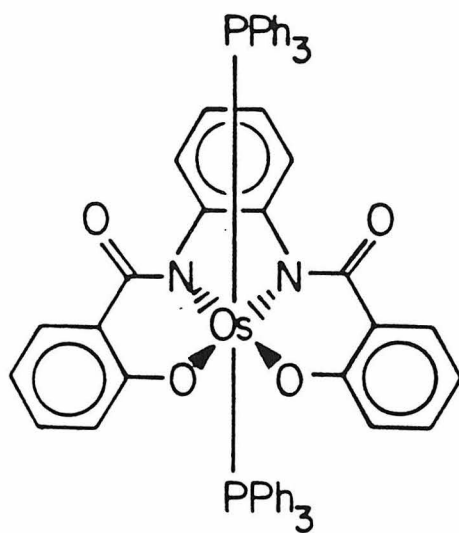
seem, however, that there is some contribution of the diimine resonance form to better donate electron density to the osmium center.

The carbonyl complex **10** is quite stable and demonstrates very little reactivity. The carbonyl ligand is not susceptible to nucleophilic attack; it does not react with a variety of nucleophiles.<sup>26</sup> The carbon monoxide ligand is also not at all labile; no reaction of **10** with two-electron donor ligands (py, PPh<sub>3</sub>) is observed thermally or photochemically. Oxidation of **10** by one-electron is possible. The cyclic voltammogram of **10** shows a reversible one-electron oxidation at +0.90 V vs. Fc<sup>+</sup>/Fc. The oxidized product is stable at room temperature on the CV time-scale but decomposes in minutes even at low temperature, so isolation of the product is not possible.

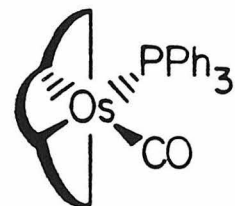
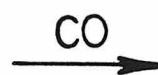
Isocyanide reacts with *trans*-Os(η<sup>4</sup>-HBA-B)(PPh<sub>3</sub>)<sub>2</sub> (**3**) in a manner similar to CO to give a *cis*-α complex. (Scheme 2.7.) Reaction of **3** with excess *t*-butylisocyanide gives *cis*-α-Os(η<sup>4</sup>-HBA-B)(PPh<sub>3</sub>)(*t*-BuNC) (**11**) in quantitative yield. The <sup>1</sup>H NMR spectrum of **11** (Table 2.2) shows twelve HBA-B ligand resonances indicating a *cis* coordination geometry. The IR spectrum of **11** has the C–N isocyanide stretch at 2135 cm<sup>-1</sup>, and two amide carbonyl stretches at 1680 and 1625 cm<sup>-1</sup>. These values for the amide bands suggest the *cis*-α formulation for **11**. (A *cis* conformation of the PAC ligand requires significant distortion of the coordinated amide groups, forming non-planar amides. The non-planar amides have higher C–O stretching frequencies than the planar amides. The IR spectrum of **11** indicates two non-planar amides, which requires the *cis*-α geometry. This isomerization phenomenon and the non-planar amide ligands are discussed in detail in Chapter 3.<sup>27</sup>) In



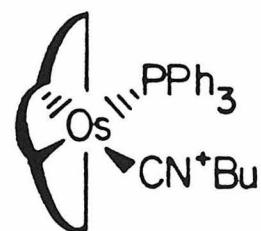
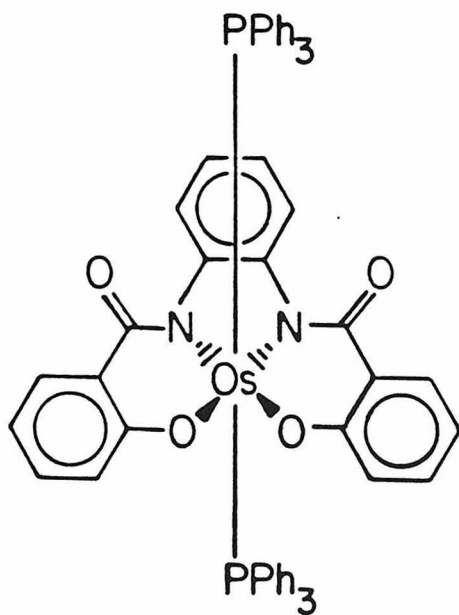
**Scheme 2.7.** Reactions of *trans*-Os( $\eta^4$ -HBA-B)(PPh<sub>3</sub>)<sub>2</sub> (3) with  $\pi$ -acid ligands.



3



10



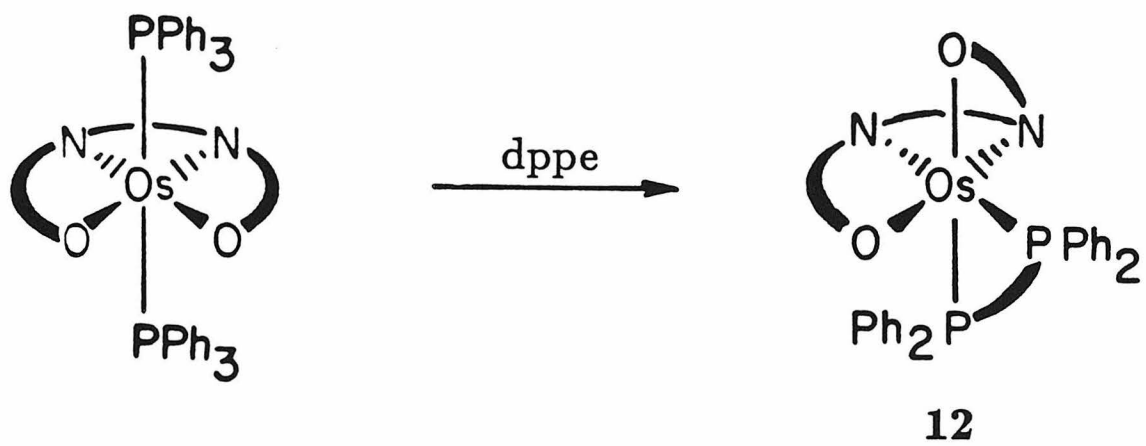
11

light of the formation of complexes with *cis- $\alpha$*  geometries, the reactivity of *trans*-Os( $\eta^4$ -HBA-B)(PPh<sub>3</sub>)<sub>2</sub> (3) with bidentate ligands was explored in an attempt to force the formation of *cis- $\alpha$*  and *cis- $\beta$*  complexes.

Reacting 1,2-bis(diphenylphosphino)ethane (dppe) with *trans*-Os( $\eta^4$ -HBA-B)(PPh<sub>3</sub>)<sub>2</sub> (3) results in substitution of the two triphenylphosphine ligands with one bidentate dppe ligand to give 12. The reaction is shown in Scheme 2.8. The elemental analysis and <sup>1</sup>H NMR spectrum of 12 are consistent with the formulation Os( $\eta^4$ -HBA-B)(dppe). The <sup>1</sup>H NMR spectrum (Table 2.2) has twelve HBA-B ligand resonances and the <sup>31</sup>P NMR spectrum has two resonances indicating that 12 has the *cis- $\beta$*  geometry as shown in Scheme 2.8.

The synthesis of *cis- $\beta$* -Os( $\eta^4$ -HBA-B)(dppe) (12) means that octahedral osmium complexes of HBA-B in all three geometries (*trans*, *cis- $\alpha$* , and *cis- $\beta$*  [Figure 2.1]) are accessible. The IR spectrum of 12 has two amide carbonyl bands at 1657 and 1600 cm<sup>-1</sup>. This IR spectrum is quite different from those of the *trans* complexes and those of the *cis- $\alpha$*  complexes. *Trans* complexes contain the HBA-B ligand in a planar geometry, and the result is one amide carbonyl stretching frequency at about 1600 cm<sup>-1</sup>. A *cis- $\beta$*  geometry requires the twisting of one arm of the HBA-B ligand into an axial position and leads to two amide carbonyl stretching frequencies. One amide stretching frequency goes up to 1657 cm<sup>-1</sup>, presumably due to the distortions of the amide group caused by twisting the phenol arm into an axial position. The other "half" of the ligand remains planar, so that amide carbonyl band remains at 1600 cm<sup>-1</sup>. The *cis- $\alpha$*  geometry requires twisting of both arms of the

**Scheme 2.8.** Reaction of *trans*-Os( $\eta^4$ -HBA-B)(PPh<sub>3</sub>)<sub>2</sub> (3) with dppe.



ligand out of the equatorial plane to occupy axial positions, so distortions are required of both amide groups. This leads to an IR spectrum showing shifting of both amide bands to higher frequencies. The infrared spectrum of a complex is then diagnostic of the geometry, and thus infrared spectroscopy is a very useful structural tool for these complexes; the IR spectrum of a new complex clearly indicates in which geometry (trans, cis- $\beta$ , or cis- $\alpha$ ) the PAC ligand coordinates.

The reaction of *trans*-Os( $\eta^4$ -HBA-B)(PPh<sub>3</sub>)<sub>2</sub> (3) with dppe to give 12 is not surprising, since as indicated above, the phosphine ligands of 3 are labile and can both be replaced by other phosphine ligands. We also know that reaction of 3 with excess pyridine leads only to mono-phosphine substitution. It will be interesting to see the results of the reaction of *trans*-Os( $\eta^4$ -HBA-B)(PPh<sub>3</sub>)<sub>2</sub> (3) with bipyridine. The reaction of 3 with either 2,2'-bipyridine (bipy), 4,4'-dimethylbipyridine (DMBP), or 1,10-phenanthroline (phen) cleanly gives a brown product. The brown product, 15, of the reaction of 3 with phen is paramagnetic with a room temperature effective magnetic moment of 1.4 BM and does not give an <sup>1</sup>H NMR spectrum at room temperature. The complex analyses as Os(HBA-B)(PPh<sub>3</sub>)(phen). The formulation of Os(HBA-B)(PPh<sub>3</sub>)(phen) means there are seven potentially coordinating atoms around the osmium center. Interest in the possibility of a seven-coordinate species<sup>28</sup> prompted an X-ray crystal structure determination. X-ray quality single crystals of 15 were isolated from a dichloromethane/ethanol solution. (Table 2.7 includes unit cell data and parameters of intensity data collection.<sup>29</sup>) Complex 15 crystallizes in the triclinic space group  $\bar{P}1$ . The complex is monomeric

**Table 2.7.** Experimental data and cell parameters for the crystal structure determination of  $\text{Os}(\eta^3\text{-}(\text{H})\text{HBA-B})(\text{PPh}_3)\text{-}(\text{phen})$  (15).

---

Formula	$\text{OsC}_{50}\text{H}_{35}\text{N}_4\text{O}_4\text{P}\cdot 2\text{C}_2\text{H}_5\text{OH}$
Formula Weight	1069.2
Unit Cell Constants	$a = 10.448(4) \text{ \AA}$ , $b = 14.454(6) \text{ \AA}$ , $c = 16.598(7) \text{ \AA}$ , $\alpha = 89.27(3)^\circ$ , $\beta = 99.74(3)^\circ$ , $\gamma = 111.44(3)^\circ$ $V = 2296(1) \text{ \AA}^3$
$D_c$ ( $Z = 2$ )	$1.546 \text{ g cm}^{-3}$
Space group	$P\bar{1}$
Crystal size	$0.26 \times 0.39 \times 0.45 \text{ mm}$
$\mu(\text{MoK}_\alpha)$	$30.4 \text{ cm}^{-1}$
Scan type and speed	$\theta - 2\theta$ , $4^\circ \text{ min}^{-1}$
Scan range	$1^\circ$ below $\text{K}_{\alpha_1}$ to $1^\circ$ above $\text{K}_{\alpha_2}$
Background counting	Stationary counts for one half of scan time at each end of scan
Collection range	$\pm h, \pm k, l$ ; $4^\circ < 2\theta < 50^\circ$ $\pm h, \pm k, -l$ ; $4^\circ < 2\theta < 40^\circ$
No. of reflections measured	13395
No. of unique data, $m$	8145
No. of data with $I > 0$	7897
No. of data with $I > 3\sigma(I)$	6986
No. of parameters refined, $p$	596
$R^a$ (for $I > 0$ )	0.054
$R$ (for $I > 3\sigma(I)$ )	0.047
Goodness of fit	2.90

---

(a)  $R = \Sigma||F_o| - |F_c||/\Sigma|F_o|$ . (b) Goodness of fit =  $[w(F_o^2 - F_c^2)^2 / (m - p)]^{1/2}$



**Figure 2.8.** ORTEP view of Os( $\eta^3$ -(H)HBA-B)(PPh<sub>3</sub>)(phen) (15).

Bond distances are in angstroms.

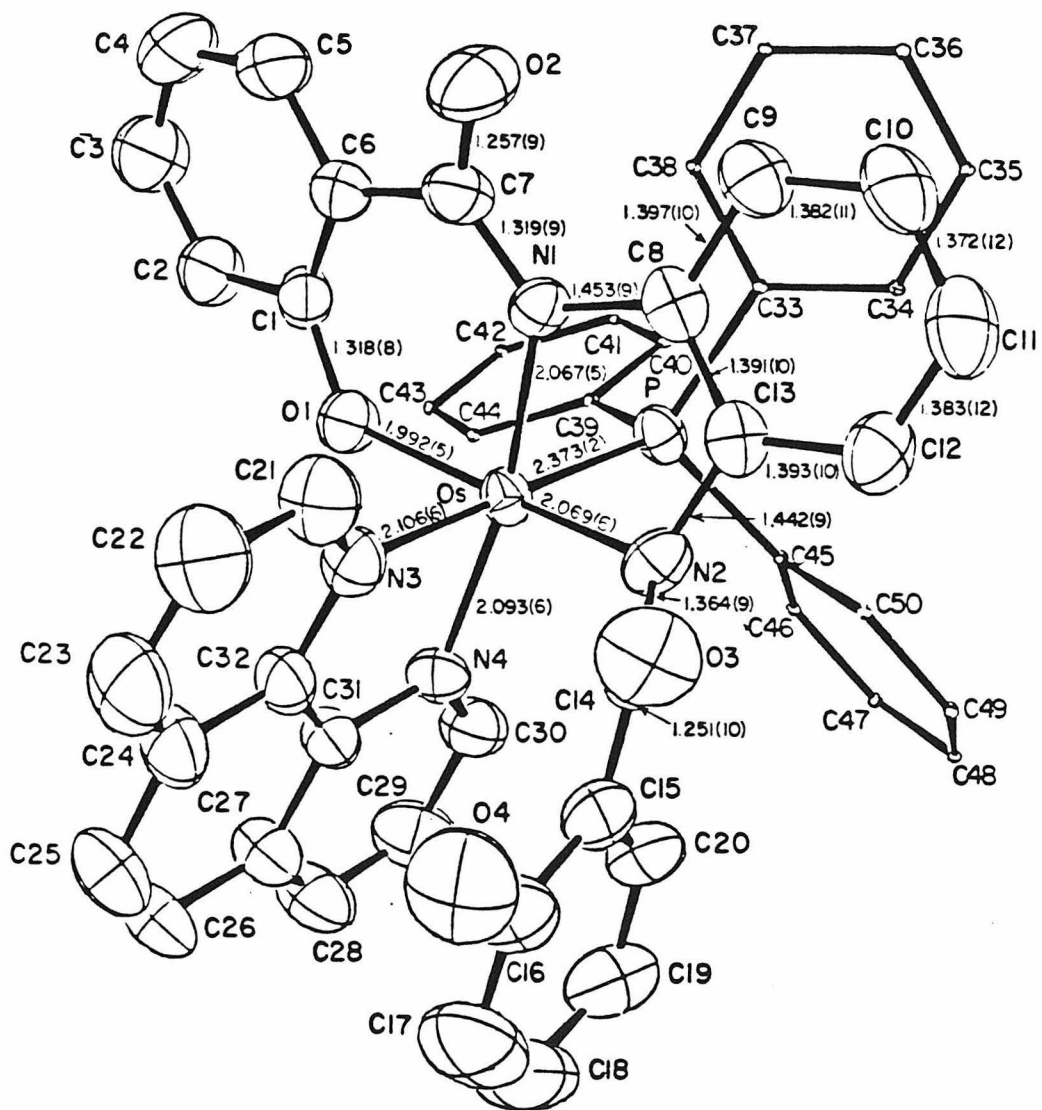


**Table 2.8.** Bond distances (Å) and angles (°) in Os( $\eta^3$ -H)HBA-B)(PPh<sub>3</sub>)(phen) (15).

Atom	Atom	Distance	Atom	Atom	Distance
Os	P	2.373(2)	Os	O1	1.922(5)
Os	N1	2.067(5)	Os	N2	2.069(6)
Os	N3	2.106(6)	Os	N4	2.093(6)
P	C33	1.838(7)	P	C39	1.836(7)
P	C45	1.832(7)	O1	C1	1.318(8)
O2	C7	1.257(9)	O3	C14	1.251(10)
O4	C16	1.352(11)	N1	C7	1.319(9)
N1	C8	1.453(9)	N2	C13	1.442(9)
N2	C14	1.364(9)	N4	C30	1.339(9)
N3	C32	1.364(9)	N3	C21	1.325(10)
N4	C31	1.374(9)	C1	C2	1.413(11)
C1	C6	1.410(10)	C2	C3	1.352(12)
C3	C4	1.401(14)	C4	C5	1.381(13)
C5	C6	1.386(11)	C6	C7	1.513(10)
C8	C9	1.397(10)	C8	C13	1.391(10)
C9	C10	1.382(11)	C10	C11	1.372(12)
C11	C12	1.383(12)	C12	C13	1.393(10)
C14	C15	1.477(11)	C15	C16	1.405(12)
C15	C20	1.381(13)	C16	C17	1.400(14)
C17	C18	1.35(2)	C18	C19	1.394(15)
C19	C20	1.381(13)	C21	C22	1.404(12)
C22	C23	1.354(13)	C23	C24	1.387(13)
C24	C25	1.431(13)	C24	C32	1.405(11)
C25	C26	1.344(14)	C26	C27	1.446(13)
C27	C28	1.388(13)	C27	C31	1.393(11)
C28	C29	1.362(13)	C29	C30	1.388(12)
C31	C32	1.419(10)	C33	C34	1.382(10)
C33	C38	1.393(10)	C34	C35	1.388(12)
C35	C36	1.354(13)	C36	C37	1.373(13)
C37	C38	1.386(12)	C39	C40	1.410(10)
C39	C44	1.378(10)	C40	C41	1.378(12)
C41	C42	1.390(12)	C42	C43	1.350(11)

Atom	Atom	Distance	Atom	Atom	distance
C43	C44	1.386(10)	C45	C46	1.390(10)
C45	C50	1.394(10)	C46	C47	1.365(13)
C47	C48	1.383(14)	C48	C49	1.377(13)
C49	C50	1.363(12)	C51	C52	1.43(3)
C52	O5	1.42(2)	O6	C54	1.31(3)
C53	C54	1.60(3)			

Atom	Atom	Atom	Angle	Atom	Atom	Atom	Angle
O1	Os	P	95.57(14)	N1	Os	P	89.3(2)
N2	Os	P	95.1(2)	N3	Os	P	178.4(2)
N4	Os	P	99.89(2)	N1	Os	O1	90.8(2)
N2	Os	O1	166.3(2)	N3	Os	O1	84.1(2)
N4	Os	O1	82.9(2)	N2	Os	N1	80.7(2)
N3	Os	N1	92.3(2)	N4	Os	N1	169.4(2)
N3	Os	N2	85.5(2)	N4	Os	N2	103.7(2)
N4	Os	N3	78.5(2)	C33	P	Os	116.5(2)
C39	P	Os	116.4(2)	C45	P	Os	113.3(2)
C39	P	C33	100.8(3)	C45	P	C33	103.4(3)
C45	P	C39	104.5(3)	C1	O1	Os	127.1(4)
C7	N1	Os	128.7(5)	C8	N1	Os	111.5(4)
C8	N1	C7	119.8(6)	C13	N2	Os	110.1(4)
C14	N2	Os	123.6(5)	C14	N2	C13	114.4(6)
C21	N3	Os	127.1(5)	C32	N3	Os	113.6(5)
C32	N3	C21	119.2(6)	C30	N4	Os	129.7(5)
C31	N4	Os	113.8(4)	C31	N4	C30	116.2(6)
C2	C1	O1	115.8(6)	C6	C1	O1	125.8(7)
C6	C1	C2	118.3(7)	C3	C2	C1	121.9(8)
C4	C3	C2	120.4(9)	C5	C4	C3	118.0(9)
C6	C5	C4	123.1(8)	C5	C6	C1	118.2(7)
C7	C6	C1	126.0(7)	C7	C6	C5	115.7(7)
N1	C7	O2	124.0(7)	C6	C7	O2	116.4(7)
C6	C7	N1	119.6(7)	C9	C8	N1	126.4(7)
C13	C8	N1	114.8(6)	C13	C8	C9	118.6(7)
C10	C9	C8	120.4(7)	C11	C10	C9	120.5(8)
C12	C11	C10	120.3(8)	C13	C12	C11	119.5(8)
C8	C13	N2	118.0(6)	C12	C13	N2	121.1(7)
C12	C13	C8	120.7(7)	N2	C14	O3	122.7(7)
C15	C14	O3	118.4(7)	C15	C14	N2	118.9(7)
C16	C15	C14	118.4(8)	C20	C15	C14	121.9(8)
C20	C15	C16	119.7(8)	C15	C16	O4	122.8(8)

Atom	Atom	Atom	Angle	Atom	Atom	Atom	Angle
C17	C16	O4	119.0(9)	C17	C16	C15	118.2(9)
C18	C17	C16	121.2(10)	C19	C18	C17	120.9(11)
C20	C19	C18	118.7(10)	C19	C20	C15	121.2(8)
C22	C21	N3	121.3(8)	C23	C22	C21	120.4(9)
C24	C23	C22	119.2(9)	C25	C24	C23	123.9(9)
C32	C24	C23	118.6(8)	C32	C24	C25	117.5(8)
C26	C25	C24	121.3(9)	C27	C26	C25	121.6(9)
C28	C27	C26	124.0(9)	C31	C27	C26	118.2(8)
C31	C27	C28	117.8(8)	C29	C28	C27	119.4(9)
C30	C29	C28	120.0(9)	C29	C30	N4	123.1(8)
C27	C31	N4	123.6(7)	C32	C31	N4	116.7(7)
C32	C31	C27	119.7(7)	C24	C32	N3	121.3(7)
C31	C32	N3	117.1(7)	C31	C32	C24	121.6(7)
C34	C33	P	123.2(6)	C38	C33	P	117.7(6)
C38	C33	C34	119.2(7)	C35	C34	C33	119.8(8)
C36	C35	C34	121.2(9)	C37	C36	C35	119.6(9)
C38	C37	C36	120.7(9)	C37	C38	C33	119.6(8)
C40	C39	P	118.9(6)	C44	C39	P	122.1(6)
C44	C39	C40	118.9(7)	C41	C40	C39	119.6(8)
C42	C41	C40	119.9(8)	C43	C42	C41	120.7(8)
C44	C43	C42	120.2(8)	C43	C44	C39	120.7(7)
C46	C45	P	123.3(6)	C50	C45	P	119.5(6)
C50	C45	C46	117.2(7)	C47	C46	C45	121.2(8)
C48	C47	C46	120.4(9)	C49	C48	C47	119.5(9)
C50	C49	C48	119.8(8)	C49	C50	C45	122.0(8)
O5	C52	C51	103.7(14)	C53	C54	O6	112(2)

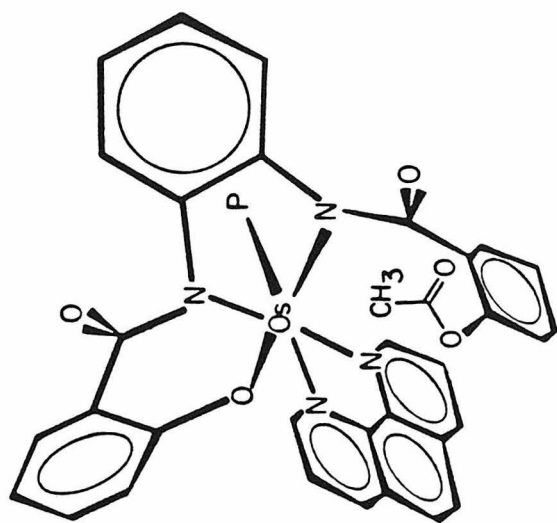
and is formulated as  $\text{Os}(\eta^3\text{-(H)HBA-B})(\text{PPh}_3)(\text{phen})$ . An ORTEP view of the molecule is shown in Figure 2.8. The most surprising feature of the structure of **15** is the coordination mode of the PAC ligand. The HBA-B ligand is three coordinate through one phenolate and two N-amido donors. The second phenol of the PAC ligand is not coordinated. (This is the first case we have observed of a three-coordinate PAC ligand of this type.<sup>30</sup>) The pseudo-octahedral coordination geometry about the osmium is completed with a bidentate phenanthroline ligand and a triphenylphosphine ligand. Table 2.8 gives a listing of important bond distances and angles in **15**. Loss of one triphenylphosphine ligand has accompanied coordination of the phenanthroline ligand, but rather than lose a second phosphine ligand, dissociation of one arm of the HBA-B ligand occurs. This is an interesting demonstration of the high affinity the osmium center has for the second phosphine ligand. No reaction of the osmium(HBA-B)-phosphine complexes has been observed to produce a complex without a phosphine ligand.

There are two possible formulations of **15**: (1) a neutral osmium(III) complex with the free phenol of the HBA-B ligand being protonated, and (2) an osmium(IV) zwitterion consisting of an osmium cation and phenolate anion. These two possibilities cannot be differentiated on the basis of the crystal structure data alone. No distinctive  $\nu(\text{OH})$  band can be located in the IR spectrum, but hydrogen bonding with the amide oxygen is expected, and the intramolecular O(3)–O(4) distance of 2.58(1) Å is consistent with such bonding.<sup>31</sup> The cyclic voltammogram of **15** (Table 2.3) shows a reversible one-electron reduction at  $-1.12$  V, a reversible one-electron oxidation at  $-0.31$  V, and a

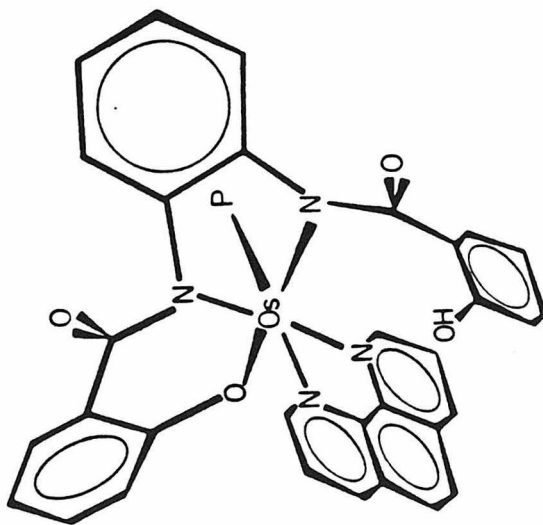


second reversible one-electron oxidation at +0.72 V vs.  $\text{Fc}^+/\text{Fc}$ . The potentials of the three reversible couples and the fact that there are two oxidations and one reduction imply that **15** is an osmium(III) complex. (Oxidation of an osmium(IV)-phenoxide zwitterion is expected to occur at a potential at least 1 V positive of that observed.) The osmium(III) formulation could also explain the absence of an NMR spectrum. Further support for this formulation is obtained by treating **15** with acetic anhydride to give the mono-acetylated product **16** as shown in Scheme 2.9. Acetylation has likely occurred at the phenol oxygen. The analysis shows that **16** is a neutral species, and has the formulation  $\text{Os}((\text{CH}_3\text{CO})\text{HBA-B})(\text{PPh}_3)(\text{phen})$  consistent with acetylation of a protonated phenol. (Acetylation of an osmium(IV) zwitterion would give a cationic species.) The cyclic voltammogram of **16** is almost identical to that of **15**, as would be expected. The formal potentials for the reversible couples of **16** are -1.11 V, -0.28 V, and +0.68 V (irreversible) vs.  $\text{Fc}^+/\text{Fc}$ . The IR spectrum of **16** is also quite similar to that of **15**, except for the new ester band at  $1767\text{ cm}^{-1}$ .

**Scheme 2.9.** Acetylation of  $\text{Os}(\eta^3\text{-H})\text{HBA-B}(\text{PPh}_3)(\text{phen})$  (**15**).



16



15

## Conclusions

The synthesis of osmium(HBA-B) compounds presented in this chapter demonstrates the wealth of ligand substitution chemistry and synthetic versatility available to these complexes. *trans*-Os( $\eta^4$ -HBA-B)-(PPh<sub>3</sub>)<sub>2</sub> has proven to be a valuable starting material to make a variety of osmium(IV) complexes, due to the lability of the phosphine ligands. Phosphine substitution will occur with neutral two-electron donor ligands (phosphines, pyridines, imidazoles), with anionic two-electron donors (chloride), and with neutral  $\pi$ -acid ligands (carbon monoxide, isocyanides). Because of the rich substitution chemistry with a variety of ligands, we were able to make a group of very different osmium complexes of HBA-B, which allowed us to study the properties of the PAC ligand in a variety of environments.

A very important property of the PAC ligands is their donating ability. The properties and reactivity of the Os(HBA-B) complexes give valuable information concerning the donating ability of the PAC ligands. The electrochemical properties of the complexes, specifically the low formal potentials of the redox couples, indicate that the PAC ligands are indeed very good electron donors. Further testimony to the powerful donating nature of the HBA-B ligand comes from the synthetic chemistry. Not only were osmium(IV) complexes of carbon monoxide and *t*-butylisocyanide synthesized and found to be quite stable, but the C $\equiv$ O and C $\equiv$ N stretching frequencies imply a degree of  $\pi$ -back-bonding that is surprising for such high oxidation state complex-

es. This is only possible because the HBA-B ligand is such a good donor to the osmium center. Perhaps this donation, and the softness of the metal center also account for the high affinity we have observed of the osmium for a soft phosphine ligand.

Included in the discussion of the donating ability of PAC ligands is the question of non-innocence of aromatic rings of the PAC ligands. We see that if the osmium center is made too electron-deficient, the PAC ligand can compensate through resonance, shifting electron density to the osmium from a benzene ring. This has important implications for the future of PAC ligand design. If the goal is to make high oxidation state complexes, PAC ligands with an aliphatic framework must be used to avoid the problems of oxidation state formalism. If the goal is to make highly oxidizing complexes this type of resonance should also be limited, so that a mechanism to lower the oxidizing power of the metal does not exist.

Another important discovery concerns the coordination geometries of the HBA-B ligand. This area was initiated by the discovery of the *cis- $\alpha$*  complexes formed with  $\pi$ -acid ligands, and led to the intentional synthesis of *cis* complexes using bidentate ligands. In thinking about inorganic PAC ligand complexes it is important to know that all coordination geometries of the PAC ligands are possible; the HBA-B ligand need not always be planar. In the case of *cis- $\beta$* -Os( $\eta^4$ -HBA-B)(dppe) the HBA-B ligand is forced to assume a non-planar geometry. In the case of *cis- $\alpha$* -Os( $\eta^4$ -HBA-B)(PPh<sub>3</sub>)(CO) and *cis- $\alpha$* -Os( $\eta^4$ -HBA-B)(PPh<sub>3</sub>)(*t*-BuNC) the HBA-B ligand is not forced to adopt a *cis* conformation by coordination of a bidentate ligand. There must be a reason for these

complexes to adopt the cis- $\alpha$  geometry. We will see in Chapter 3 that a significant change in the donating ability of the PAC ligand accompanies the change in coordination geometry and drives the formation of cis- $\alpha$  complexes.

## Experimental

**Materials.** Acetone (Mallinckrodt), benzene (thiophene free, Aldrich), di-*n*-butyl ether (EM Science), diethyl ether (Baker), ethanol (U.S. Industrial), hexanes (Aldrich), and methanol (Baker) were reagent grade and were used as received, unless otherwise noted. Dichloromethane (Baker) and tetrahydrofuran (Baker) were distilled from calcium hydride prior to use. Acetic anhydride (Mallinckrodt), 2-acetylsalicylic acid (Aldrich), *t*-butylisocyanide (Alfa), 4-*t*-butylpyridine (Aldrich), carbon monoxide (Matheson), 4-(*N,N*-dimethylamino)pyridine (Aldrich), 4,4'-dimethylbipyridine (Fluka), 2,2'-dipyridyl (99%, Aldrich), ethylene-bis-(diphenylphosphine) (97%, Aldrich), hydrochloric acid (conc., Mallinckrodt), imidazole (MCB), methyl iodide (Aldrich), osmium tetroxide (99.8%, Alfa), 1,10-phenanthroline (Aldrich), 4-picoline (MCB), potassium hydroxide (Baker), pyridine (Baker), sodium hydroxide (Baker), tetra-*n*-butylammonium chloride (Kodak), tri-*n*-butylphosphine (Aldrich), triethylamine (reagent, MCB), trifluoroacetic acid (98.5%, MCB), and triphenylphosphine (99%, Aldrich) were all used as received. Oxalyl chloride (Aldrich) was freshly distilled under nitrogen prior to use. The *o*-phenylenediamine (Aldrich) was recrystallized from toluene (Baker). Silica gel used in column chromatography was 60-200 mesh (Davison).

**Physical Measurements.**  $^1\text{H}$  NMR spectra were recorded at 90 MHz on a Varian EM-390 spectrometer, at 89.83 MHz on a JEOL FX90-Q spectrome-

ter, at 399.7822 MHz on a JEOL GX-400 spectrometer, or at 500.135 MHz on a Bruker WM-500 spectrometer.<sup>32</sup>  $^1\text{H}$  chemical shifts are reported in ppm( $\delta$ ) vs.  $\text{Me}_4\text{Si}$  with the solvent ( $\text{CDCl}_3$ ,  $\delta$  7.24; acetone- $\text{d}_6$ ,  $\delta$  2.04) as internal standard.  $^{31}\text{P}$  NMR spectra were recorded at 36.28 MHz on a JEOL FX90-Q spectrometer.  $^{31}\text{P}$  chemical shifts are reported in ppm( $\delta$ ) vs. an 85% phosphoric acid external standard. Infrared spectra were recorded on a Beckman IR 4240 spectrometer. Magnetic moments were obtained on a Cahn Faraday magnetic susceptibility balance equipped with a permanent magnet. The magnetic balance was calibrated using  $\text{HgCo}(\text{SCN})_4$ . Elemental analyses were obtained at the Caltech analytical facility. Solvents of crystallization were quantified by  $^1\text{H}$  NMR spectroscopy of the authentic samples submitted for elemental analyses.

**Electrochemical Procedures.** Dichloromethane (Mallinckrodt) used in cyclic voltammetric experiments was reagent grade and was further purified by distillation from calcium hydride. TBAP supporting electrolyte (Southwestern Analytical Chemicals) was dried, recrystallized twice from acetone/diethyl ether, and then dried under vacuum. The TBAP concentration in all solutions was 0.1 M. BPG electrodes (Union Carbide Co., Chicago) used for cyclic voltammetry were cut and mounted as previously described.<sup>33</sup> The reference electrode was a saturated KCl silver/silver chloride electrode ( $\text{Ag}/\text{AgCl}$ ). In all cases ferrocene was added at the conclusion of the experiment as an internal potential standard.<sup>16</sup> All potentials are quoted with respect to the formal potential of the ferrocinium/ferrocene couple which, under



these conditions, we have consistently measured as +0.48 V vs. SCE, or ca. +0.70 V vs. NHE.

Cyclic voltammetry and controlled potential electrolyses were performed with a Princeton Applied Research Model 173/179 potentiostat/digital coulometer equipped with positive feedback IR-compensation and a Model 175 universal programmer. Current-voltage curves were recorded on a Houston Instruments Model 2000 X-Y recorder.

**X-ray Data Collection and Structure Determination of 10.** A crystal approximately  $0.1 \times 0.1 \times 0.3$  mm of *cis*- $\alpha$ -Os( $\eta^4$ -HBA-B)(PPh<sub>3</sub>)(CO) was obtained from an dichloromethane/ethanol solution. Oscillation and Weissenberg photographs indicated a monoclinic space group, and the systematic absences ( $h0l$ ,  $l = 2n+1$ ;  $0k0$ ,  $k = 2n+1$ ) verified the space group  $P2_1/c$  ( $C_{2h}^5$ , No. 14). The intensity data were collected on an Enraf-Nonius CAD4 diffractometer with graphite monochromator and Mo K $\alpha$  radiation ( $\lambda = 0.7107$  Å). The unit cell parameters were obtained by least-squares refinement of the orientation matrix based on twenty-five reflections in the range:  $15.0^\circ < 2\theta < 24.1^\circ$ . The intensity measurements were recorded for all reflections in one hemisphere ( $4.0^\circ < 2\theta < 50^\circ$ ) using  $\theta-2\theta$  scans at a variable scan speed. The three check reflections indicated no decomposition, and the data were reduced to  $F_o^2$ 's; the variances of the intensities were obtained from counting statistics plus an additional term  $(0.02 \times \text{scan counts})^2$ . The form factors were taken from *The International Table for X-ray Crystallography, Vol. IV, Table 2.2B*.<sup>3 4</sup> Those of osmium and phosphorus were corrected for anomalous dispersion. Details of the data

collection are summarized in Table 2.5.

The atomic position of the Os atom was derived from the Patterson map. Subsequent Fourier and difference maps revealed all non-hydrogen atoms of the ligands. After several cycles of least-squares refinement, hydrogen atoms were placed at a distance of 0.95 Å from their respective carbon atoms by assuming ideal geometry, with fixed  $U = 0.065 \text{ \AA}^2$ . Several cycles of full-matrix least-squares refinement minimizing  $\sum w [F_o^2 - (F_c/k)^2]^2$  on all non-hydrogen atoms with anisotropic thermal parameters for Os and P, and isotropic thermal parameters for all other atoms, yielded  $R_F = 0.059$ ,  $R_{3\sigma} = 0.044$ , and GOF = 2.62; data-to-parameter ratio = 10.6.

**X-ray Data Collection and Structure Determination of 15.** A crystal of  $\text{Os}(\eta^3\text{-(H)HBA-B})(\text{PPh}_3)(\text{phen})$  was obtained from a dichloromethane/ethanol solution. Intensity data were collected on a Nicolet P2<sub>1</sub> diffractometer using the  $\theta$ - $2\theta$  scanning technique. Three check reflections monitored every 100 data measurements showed a decrease in intensity of about 2% during the 250 hours of X-ray exposure. The intensities were corrected for a linear decay and reduced to  $|F_o|$ 's. Multiple observations were averaged to yield 8145 independent reflections. No absorption correction was applied.

The positions of the osmium and phosphorous atoms were obtained from a three-dimensional Patterson function and the rest of the non-hydrogen atoms were recovered from subsequent Fourier and difference Fourier syntheses. The  $R$  factor was 0.25.

Refinement was carried out by full-matrix least-squares methods. The quantity minimized was  $\sum w (F_o^2 - F_c^2)^2$ , with weight  $w = 1/\sigma^2(F_o^2)$ .

Atomic scattering factors with the real part of anomalous dispersion applied to these for osmium and phosphorous were obtained from the International Tables.<sup>3 4</sup> Calculations were carried out on a VAX 11750 computer using the CRYM system.

After several cycles of least-squares adjustment of the coordinates for all non-hydrogen atoms, anisotropic thermal parameters for osmium and phosphorous, and isotropic thermal parameters for the rest, the *R* factor was reduced to 0.066. At this stage all hydrogen atoms, except those attached to oxygen atoms, were inserted in their calculated positions with assigned isotropic thermal parameters the same as their parent carbon atoms. During the last four cycles a list of 596 parameters was adjusted: atomic coordinates and anisotropic thermal parameters of all the non-hydrogen atoms, a scale factor and a secondary extinction coefficient. Atomic coordinates of all except the solvent atoms were kept in one matrix, the scale factor, the secondary extinction coefficient, and the anisotropic thermal parameters of all except the carbon atoms in the triphenylphosphine group of the osmium complex in a second matrix, and the rest of the parameters in a third matrix. Parameters of the hydrogen atoms were not refined.

The final *R* index for 7897 reflections was 0.054 and the final value of the secondary extinction parameter was  $(0.26 \pm 0.03) \times 10^{-7}$ .

A list of experimental parameters is given in Table 2.7.

**Syntheses.** All reactions were carried out in air unless otherwise noted.  $K_2[Os(OH)_4(O)_2]$  was prepared as described in the literature.<sup>3 5</sup>

**H<sub>4</sub>HBA-B (1).** 2-Acetylsalicylic acid (50.0 g; 0.27 mol) was heated at 30°C in oxalyl chloride under a nitrogen atmosphere (4 h). Excess oxalyl chloride was removed under reduced pressure. The residue was dissolved in dichloromethane (30 mL) and the dichloromethane was removed under vacuum. This washing process was repeated three times. The residue was then dissolved in dichloromethane (100 mL) and chilled to 0°C. This solution was added dropwise to a stirred, chilled solution of *o*-phenylenediamine (15.0 g; 0.138 mol) in dichloromethane (100 mL) that was cooled continuously in an ice-bath. The mixture was stirred (1 h), excess (>2 equivalent) triethylamine was added, and the mixture was again stirred (0.5 h). The mixture was treated with 6 M NaOH solution (100 mL) and the organic volatiles were removed on a rotary evaporator. The remaining aqueous solution was decanted from the undissolved organic residue. The residue was dissolved in a small amount of acetone and then treated with an additional portion of 6 M NaOH solution (100 mL). The aqueous solutions were combined and slowly acidified with concentrated HCl. The precipitate was collected, washed with water, and recrystallized from acetone/water. Yield: 78.3 g (81%). Anal. Calcd for C<sub>20</sub>H<sub>16</sub>N<sub>2</sub>O<sub>4</sub>: C, 68.96; H, 4.63; N, 8.04. Found: C, 69.04; H, 4.75; N, 8.14. IR (Nujol): 1640 cm<sup>-1</sup> (s),  $\nu$ (amide); 1610 cm<sup>-1</sup> (s),  $\nu$ (amide); 1590 cm<sup>-1</sup> (s),  $\nu$ (amide). <sup>1</sup>H NMR: See Table 2.2.

**K<sub>2</sub>[*trans*-Os( $\eta^4$ -HBA-B)(O)<sub>2</sub>] $\cdot$ H<sub>2</sub>O (2).** A solution of K<sub>2</sub>[Os(OH)<sub>4</sub>(O)<sub>2</sub>] (2.01 g; 5.46 mmol) in methanol (500 mL) was added to a solution of H<sub>4</sub>HBA-B (1.90 g; 5.46 mmol) in THF (200 mL) that was continuously stirred. The solution was heated on a hotplate (ca.

40°C; 0.5 h). After cooling, the clear brown solution was evaporated to dryness on a rotary evaporator. The residue was dissolved in ethanol, di-*n*-butyl ether was added and the ethanol was removed on a rotary evaporator to give brown crystals. The product was filtered and washed with diethyl ether. Yield: 3.60 g (100%). Anal. Calcd for  $C_{20}H_{12}N_2K_2O_4Os \cdot H_2O$ : C, 36.25; H, 2.13; N, 4.23. Found: C, 36.35; H, 2.40; N, 4.07. IR (Nujol): 1600  $cm^{-1}$  (vs),  $\nu$ (amide); 822  $cm^{-1}$  (s),  $\nu_{as}(Os(O)_2)$ .  $^1H$  NMR: See Table 2.2.

*trans*-Os( $\eta^4$ -HBA-B)(PPh<sub>3</sub>)<sub>2</sub> (3).  $K_2[trans-Os(\eta^4-HBA-B)(O)_2] \cdot H_2O$  (1.02 g; 1.58 mmol) and triphenylphosphine (2.0 g; 6.32 mmol) were dissolved in a mixture of ethanol (25 mL) and THF (45 mL). Excess CF<sub>3</sub>CO<sub>2</sub>H (0.5 mL) was added and the solution was stirred at room temperature (10 min), after which the solution turned from brown to dark green. Ethanol (20 mL) was added and the THF was removed on a rotary evaporator to give dark green crystals. The product was filtered and washed with ethanol and hexanes. The solid was recrystallized from dichloromethane/ethanol containing PPh<sub>3</sub> (250 mg). The final product was filtered and washed with ethanol and hexanes. Yield: 1.23 g (73%). Anal. Calcd for  $C_{56}H_{42}N_2O_4OsP_2 \cdot 0.5(H_2O) \cdot 0.5(CH_3CH_2OH)$ : C, 62.74; H, 4.26; N, 2.57. Found: C, 62.67; H, 4.44; N, 2.45. IR (Nujol): 1600  $cm^{-1}$  (s),  $\nu$ (amide).  $^1H$  NMR: See Table 2.2.

*trans*-Os( $\eta^4$ -HBA-B)(PBu<sub>3</sub>)<sub>2</sub> (4). Benzene (100 mL) was degassed by bubbling nitrogen through it (20 min). *trans*-Os( $\eta^4$ -HBA-B)(PPh<sub>3</sub>)<sub>2</sub> (200 mg; 0.19 mmol) was dissolved, and PBu<sub>3</sub> (1.0 mL; 4.0 mmol) was added via gastight syringe. The solution was stirred under N<sub>2</sub> at room temperature (6 h). The solvent was removed on a rotary evaporator and

the residue was dissolved in a minimum of dichloromethane. The solution was purified by chromatography on a silica gel column eluting with dichloromethane. The red-brown band was collected and the product crystallized from a small amount of pentane. Yield: 100 mg (56%). Anal. Calcd for  $C_{44}H_{66}N_2O_4OsP$ : C, 56.27; H, 7.08; N, 2.98. Found: C, 56.39, H, 6.89; N, 3.06. IR (Nujol):  $1604\text{ cm}^{-1}$  (s),  $\nu$ (amide).  $^1\text{H NMR}$ : See Table 2.2.

*trans*-Os( $\eta^4$ -HBA-B)(PPh<sub>3</sub>)(py) (5). *trans*-Os( $\eta^4$ -HBA-B)(PPh<sub>3</sub>)<sub>2</sub> (98 mg;  $9.25 \times 10^{-5}$  mol) was dissolved in dichloromethane (15 mL). Excess pyridine (0.25 mL) was added and the solution was stirred at room temperature (5 min). The solution was stripped to dryness on a rotary evaporator and the residue was dissolved in a minimum of dichloromethane. The product was purified by chromatography on a short silica gel column, eluting first with dichloromethane to remove excess PPh<sub>3</sub>, and then with 4/1 dichloromethane/acetone to remove the purple product. The compound was crystallized from dichloromethane/hexanes. Yield: 77 mg (92%). Anal. Calcd for  $C_{43}H_{32}N_3O_4OsP \cdot 0.33(C_6H_{14})$ : C, 59.74; H, 4.09; N, 4.65. Found: C, 59.71; H, 4.12; N, 4.62. IR (Nujol):  $1604\text{ cm}^{-1}$  (s),  $\nu$ (amide).  $^1\text{H NMR}$ : See Table 2.2.

*trans*-Os( $\eta^4$ -HBA-B)(PPh<sub>3</sub>)(*t*-Bupy) (6). *trans*-Os( $\eta^4$ -HBA-B)(PPh<sub>3</sub>)<sub>2</sub> (121 mg; 0.11 mmol) was dissolved in dichloromethane (15 mL). Excess 4-*t*-butylpyridine (0.25 mL) was added and the solution was stirred at room temperature (5 min). The solution was stripped to dryness on a rotary evaporator and the residue was dissolved in a minimum of dichloromethane. The purple solution was purified by column chromatography on silica gel, eluting first with dichloromethane to remove ex-

cess  $\text{PPh}_3$ , and then with 4/1 dichloromethane/acetone to remove the product. The product was crystallized from dichloromethane/hexanes. Yield: 83 mg (78%). Anal. Calcd for  $\text{C}_{52}\text{H}_{40}\text{N}_3\text{O}_4\text{OsP} \cdot 0.33(\text{C}_6\text{H}_{14})$ : C, 61.25; H, 4.69; N, 4.38. Found: C, 61.28; H, 4.66; N, 4.37. IR (Nujol):  $1603\text{ cm}^{-1}$  (s),  $\nu(\text{amide})$ .  $^1\text{H NMR}$ : See Table 2.2.

*trans*-Os( $\eta^4$ -HBA-B)( $\text{PPh}_3$ )(4-pic) (7). *trans*-Os( $\eta^4$ -HBA-B)( $\text{PPh}_3$ )<sub>2</sub> (300 mg; 0.28 mmol) and 4-picoline (0.3 mL) were dissolved in dichloromethane (25 mL). The solution was stirred at room temperature (5 min). The resulting purple solution was stripped to dryness on a rotary evaporator. The residue was dissolved in a minimum of dichloromethane and purified by chromatography on a silica gel column. Elution was done first with dichloromethane to remove excess  $\text{PPh}_3$ , and then with 4/1 dichloromethane/acetone to remove the purple product. Crystallization was from dichloromethane/hexanes. Yield: 200 mg (79%). Anal. Calcd for  $\text{C}_{44}\text{H}_{34}\text{N}_3\text{O}_4\text{OsP} \cdot 0.33(\text{CH}_2\text{Cl}_2) \cdot 0.33(\text{H}_2\text{O})$ : C, 58.00; H, 3.81; N, 4.58. Found: C, 57.89; H, 3.92; N, 4.54. IR (Nujol):  $1604\text{ cm}^{-1}$  (s),  $\nu(\text{amide})$ .  $^1\text{H NMR}$ : See Table 2.2.

*trans*-Os( $\eta^4$ -HBA-B)( $\text{PPh}_3$ )(ImH) (8). *trans*-Os( $\eta^4$ -HBA-B)( $\text{PPh}_3$ )<sub>2</sub> (400 mg; 0.38 mmol) was dissolved in dichloromethane (25 mL) and imidazole (80 mg; 1.2 mmol) was added. The mixture was stirred at room temperature (5 min). The solvent was removed on a rotary evaporator and the residue was dissolved in a small amount of dichloromethane. The solution was run down a silica gel column eluting the excess  $\text{PPh}_3$  with dichloromethane, and eluting the product as a purple band with 4/1 dichloromethane/acetone. The product was crystallized from dichloromethane/hexanes. Yield: 289 mg (88%). Anal. Calcd for

$C_{41}H_{31}N_4O_4OsP \cdot 0.13(CH_2Cl_2) \cdot 0.13(C_2H_5OH)$ : C, 56.47; H, 3.65; N, 6.35. Found: C, 56.50; H, 3.64; N, 6.31. IR (Nujol):  $1596\text{ cm}^{-1}$  (s),  $\nu$ (amide).  $^1H$  NMR: See Table 2.2.

$(NBu_4)[trans-Os(\eta^4-HBA-B)(PPh_3)(Cl)]$  (9).  $trans-Os(\eta^4-HBA-B)(PPh_3)_2$  (200 mg; 0.19 mmol) and  $NBu_4Cl$  were dissolved in dichloromethane (40 mL). The solution was stirred at room temperature (45 min), and the solvent was removed on a rotary evaporator. The residue was dissolved completely in a small amount of ethanol (5 mL). After a minute or two crystals of the product came out of solution. The mixture was allowed to stand (1 h) to allow full crystallization. The purple crystals were filtered and washed with a small amount of ethanol, and diethyl ether. Yield: 162 mg (80%). Anal. Calcd for  $C_{54}H_{63}N_3ClO_4OsP \cdot 0.25(CH_2Cl_2)$ : C, 59.45; H, 5.84; N, 3.83. Found: C, 59.27; H, 5.78; N, 3.86. IR (Nujol):  $1600\text{ cm}^{-1}$  (s),  $\nu$ (amide).  $^1H$  NMR: See Table 2.2.

$cis-\alpha-Os(\eta^4-HBA-B)(PPh_3)(CO)$  (10). Benzene (100 mL) was deoxygenated by bubbling a nitrogen stream through it (20 min).  $trans-Os(\eta^4-HBA-B)(PPh_3)_2$  (500 mg; 0.47 mmol) was dissolved in the benzene and carbon monoxide was bubbled through the solution at room temperature (1.5 h). Methyl iodide (1 mL) was added and CO bubbling was continued (0.5 h). Another portion of MeI (1 mL) was added and CO bubbling continued (0.5 h). The resulting violet solution was passed down a silica gel column by elution with a large quantity of benzene until the eluent was colorless. The benzene was removed on a rotary evaporator and the residue was crystallized from dichloromethane/ethanol to yield violet crystals. Yield: 125 mg (32%). Anal. Calcd for



$C_{39}H_{27}N_2O_5OsP$ : C, 56.79; H, 3.30; N, 3.40. Found: C, 56.59; H, 3.44; N, 3.38. IR ( $CH_2Cl_2$ ):  $1985\text{ cm}^{-1}$  (vs),  $\nu(C\equiv O)$ ;  $1695\text{ cm}^{-1}$  (s),  $\nu(\text{amide})$ ;  $1640\text{ cm}^{-1}$  (s),  $\nu(\text{amide})$ .  $^1H$  NMR: See Table 2.2.

*cis- $\alpha$ -Os( $\eta^4$ -HBA-B)(PPh<sub>3</sub>)(*t*-BuNC)* (11). Benzene (100 mL) was deoxygenated with a nitrogen stream (20 min). *trans*-Os( $\eta^4$ -HBA-B)(PPh<sub>3</sub>)<sub>2</sub> (500 mg; 0.47 mmol) was dissolved, and excess *t*-butylisocyanide (0.10 mL; 0.89 mmol) was added. The solution was stirred under a nitrogen atmosphere (30 min) at room temperature and then reduced to a small volume on a rotary evaporator. The solution was placed on a short silica gel column and eluted with dichloromethane. The violet solution was collected, the solvents were removed on a rotary evaporator, and the product was crystallized from dichloromethane/hexanes. The violet microcrystalline solid was filtered and washed with ice-cold hexanes. Yield: 402 mg (97%). Anal. Calcd for  $C_{43}H_{36}N_3O_4OsP \cdot 0.75$  ( $CH_2Cl_2$ ): C, 55.69; H, 4.01; N, 4.45. Found: C, 55.60; H, 4.17; N, 4.43. IR (Nujol):  $2135\text{ cm}^{-1}$  (vs),  $\nu(C\equiv N)$ ;  $1680\text{ cm}^{-1}$  (s),  $\nu(\text{amide})$ ;  $1625\text{ cm}^{-1}$  (s),  $\nu(\text{amide})$ .  $^1H$  NMR: See Table 2.2.

*cis- $\beta$ -Os( $\eta^4$ -HBA-B)(dppe)* (12). *trans*-Os( $\eta^4$ -HBA-B)(PPh<sub>3</sub>)<sub>2</sub> (500 mg; 0.47 mmol) and diphenylphosphinoethane (200 mg; 2.36 mmol) were dissolved in dichloromethane (100 mL) and the solution was stirred overnight at room temperature. Ethanol was added and the dichloromethane was removed on a rotary evaporator to produce a green solid. The solid was filtered and washed with a small portion of ice-cold ethanol, and hexanes. Yield: 359 mg (82%). Anal. Calcd for  $C_{46}H_{36}N_2O_4OsP_2$ : C, 59.22; H, 3.89; N, 3.00. Found: C, 59.22; H, 3.89; N, 3.04. IR (Nujol):  $1657\text{ cm}^{-1}$  (s),  $\nu(\text{amide})$ ;  $1600\text{ cm}^{-1}$  (s),  $\nu(\text{amide})$ .

$^1\text{H}$  NMR: See Table 2.2.  $^{31}\text{P}$  NMR ( $\text{CDCl}_3$ ):  $\delta$  -64.08 (s, 1P); -86.55 (s, 1P).

**Os( $\eta^3$ -(H)HBA-B)(PPh<sub>3</sub>)(bipy) (13).** *trans*-Os( $\eta^4$ -HBA-B)(PPh<sub>3</sub>)<sub>2</sub> (500 mg; 0.47 mmol) and 2,2'-bipyridine (125 mg; 0.80 mmol) were dissolved in dichloromethane (100 mL) and the solution was stirred at room temperature (18 h). Ethanol was added and the dichloromethane was removed on a rotary evaporator to effect crystallization. The brown crystals were filtered washing with ethanol and hexanes. Yield: 381 mg (85%). Anal. Calcd for C<sub>48</sub>H<sub>36</sub>N<sub>4</sub>O<sub>4</sub>OsP•(H<sub>2</sub>O): C, 59.31; H, 3.94; N, 5.76. Found: C, 59.40; H, 4.10; N, 5.78. IR (Nujol): 1620 cm<sup>-1</sup> (s),  $\nu$ (amide); 1600 cm<sup>-1</sup> (s),  $\nu$ (amide).

**Os( $\eta^3$ -HBA-B)(PPh<sub>3</sub>)(DMBP) (14).** *trans*-Os( $\eta^4$ -HBA-B)(PPh<sub>3</sub>)<sub>2</sub> (200 mg; 0.19 mmol) and 4,4'-dimethylbipyridine (50 mg; 0.27 mmol) were dissolved in dichloromethane (50 mL) and the solution was stirred at room temperature (7.5 h). Ethanol was added and the dichloromethane was removed on a rotary evaporator to give brown crystals. The product was filtered and washed with ethanol and diethyl ether. Yield: 160 mg (86%). Anal. Calcd for C<sub>50</sub>H<sub>40</sub>N<sub>4</sub>O<sub>4</sub>OsP: C, 61.15; H, 4.11; N, 5.70. Found: C, 60.56; H, 4.12; N, 5.65. IR (Nujol): 1620 cm<sup>-1</sup> (s),  $\nu$ (amide); 1600 cm<sup>-1</sup> (s),  $\nu$ (amide).

**Os( $\eta^3$ -HBA-B)(PPh<sub>3</sub>)(phen) (15).** *trans*-Os( $\eta^4$ -HBA-B)(PPh<sub>3</sub>)<sub>2</sub> (1.00 g; 0.94 mmol) and 1,10-phenanthroline (200 mg; 1.11 mmol) were dissolved in dichloromethane (100 mL) and the solution was stirred at room temperature (30 min). Ethanol was added and the product was crystallized by removal of dichloromethane on a rotary evaporator. The brown crystals were filtered and washed with ethanol and diethyl

ether. Yield: 846 mg (92%). Anal. Calcd for  $C_{50}H_{36}N_4O_4OsP$ : C, 61.40; H, 3.71; N, 5.73. Found: C, 60.95; H, 3.86; N, 5.56. IR (Nujol):  $1610\text{ cm}^{-1}$  (s),  $\nu$ (amide);  $1595\text{ cm}^{-1}$  (s),  $\nu$ (amide).

**Os( $\eta^3$ -(CH<sub>3</sub>CO)HBA-B)(PPh<sub>3</sub>)(phen) (16).** Os( $\eta^3$ -(H)HBA-B)(PPh<sub>3</sub>)-(phen) (50 mg;  $1.1 \times 10^{-6}$  mol) was dissolved in dichloromethane (10 mL). 4-(N,N-dimethylamino)pyridine (5 mg;  $4.1 \times 10^{-5}$  mol), triethylamine (1 mL), and acetic anhydride (1–2 mL) were added. The solution was stirred at room temperature (20 min). The solution was stripped to dryness on a rotary evaporator and the residue was dissolved in a small amount of dichloromethane. The mixture was columned on silica gel eluting first with dichloromethane and then with 3/2 dichloromethane/acetone to remove the brown product. The product was crystallized from dichloromethane/hexanes. Yield: 35 mg (67%). Anal. Calcd for  $C_{52}H_{38}N_4O_5OsP \cdot (C_6H_6)$ : C, 63.43; H, 4.04; N, 5.10. Found: C, 63.49; H, 4.11; N, 5.09. IR (Nujol):  $1767\text{ cm}^{-1}$  (m),  $\nu$ (C=O, ester);  $1600\text{ cm}^{-1}$  (s),  $\nu$ (amide).

References

1. (a) Anson, F.C.; Christie, J.A.; Collins, T.J.; Coots, R.J.; Furutani, T.T.; Gipson, S.L.; Keech, J.T.; Krafft, T.E.; Santarsiero, B.D.; Spies, G.H. *J. Am. Chem. Soc.* **1984**, *106*, 4460-72. (b) Keech, J.T. Ph.D. Dissertation, California Institute of Technology, Pasadena, California, 1987.
2. (a) Collins, T.J.; Richmond, T.G.; Santarsiero, B.D.; Treco, B.G.R.T. *J. Am. Chem. Soc.* **1986**, *108*, 2088-90. (b) Treco, B.G.R.T., unpublished results.
3. Christie, J.A.; Collins, T.J.; Krafft, T.E.; Santarsiero, B.D.; Spies, G.H. *J. Chem. Soc., Chem. Commun.* **1984**, 198-9.
4. This generalized synthesis was developed by George Spies. Spies, G.H. Ph.D. Dissertation, California Institute of Technology, Pasadena, California, 1985.
5. (a) Schröder, M. *Chem. Rev.* **1980**, *80*, 187-213. (b) Griffith, W.P.; Rossetti, R. *J. Chem. Soc., Dalton Trans.* **1972**, 1449-53. (c) Griffith, W.P. *J. Chem. Soc. (A)* **1969**, 211-18.
6. (a) Sargeson, A.M.; Searle, G.H. *Nature* **1963**, *200*, 356-7. (b) Sargeson, A.M.; *Inorg. Chem.* **1965**, *4*, 45-52.
7. Treco, B.G.R.T., unpublished results.
8. We have verified that triphenylphosphine oxide is a product of the reduction reaction.
9. "Forcing conditions" means heated at reflux in neat *t*-butylpyridine (b.p. = 196-197°C) for an extended period.
10. This kinetic study was carried out by Sonny Lee. Lee, S.C., un-

published results.

11. (a) Huheey, J.E. "Inorganic Chemistry", 2nd ed.; Harper and Row, New York, 1978; p. 491. (b) Cotton, F.A.; Wilkinson, G. "Advanced Inorganic Chemistry", 4th ed.; John Wiley & Sons, New York, 1980; p. 1200.
12. Figgis, B.N.; Lewis, J. *Prog. Inorg. Chem.* 1964, 6, 37-239.
13. (a) Given, K.W.; Wheeler, S.H.; Jick, B.S.; Maheu, L.J.; Pignolet, L.H. *Inorg. Chem.* 1979, 18, 1261-6. (b) Gunz, H.P.; Leigh, G.L. *J. Chem. Soc. (A)* 1971, 2229-33. (c) Randall, E.W.; Shaw, D. *J. Chem. Soc. (A)* 1969, 2867-72.
14. The 2D-( $^1\text{H}$ - $^1\text{H}$ ) COSY spectrum and the difference NOE spectra were obtained with the help of Doug Meinhart.
15. (a) Mersh, J.D.; Sanders, J.K.M. *Org. Mag. Res.* 1982, 18, 122-4. (b) Sanders, J.K.M.; Mersh, J.D. *Prog. NMR Spect.* 1982, 15, 353-400.
16. When reporting electrochemical potentials measured in non-aqueous solvents it is useful to use the  $\text{Fc}^+/\text{Fc}$  couple as an internal potential standard. Gagné, R.R.; Koval, C.A.; Lisensky, G.C. *Inorg. Chem.* 1980, 19, 2854-5.
17. Keech, J.T. Ph.D. Dissertation, California Institute of Technology, Pasadena, California, 1987.
18. Treco, B.G.R.T. unpublished results.
19. Armstrong, J.E.; Robinson, W.R.; Walton, R.A. *Inorg. Chem.* 1983, 22, 1301-6.
20. Reagents used for the oxidations were: ferricinium hexafluorophosphate, ceric ammonium nitrate, hydrogen peroxide (30%),

nitrosonium hexafluorophosphate, and silver perchlorate. In all cases the reactions resulted in complex mixtures of species.

21. The structural study of 10 was carried out in collaboration with Dr. Robert Coots.
22. At the present time many complexes of several PAC ligands having cis geometries have been prepared. Keech, J.T.; Lee, S.C.; Barner, C.J. unpublished results. Also see reference 1 of this chapter.
23. Several osmium(IV) carbonyl complexes with highly donating ligands have been reported. (a) Nowell, I.W.; Tabatabaian, K.; White, C.J. *J. Chem. Soc., Chem. Commun.* 1979, 547-8. (b) Hoyano, J.K.; Graham, W.A.G. *J. Am. Chem. Soc.* 1982, 104, 3722-3. (c) Millar, M.M.; O'Sullivan, T.; deVries, N.; Koch, S.A. *J. Am. Chem. Soc.* 1985, 107, 3714-15.
24. Collman, J.P.; Hegedus, L.S. "Principles and Applications of Organotransition Metal Chemistry"; University Science Books, Mill Vallely, California, 1980; pp. 85-86.
25. (a) Buchanan, R.M.; Pierpont, C.G. *J. Am. Chem. Soc.* 1980, 102, 4951-7, and references therein. (b) Lynch, M.W.; Hendrickson, d.N.; Fitzgerald, B.J.; Pierpont, C.G. *J. Am. Chem. Soc.* 1984, 106, 2041-9. (c) Smolenaers, P.J.; Beattie, J.K.; Hutchinson, N.D. *Inorg. Chem.* 1981, 20, 2202-6. (d) Malin, J.M.; Schlemper, D.O.; Murmann, R.K. *Inorg. Chem.* 1977, 16, 615-19. (e) Chaudret, B.; Köster, H.; Poilblanc, R. *J. Chem. Soc., Chem. Commun.* 1981, 266-8. (f) Staal, L.H.; Polm, L.H.; Balk, R.W.; van Koten, G.; Vrieze, K.; Brouwers, A.M.F. *Inorg.*

- Chem.* 1980, 19, 3343–51.
26. Nucleophiles tried include  $\text{OH}^-$ ,  $\text{NaBH}_4$ ,  $(\text{NBu}_4)\text{OH}$ , and  $\text{LiMe}$ . There was no reaction observed with  $\text{OH}^-$  and  $\text{NaBH}_4$ , while  $(\text{NBu}_4)\text{OH}$  and  $\text{LiMe}$  reduced the osmium complexes without attack on the carbonyl. Also, prolonged reaction of 10 with  $\text{H}_2^{18}\text{O}$  gave no exchange into the carbonyl ligand.
  27. See also: Collins, T.J.; Coots, R.J.; Furutani, T.T.; Keech, J.T.; Peake, G.T.; Santarsiero, B.D. *J. Am. Chem. Soc.* 1986, 108, 5333–9.
  28. Besides the general interest in seven-coordinate species, such a species would be interesting in considering possible coordination of an organic substrate to a similar osmium complex, and subsequent oxidation of the substrate.
  29. The crystal structure study of 15 was done entirely by Dr. Ting Lai of the University of Hong Kong.
  30. At the present time, compounds 13, 14, 15 and 16 are the only cases of complexes containing PAC ligands with  $\eta^3$ -coordination.
  31. Pimentel, G.C.; McClellan, A.L. "The Hydrogen Bond"; W.H. Freeman and Co., San Francisco, 1960, p. 260.
  32. All 500 MHz NMR spectra were taken at the Southern California Regional NMR Facility.
  33. Oyama, N.; Anson, F.C. *J. Am. Chem. Soc.* 1979, 101, 3450–6.
  34. Ibers, J.A.; Hamilton, W.C., eds. "International Tables for X-ray Crystallography"; The Kynoch Press, Birmingham, England, 1974.
  35. Malin, J.M. *Inorg. Syn.* 1980, 20, 61–3.

### Chapter 3

#### Nonplanar amide ligands



## Introduction

The results in Chapter 2 demonstrated the synthetic value of *trans*-Os( $\eta^4$ -HBA-B)(PPh<sub>3</sub>)<sub>2</sub> (3). The lability of the phosphines allowed the synthesis of many osmium(IV) species with varied auxiliary ligands. Reaction of 3 with carbon monoxide resulted in a *cis*- $\alpha$  complex, coordinating the tetradentate ligand in a nonplanar geometry. Following this discovery, other PAC ligand complexes with *cis* geometries were synthesized. For instance, reaction of 3 with 1,2-bis-(diphenylphosphino)ethane (dppe) gave *cis*- $\beta$ -Os( $\eta^4$ -HBA-B)(dppe) (12). John Keech<sup>1</sup> found in his work with the PAC ligand CHBA-DCB that *cis*- $\beta$ -Os( $\eta^4$ -CHBA-DCB)(bipy)<sup>2</sup> and *cis*- $\alpha$ -Os( $\eta^4$ -CHBA-DCB)(PPh<sub>3</sub>)(*t*-BuNC)<sup>3</sup> (H<sub>4</sub>CHBA-DCB  $\equiv$  1,2-bis(3,5-dichloro-2-hydroxybenzamido)-4,5-dichlorobenzene) could be made.

When the tetradentate HBA-B ligand changes from planar coordination in a *trans* complex to nonplanar coordination in a *cis* complex, what are the accompanying structural changes in the HBA-B ligand? Examination of crystal structures of *cis*- $\alpha$  complexes shows that twisting the planar ligand in a *trans* complex to be nonplanar in a *cis*- $\alpha$  complex results in substantial rotation about the amide C-N bonds, forming nonplanar amide ligands.

Nonplanar amides in organic molecules are rare, and the PAC ligand complexes discussed here contain the first examples of nonplanar N-amido ligands. A review of the crystallographic database for all secondary amide ligands demonstrates that the degree of non-pla-

narity of the amide ligands in the osmium PAC ligand complexes is indeed unusual.

Rotation about amide C–N bonds disrupts amide resonance delocalization and consequently rotation is subject to substantial activation barriers (10–35 kcal·mol<sup>-1</sup>).<sup>4</sup> Formation of nonplanar amide ligands must be accompanied by an energy gain that makes the process favorable. We have discovered three causes for the formation of nonplanar amide ligands: (1) structural constraints of the coordination sphere force the formation of nonplanar amides, (2) formation of nonplanar amides is thermodynamically favored because of increased metal-ligand bonding of the nonplanar compared to the planar N–amido ligand, and (3) non-planarity is caused by steric constraints. All three types of nonplanar N–amido ligands are demonstrated by osmium complexes of HBA-B.

## Results and Discussion

Our interest in osmium-PAC ligand complexes with *cis- $\alpha$*  and *cis- $\beta$* <sup>5</sup> geometries began with the discovery of the *cis* complexes. As discussed in Chapter 2, reaction of *trans*-Os( $\eta^4$ -HBA-B)(PPh<sub>3</sub>)<sub>2</sub> (3) with carbon monoxide leads to a tetradentate ligand isomerization and the product *cis- $\alpha$* -Os( $\eta^4$ -HBA-B)(PPh<sub>3</sub>)(CO) (10). The geometry of 10 is determined from the crystal structure, which is also reported in Chapter 2. For the isomerization of the HBA-B ligand from its coordination geometry in a *trans* complex to its coordination geometry in a *cis* complex to occur, what structural changes of the HBA-B ligand are necessary? That is, what are the degrees of freedom in the PAC ligand that allow it to twist from a planar arrangement and adopt a *cis* geometry? A close examination of the crystal structure of the *cis- $\alpha$*  complex, *cis- $\alpha$* -Os( $\eta^4$ -HBA-B)(PPh<sub>3</sub>)(CO) (10), answers this question.

Figure 3.1 shows an ORTEP view of 10. (An alternate view is shown in Figure 2.6.) In this particular view, the viewing axis is along one of the coordinated amide carbon-nitrogen bonds. The C14–O4 vector lies at an angle of 76° from the amide nitrogen plane defined by N2, Os, C13, and C14. The phenol arm of the HBA-B ligand (O2, C15, C16, C17, C18, C19, C20) and the amide carbonyl group (C14, O4) are still planar, and the phenylene bridge with the amide nitrogen atoms (C8, C9, C10, C11, C12, C13, N1, N2) is also planar. (The other amide group shows a similar distortion.) In forming a *cis- $\beta$*  complex from a *trans* complex, one arm of the PAC ligand moves from an equatorial co-

**Figure 3.1.** ORTEP view of *cis*- $\alpha$ -Os( $\eta^4$ -HBA-B)(PPh<sub>3</sub>)(CO) (10) showing nonplanar amide groups.



ordination site to an axial site. A cis- $\alpha$  complex is formed by twisting both arms of the PAC ligand out of the equatorial plane to occupy axial positions. (See Figure 2.1.) The major deformation in the HBA-B ligand resulting from the twisting of an arm to an axial position is rotation about the amide C-N bond. The rotation about these bonds results in nonplanar amide ligands. A cis- $\beta$  PAC ligand complex contains one nonplanar amide ligand and a cis- $\alpha$  complex contains two nonplanar amide ligands.

In organic chemistry, nonplanar amides are quite rare. The reason for this is the amide resonance delocalization shown in Scheme 3.1. This resonance requires a planar amide group, demonstrated by high barriers to rotation ( $10\text{--}35 \text{ kcal}\cdot\text{mol}^{-1}$ )<sup>4</sup> about the amide C-N bonds. Nonplanar amides have been recognized in several instances. These include formamide,<sup>6</sup> some constrained molecules such as certain lactams<sup>7</sup> (including penicillin and cephalosporin antibiotics<sup>8</sup>), polycyclic spirodilactams,<sup>9</sup> and anti-Bredt bridgehead nitrogen compounds.<sup>10</sup> (Figure 3.2.)

Dunitz and Winkler have carried out a detailed structural analysis of nonplanar organic amides. They define three parameters  $\tau$ ,  $\chi_N$ , and  $\chi_C$ , to describe nonplanar amides.<sup>11</sup> The most obvious deformation of a planar amide to a nonplanar amide is twisting about the amide C-N bond. Dunitz and Winkler have found that accompanying this twisting is a degree of pyramidalization at both the amide nitrogen and carbon atoms.  $\tau$  approximates the angle between the unperturbed nitrogen and carbonyl-carbon p- $\pi$ -orbitals and measures the twisting about the C-N bond.  $\chi_N$  and  $\chi_C$  are measures of the out-of-plane bending around the

**Scheme 3.1.** Organic amide resonance.

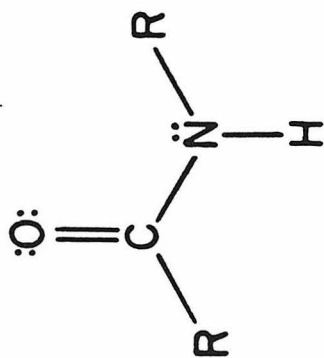
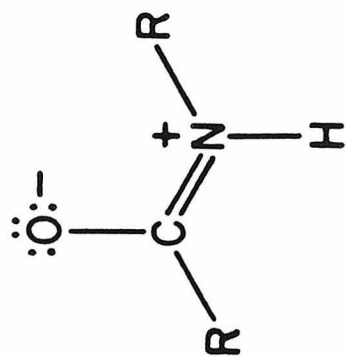
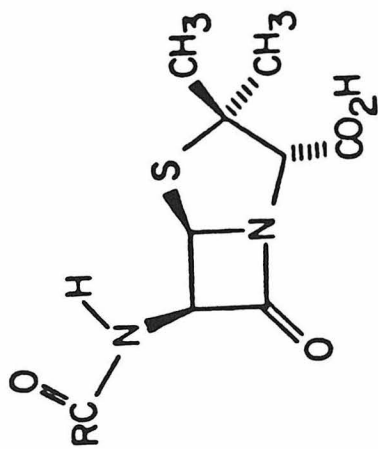
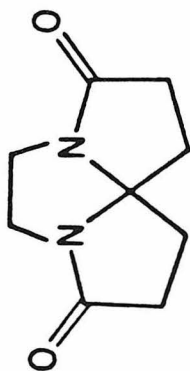




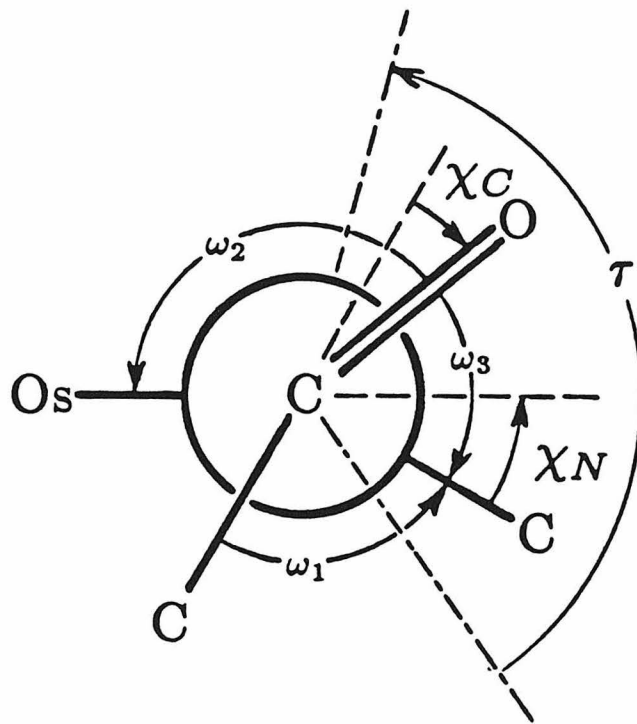
**Figure 3.2.** Organic molecules containing nonplanar amide groups: penicillin, a spirodilactam, and an anti-Bredt bridgehead nitrogen molecule.



nitrogen and carbon atoms, respectively.<sup>1,2</sup> Figure 3.3 shows how these three parameters are derived from three amide torsion angles,  $\omega_1$ ,  $\omega_2$ , and  $\omega_3$ , calculated from the structural data. (The figure shows a projection down the amide C–N bond, with the nitrogen directly behind the carbon. The nitrogen is shown bound to osmium. In an organic amide the Os is replaced by H.) For a rigorously planar amide, both the nitrogen and carbonyl carbon atoms are  $sp^2$  hybridized and  $\chi_N$  and  $\chi_C$  are both equal to  $0^\circ$ . However, the value of  $\tau$  can be either  $0^\circ$  or  $180^\circ$  depending upon whether the parent organic chain of the amide has a cisoid or transoid geometry. The limiting values of these parameters for a totally nonplanar amide and  $sp^3$  hybridization at nitrogen and carbon are  $\tau = \pm 90^\circ$ ,  $\chi_N, \chi_C = \pm 60^\circ$ . We have defined a modified version of  $\tau$ ,  $\bar{\tau}$ , such that  $\bar{\tau} = (\tau) \bmod \pi$ . In contrast to  $\tau$ , this term does not distinguish cisoid and transoid geometries. However,  $\bar{\tau}$  provides an approximate measure of the smaller angle between the unperturbed nitrogen and carbonyl carbon  $\pi$  orbitals, and is easily visualized ( $-90^\circ \leq \bar{\tau} \leq 90^\circ$ ).

These amide angular parameters have been calculated for the two amides in *cis*- $\alpha$ -Os( $\eta^4$ -HBA-B)(PPh<sub>3</sub>)(CO) (10). The  $\bar{\tau}$  values of  $46^\circ$  and  $73^\circ$  indicate that both amide groups are decidedly nonplanar. Since nonplanar organic amides are so rare, we wondered if these nonplanar amide ligands were unusual in inorganic chemistry. As measured by the angular parameters  $\bar{\tau}$ ,  $\chi_N$ , and  $\chi_C$ , all amide ligands will exhibit some degree of nonplanarity. In order to evaluate the degree of nonplanarity of the amide ligands in 10 an extensive study was carried out. A search of the Cambridge crystallographic database was undertaken for

**Figure 3.3.** Projection down the amide C–N bond of a coordinated amide showing the derivation of the angular parameters.



$$\tau = ((\omega_1 + \omega_2)/2) \bmod 2\pi$$

$$\chi_N = (\omega_2 - \omega_3 + \pi) \bmod 2\pi$$

$$\chi_C = (\omega_1 - \omega_3 + \pi) \bmod 2\pi$$

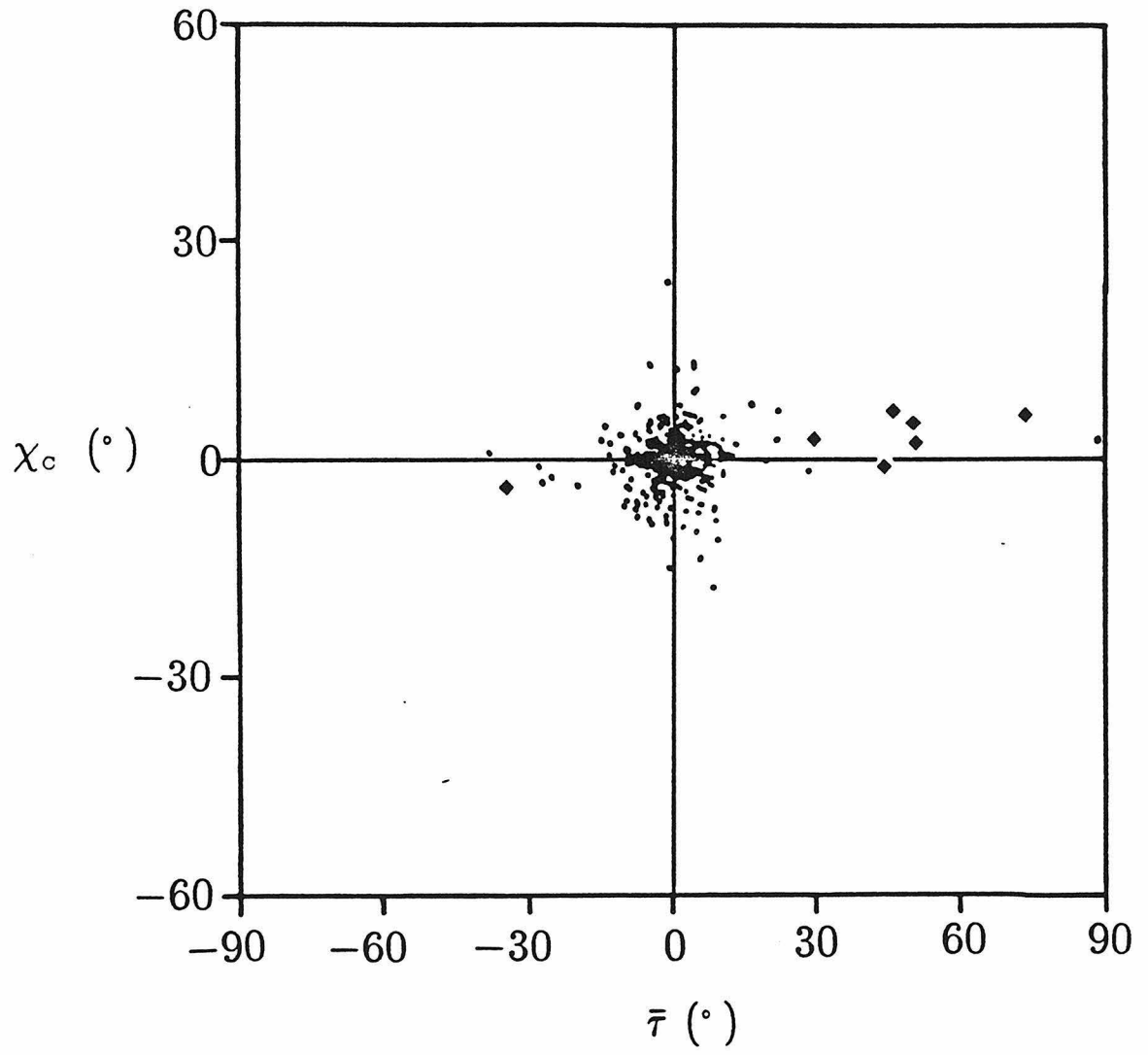
all structurally characterized N-coordinated secondary amide ( $\text{RC(O)NR}'\text{M}$  and  $\text{RC(OM}')\text{NR}'\text{M}$ , R and R' are general groups but do not include H) functionalities. Bibliographic references and coordinate data were obtained, calculations to give the  $\bar{\tau}$ ,  $\chi_{\text{N}}$ , and  $\chi_{\text{C}}$  parameters for each N-amido ligand were carried out, and the results were compiled using the Cambridge database programs. In Figure 3.4(A and B) the calculated values of  $\bar{\tau}$ ,  $\chi_{\text{N}}$ , and  $\chi_{\text{C}}$  are plotted. Each point represents an amide ligand. There are 457 data points in Figure 3.4(A and B), which include the data obtained from the Cambridge files,<sup>13</sup> and the data from structurally characterized PAC ligand complexes prepared in our group.<sup>14</sup> Of the 457 data points, 118 represent cases of monodentate N-amido ligands where the parent free-base ligand is a secondary organic amide functional group. These data are plotted separately in Figure 3.4(C and D). The dots represent points from the literature, and the diamonds represent points for osmium complexes of PAC ligands where  $|\bar{\tau}|$  values of  $> 25^\circ$  are found.

The first thing to notice in these plots is that the scattering is greater along the  $\chi_{\text{N}}$  axis than it is along the  $\bar{\tau}$  or  $\chi_{\text{C}}$  axes. This agrees with several theoretical studies<sup>11b,15</sup> which conclude that pyramidalization at nitrogen is energetically less demanding than pyramidalization at carbon or rotation about the C-N bond. The plots also show that  $\chi_{\text{C}}$  is always quite small.

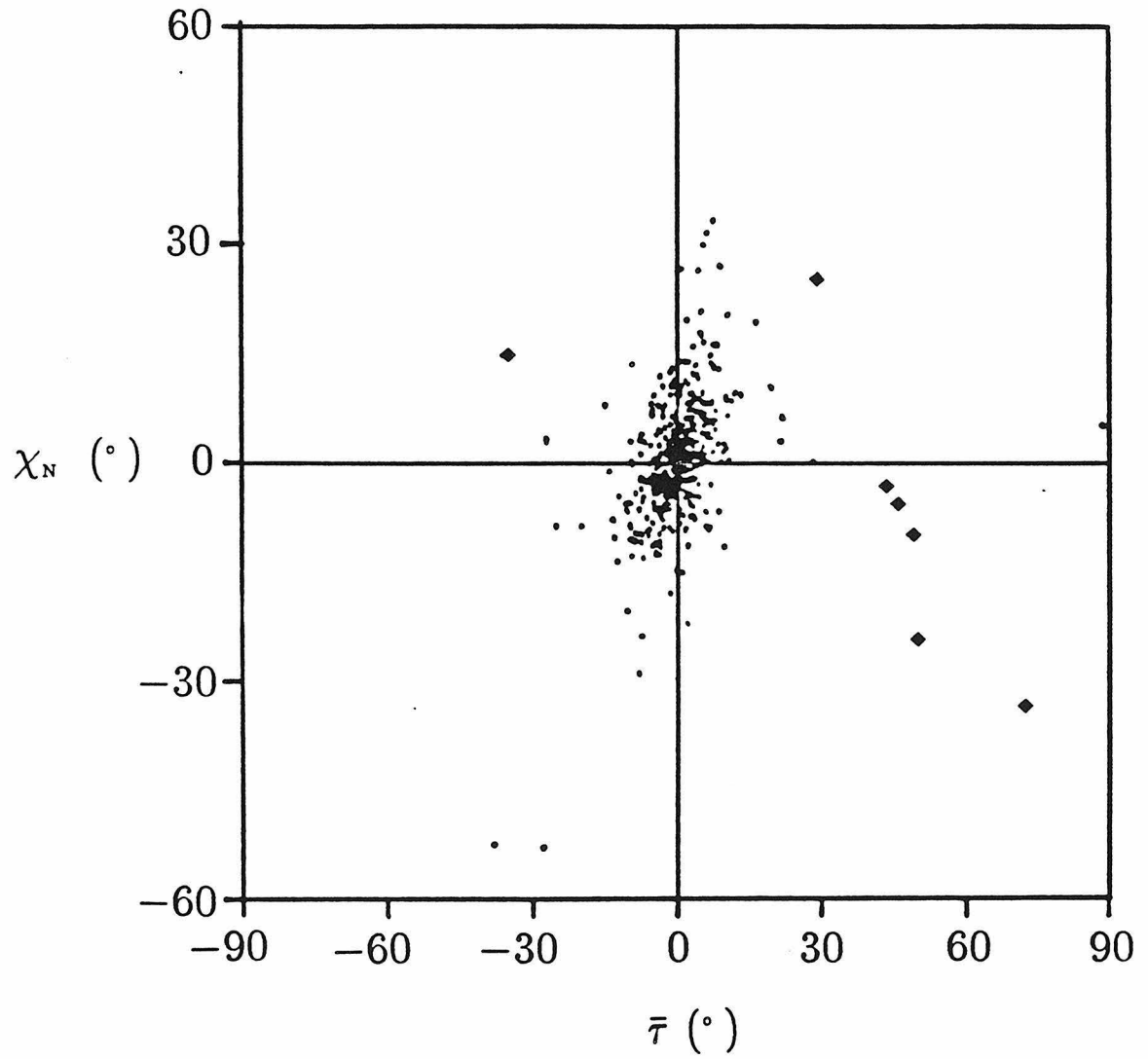
The second thing to notice is that very few amides have high  $\bar{\tau}$  values ( $|\bar{\tau}| > 25^\circ$ ) indicating substantial twisting about the amide C-N bond. Table 3.1 shows all the complexes with  $\text{RC(O)NR}'\text{M}$  or  $\text{RC(OM}')\text{NR}'\text{M}$  fragments where  $|\bar{\tau}| > 25^\circ$ , and lists their angular parameters. Com-

**Figure 3.4.** Plots of angular parameters for all structurally characterized  $\text{RC}(\text{O})\text{NR}'\text{M}$  and  $\text{RC}(\text{OM}')\text{NR}'\text{M}$  fragments. Dots represent literature points. Diamonds represent points for PAC ligand complexes with  $|\bar{\tau}| > 25^\circ$ . (A and B): all data. (B and C): all points for fragments where the free base ligand is a secondary amide.

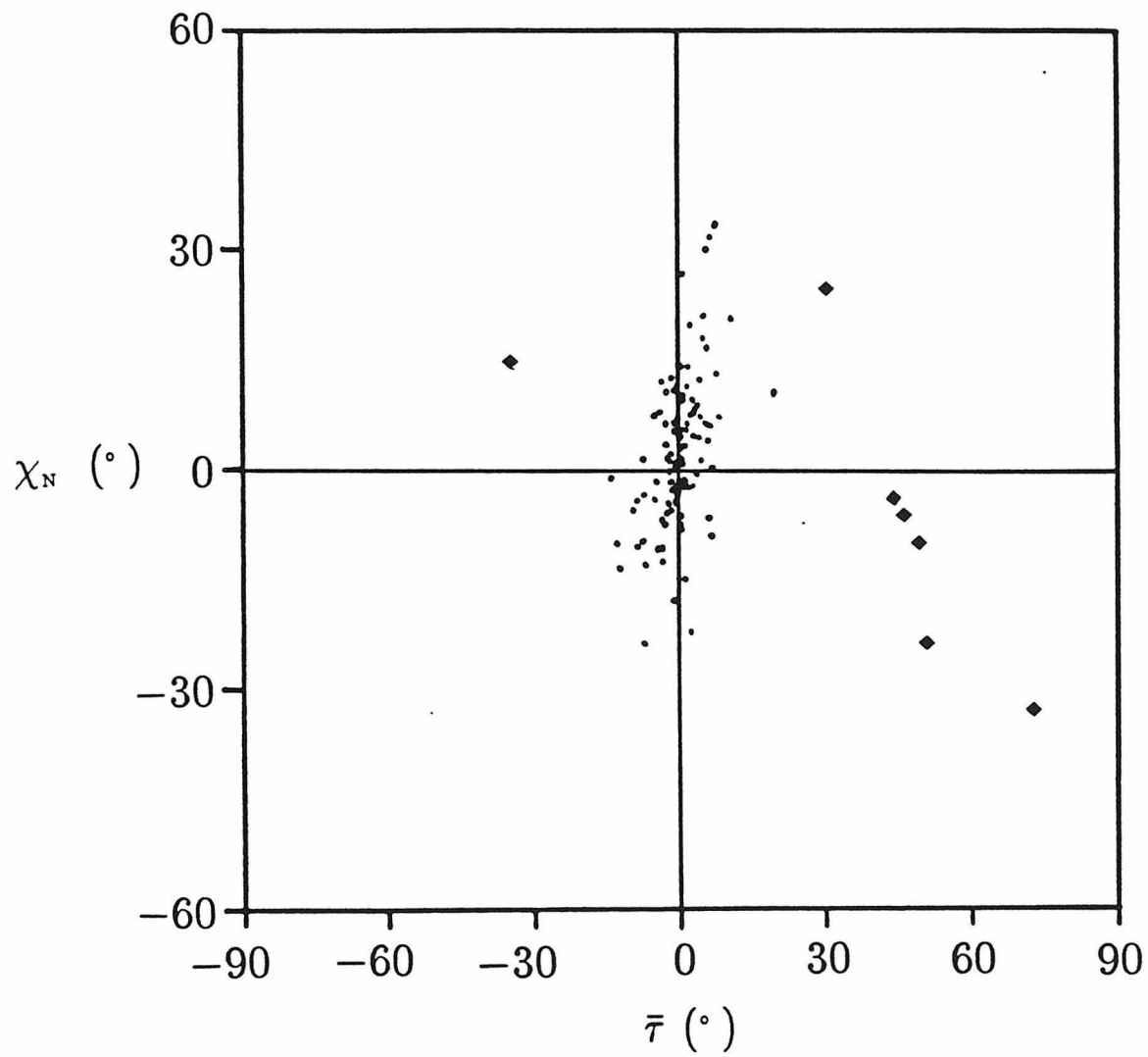
A



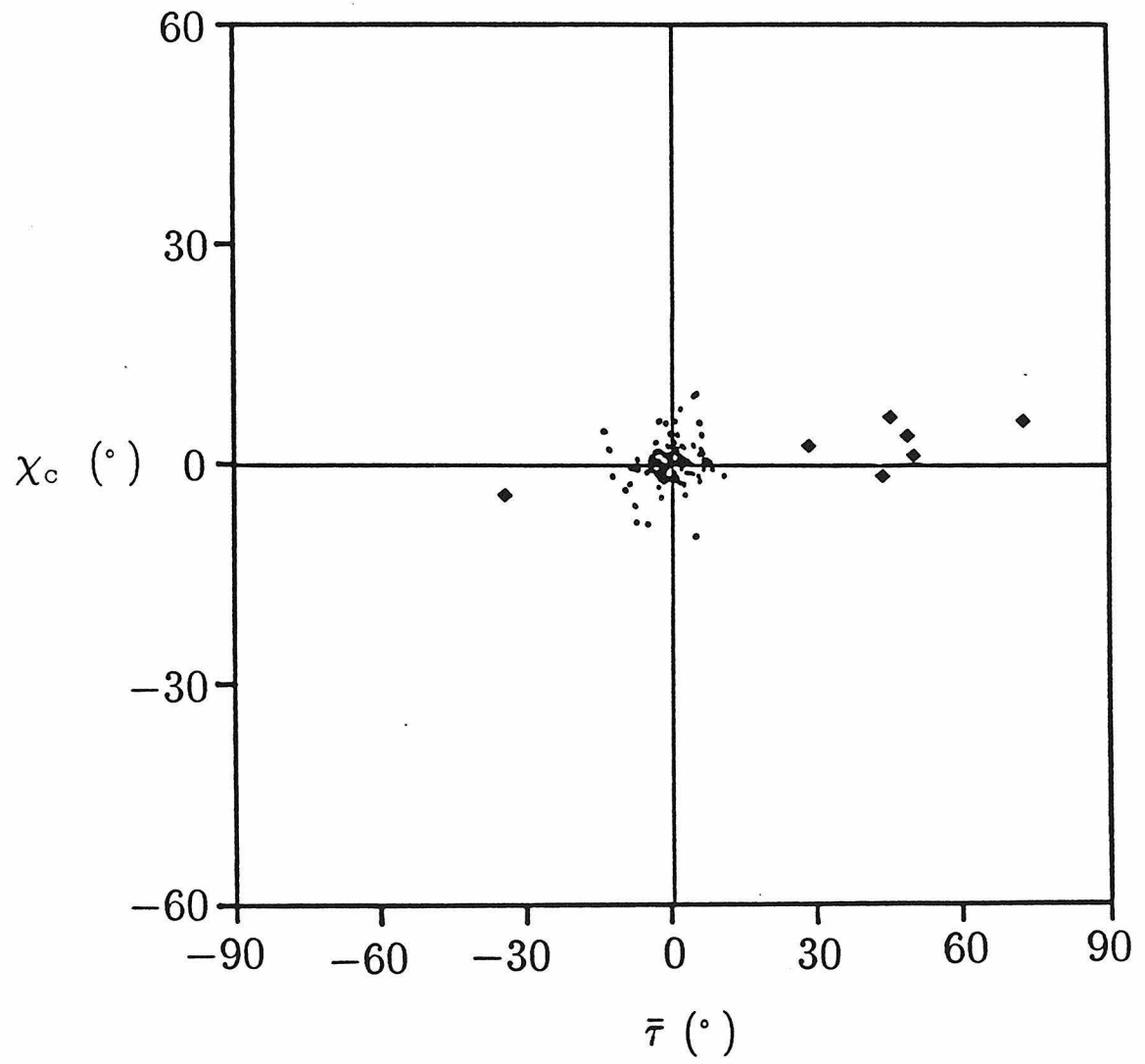


**B**

C



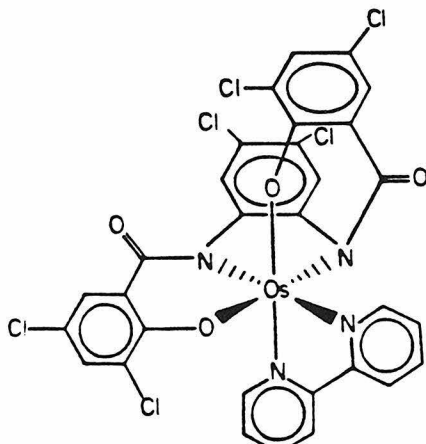
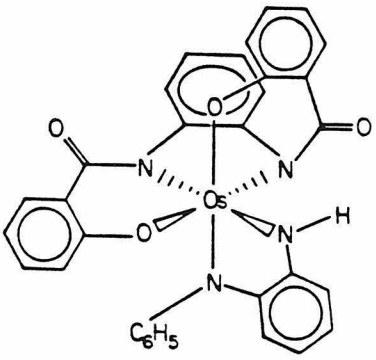
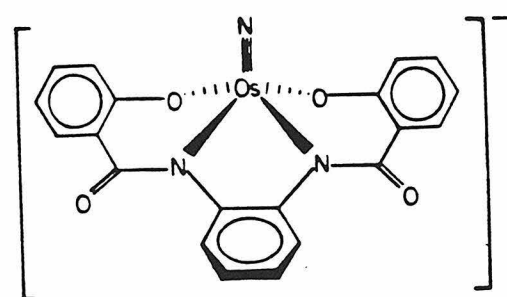
D

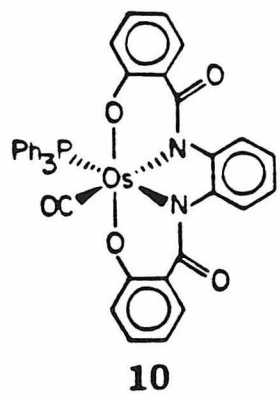


pounds 18 and 19 are PAC ligand compounds with a bidentate auxiliary ligand and a  $\text{cis-}\beta$  coordination geometry. They apparently exhibit large  $\bar{\tau}$  values because the structural constraints of the coordination sphere force the formation of nonplanar N-amido ligands. Compounds 10 and 17 are  $\text{cis-}\alpha$ -PAC ligand complexes so each has two nonplanar amide ligands. The nonplanarity of the N-amido ligand in 20 is likely a result of the distortions of the PAC ligand arising from the osmium atom sitting 0.55 Å out of plane of the nitrogen and oxygen atoms.<sup>14a</sup> In the other four cases where the  $\bar{\tau}$  values are large, the amide nitrogen atom is involved in formal multiple bonding with its R' ligand and/or the C(O) group is involved in multiple bonding with its R ligand. This allows resonance delocalization further than the amide fragment. None of the  $\text{RC(O)NR}'$  ligands in these four cases is derived from a parent organic amide functional group.

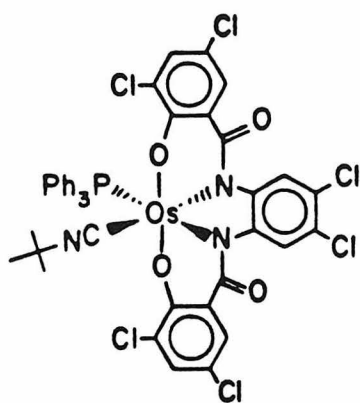
If we adopt the somewhat arbitrary criterion that an amide with  $|\bar{\tau}| > 25^\circ$  is a nonplanar amide, the plots in Figure 3.4 and Table 3.1 demonstrate that there are very few nonplanar amide ligands. The osmium complexes of PAC ligands form "very" nonplanar amide ligands, and are the only nonplanar amide ligands derived from parent organic amide functional groups. They also demonstrate one of the reasons for the formation of nonplanar amides in the PAC ligand complexes. Structural constraints imposed on the coordination sphere can force the PAC ligand to coordinate in a geometry that requires nonplanar amides. Complexes 10 and 17 also contain the PAC ligands in geometries requiring nonplanar amides, but in these cases no structural constraints exist. An energy stabilization of the  $\text{cis-}\alpha$  isomers must exist for

**Table 3.1.** Angular parameters for  $\text{RC(O)NR}'\text{M}$  and  $\text{RC(OM}')\text{NR}'\text{M}$  fragments with  $|\bar{\tau}| > 25^\circ$ .

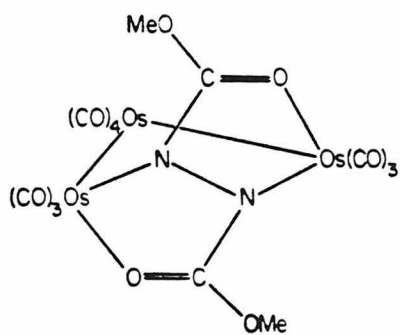
Compound	$\bar{\tau}(\circ)$	$\chi_N(\circ)$	$\chi_C(\circ)$	Note
 <p style="text-align: center;"><b>18</b></p>	-35 1	15 5	-4 3	a
 <p style="text-align: center;"><b>19</b></p>	22 44	6 -47	7 -1	b
 <p style="text-align: center;"><b>20</b></p>	30 5	25 7	3 0	b



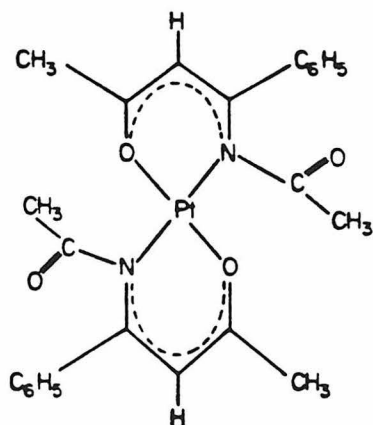
44	-6	6	c
73	-33	6	



49	-10	4	d
50	-24	2	



-28	-53	-1	e
-38	-52	1	



88	5	3	f
----	---	---	---

<p>The structure shows a central nickel atom (Ni) coordinated to two thiazole rings. Each thiazole ring consists of a five-membered ring with two sulfur atoms and one nitrogen atom. The nickel atom is also coordinated to the nitrogen atom of a benzamide group (-NH-C(=O)-N-C<sub>6</sub>H<sub>5</sub>) which is bonded to one of the thiazole rings.</p>	29	0	-2	g
<p>The structure shows a central nickel atom (Ni) coordinated to two triethylphosphine ligands ((C<sub>2</sub>H<sub>5</sub>)<sub>3</sub>P)<sub>2</sub> and two nitrogen atoms of a phthalazine derivative. The phthalazine derivative is a six-membered ring with two nitrogen atoms and two carbonyl groups (C=O). Each nitrogen atom of the phthalazine derivative is also bonded to a phenyl group (C<sub>6</sub>H<sub>5</sub>).</p>	-27	3	-3	h
	-15	8	3	

<sup>a</sup> See ref. 2.

<sup>b</sup> See ref. 14a.

<sup>c</sup> Reported in this chapter.

<sup>d</sup> See ref. 3.

<sup>e</sup> Einstein, F.W.B.; Nussbaum, S.; Sutton, D.; Willis, A.C. *Organometallics* **1984**, *3*, 568-74.

<sup>f</sup> Uchiyama, T.; Takagi, K.; Matsumoto, K.; Ooi, S.; Nakamura, Y.; Kawaguchi, S. *Chem. Lett.* **1979**, 1197-200.

<sup>g</sup> Weiss, J.; Thewalt, U. *Z. Anorg. Allg. Chem.* **1966**, *343*, 274-89.

<sup>h</sup> Hoberg, H.; Oster, B.W.; Kruger, C.; Tsay, Y.H. *J. Organomet. Chem.* **1983**, *252*, 365-73.



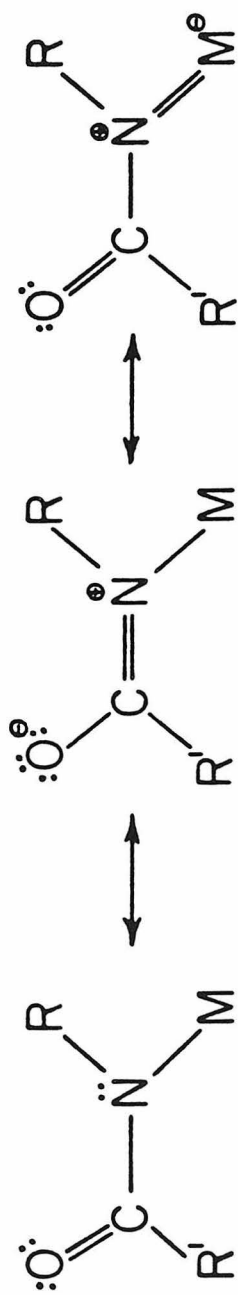
these complexes to offset the loss in energy from twisting the amide C–N bonds.

As discussed above, the major change in the PAC ligand upon isomerization from a trans complex to a cis complex is the formation of nonplanar amide groups. This is necessarily the result of isomerization, because twisting about the amide C–N bond is the only way to allow a cis coordination geometry of the tetradentate PAC ligands. We now show that in the cases of complexes 10 and 17, nonplanar amides are thermodynamically favored, and isomerization occurs in order to form nonplanar amide ligands. To explain why this is the case we must look in more detail at the resonance picture of amides.

Scheme 3.2 shows resonance structures important for a coordinated amide group. The structure with delocalization of negative charge to the electronegative oxygen atom is an important contributor to the overall structure. In a nonplanar amide twisting about the C–N bond will limit the contribution from this resonance structure, and the other resonance structures will dominate.

Examination of the IR spectra of some representative complexes confirms the presence of this effect. The planar amides of the HBA-B ligand, for example in *trans*-Os( $\eta^4$ -HBA-B)(PPh<sub>3</sub>)<sub>2</sub>, give rise to amide carbonyl stretches at 1600 cm<sup>-1</sup>. The *cis*- $\beta$ -Os( $\eta^4$ -HBA-B)(dppe) complex contains one planar amide and one nonplanar amide. The IR spectrum shows a carbonyl stretch at 1600 cm<sup>-1</sup> for the planar amide. The nonplanar amide stretch is at 1657 cm<sup>-1</sup>, as a result of the decrease in importance of the delocalization resonance structure and an accompanying increase in the C–O bond order. In a *cis*- $\alpha$  complex such as

**Scheme 3.2** Resonance in a coordinated amide.



*cis*- $\alpha$ -Os( $\eta^4$ -HBA-B)(PPh<sub>3</sub>)(CO) (10) or *cis*- $\alpha$ -Os( $\eta^4$ -HBA-B)(PPh<sub>3</sub>)(*t*-BuNC) (11) both amide groups are nonplanar, and we observe a shift of both amide stretches to higher frequency: 1695 and 1640 cm<sup>-1</sup> for 10 and 1680 and 1625 cm<sup>-1</sup> for 11. As pointed out in chapter 2, this effect makes IR spectroscopy a good structural indicator for these complexes.

The reduction in amide delocalization in a nonplanar amide makes this amide ligand a better donor than the planar amide. The increase in basicity (a deprotonated amine vs. a deprotonated amide) would make the nonplanar amide a better  $\sigma$ -donor. The localization of the nitrogen  $p$ - $\pi$  electrons on the amide nitrogen would make the nonplanar amide a better  $\pi$ -donor. This difference in donation ability between planar and nonplanar amide ligands is beautifully demonstrated by the electrochemistry of some osmium(CHBA-DCB) complexes prepared by John Keech.<sup>1,16</sup> All three isomers (trans, *cis*- $\beta$  and *cis*- $\alpha$ ) of Os( $\eta^4$ -CHBA-DCB)(*p*-Clpy)<sub>2</sub> have been isolated. Table 3.2 lists the electrochemical data for these three isomers. The formal reduction potentials for the reversible couples of the *cis*- $\alpha$  isomer are lower than those for the *cis*- $\beta$  isomer which are in turn lower than those for the trans isomer. Clearly, the donating ability of the PAC ligand is different depending on the coordination geometry, with the order of decreasing donating ability being *cis*- $\alpha$  > *cis*- $\beta$  > trans.<sup>17</sup> The *cis*- $\alpha$  isomer of the PAC ligand has two nonplanar amides, the *cis*- $\beta$  isomer has one nonplanar amide, and the trans isomer does not have any nonplanar amides. Since nonplanar amides are better donors than the planar amides, the PAC ligand coordinated in the *cis*- $\alpha$  geometry is the strongest donor, and

**Table 3.2.** Formal potentials of the redox couples of the three isomers of  $\text{Os}(\eta^4\text{-CHBA-DCB})(p\text{-chloropyridine})_2$ . Measured in  $\text{CH}_2\text{Cl}_2/0.1\text{ M TBAP}$  and referenced to the  $\text{Fc}^+/\text{Fc}$  couple.

<u>isomer</u>	<u>Os(III/II)</u>	<u>Os(IV/III)</u>	<u>Os(V/IV)</u>
trans	-1.59	-0.39	+0.74
cis- $\beta$	-	-0.48	+0.60
cis- $\alpha$	-1.81	-0.89	+0.58

---

the PAC ligand coordinated in the trans geometry is the weakest donor.

Another explanation can be suggested as to why a PAC ligand coordinated in a cis complex is a better donor than if it were coordinated forming a trans complex. It could be argued that a different arrangement of donor groups about the metal leads to a change in donating power. In a trans complex the powerful donating groups of the PAC ligand are all coordinated in the equatorial plane, while the auxiliary ligands occupy the axial sites. In this case the four strong donor groups of the PAC ligand are all interacting with the same two metal orbitals. In a cis- $\alpha$  complex two of the PAC ligand donors are in equatorial positions and two are in axial positions, so they have more metal orbitals available for interaction. This arrangement of donating atoms could lead to better donation by the cis- $\alpha$  complex than by the trans.

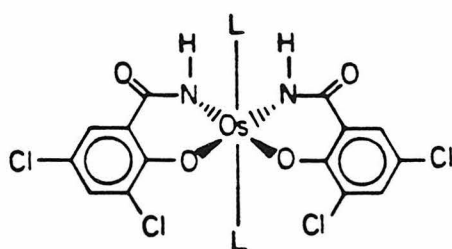
This argument can be discounted by the following observations. Table 3.3 shows the cis- $\alpha$  and trans diastereomers of  $\text{Os}(\eta^2\text{-CHBA})_2(t\text{-Bupy})_2$  ( $\text{H}_2\text{CHBA} \equiv 3,5\text{-dichloro-2-hydroxybenzamide}$ ). These complexes have both been isolated and their cyclic voltammograms recorded.<sup>18</sup> Table 3.3 also lists the formal reduction potentials for these two diastereomers. The table shows that there is essentially no difference in the formal potentials in going from the trans to the cis- $\alpha$  isomer. The differences in formal potentials for a reversible couple between the trans and cis- $\alpha$  isomers of an  $\text{Os}(\eta^4\text{-CHBA-DCB})(\text{L})_2$  complex can be as much as 500 mV.<sup>16</sup> In the osmium-(CHBA-DCB) case the two arms of the ligand are connected by the phenylene bridge, which, as we have shown, leads to distinctly nonplanar amide groups in cis- $\alpha$  com-

**Table 3.3.** Electrochemical data for the trans and cis- $\alpha$  isomers of  $\text{Os}(\text{n}^2\text{-CHBA})_2(\text{py})_2$ . Potentials were measured in  $\text{CH}_2\text{Cl}_2/0.1\text{ M}$  TBAP.



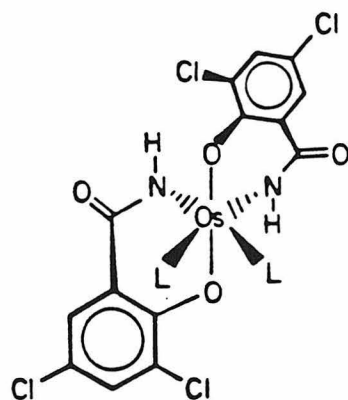
Standard Reduction Potentials in Volts vs. Fc<sup>+</sup>/Fc.

<u>Compound</u>	<u>III/II</u>	<u>IV/III</u>
-----------------	---------------	---------------



-1.97

-0.71



-1.99

-0.71

---

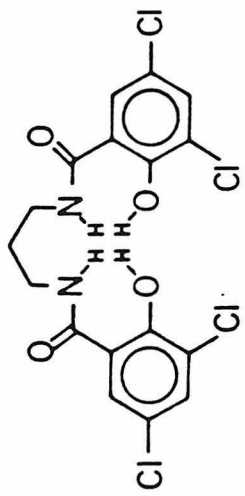
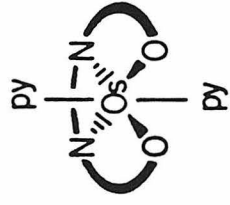
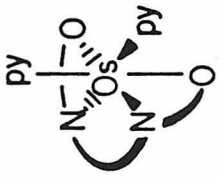
**L = py**

plexes. In the case of  $\text{Os}(\text{CHBA})_2$  complexes, there is no bridge connecting the two bidentate ligands, so an additional degree of freedom exists. Isomerization from the trans diastereomer to the cis- $\alpha$  diastereomer can occur with rotation about the Os-N bonds moving the amide hydrogens out of the equatorial plane, leaving the amide ligands planar. The cis- $\alpha$  and trans complexes of  $\text{Os}(\eta^2\text{-CHBA})_2(t\text{-Bupy})_2$  have different arrangements of donor atoms about the osmium center, but contain no nonplanar amides, and there is no difference in their redox potentials. The increased donor ability of the cis- $\alpha$  geometries of the tetradentate PAC ligands HBA-B and CHBA-DCB is certainly due to the presence of nonplanar amide ligands.

Further evidence against the argument of better donation through a different arrangement of the donor atoms comes from some osmium chemistry with the PAC ligand CHBA-Pr. Table 3.4 shows the three isomers (trans, cis- $\beta$ , and cis- $\alpha$ ) of  $\text{Os}(\eta^4\text{-CHBA-Pr})(\text{py})_2$  ( $\text{H}_4\text{CHBA-Pr} = 1,3\text{-bis}(3,5\text{-dichloro-2-hydroxybenzamido})\text{propane}$ ) and the electrochemical and infrared data for these complexes.<sup>19</sup> As with the  $\text{Os}(\eta^2\text{-CHBA})_2(\text{L})_2$  complexes, there is little change in the redox potentials between isomers. Apparently the propane bridge has enough flexibility to allow formation of cis- $\beta$  and cis- $\alpha$  complexes, without the formation of nonplanar amides. The amide CO stretching frequencies for the different isomers are identical, implying there is no formation of nonplanar amide groups.

With the knowledge that the HBA-B ligand, coordinated in a cis- $\alpha$  or cis- $\beta$  complex, contains nonplanar amide groups, and that nonplanar amides are much better donors than planar amides, we can now explain

**Table 3.4.** Electrochemical and IR data for isomers of  $\text{Os}(\eta^4\text{-CHBA-Pr})(\text{py})_2$ . Potentials were measured in  $\text{CH}_2\text{Cl}_2$  with 0.1 M TBAP, and are references to the  $\text{Fc}^+/\text{Fc}$  couple.

	$E^f \text{Os}^{\text{III}}/\text{Os}^{\text{I}}$	$E^f \text{Os}^{\text{IV}}/\text{Os}^{\text{III}}$	$E^f \text{Os}^{\text{IV/IV}}$	$\nu_{\text{CO}} \text{Os}^{\text{IV}}$
	-1.91	-0.62	(0.74)	1595
	-1.87	-0.66	(0.72)	1595
	-2.08	-0.81	0.63	1595

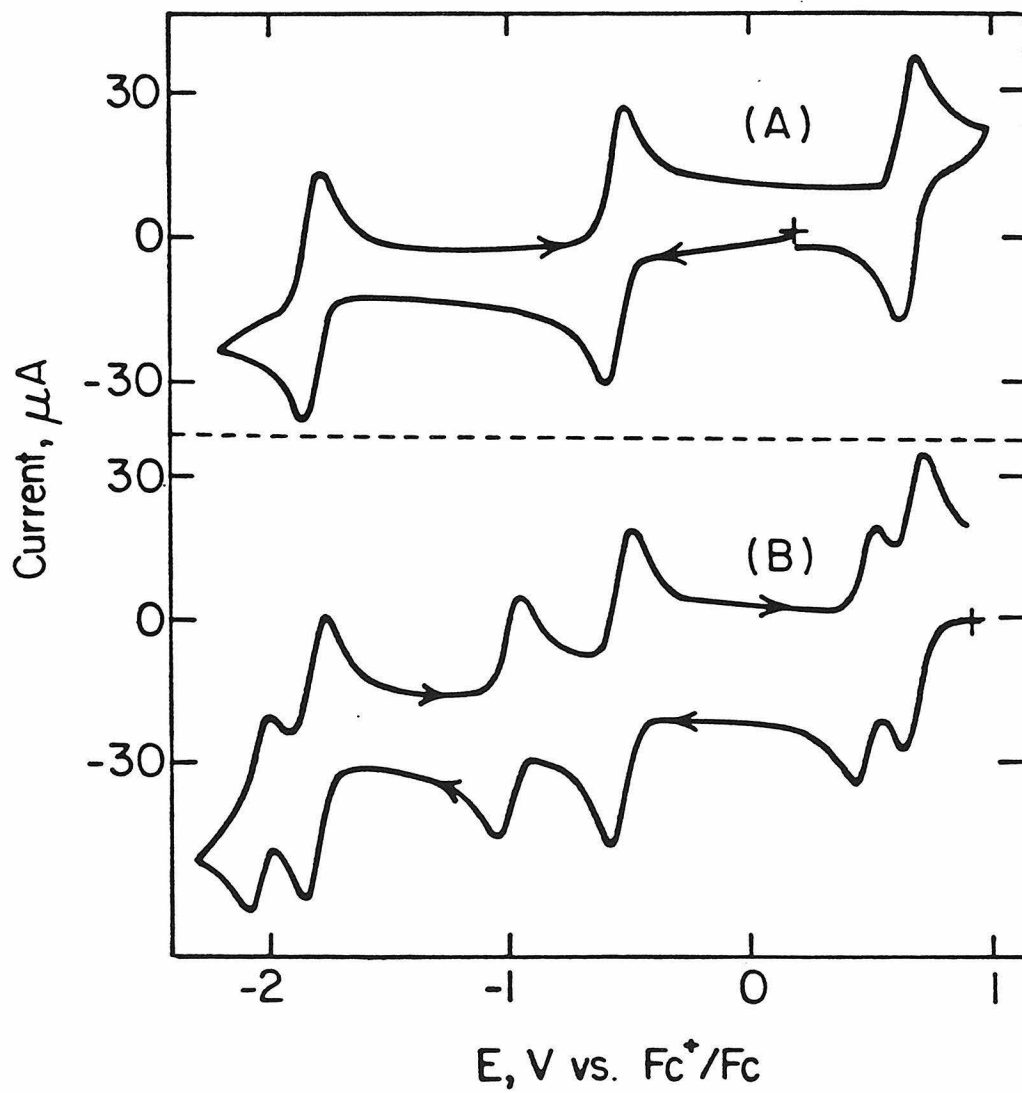
the ligand isomerizations in the formation of 10 and 11. PAC ligand isomerization, if not forced by coordination of a bidentate auxiliary ligand, can still occur to change the donating properties of the PAC ligand. Consider the *cis- $\alpha$*  carbonyl complex 10. To make this complex, we react carbon monoxide with the *trans* complex  $\text{trans-Os}(\eta^4\text{-HBA-B})(\text{PPh}_3)_2$ . A phosphine ligand is replaced by a carbon monoxide ligand. For carbon monoxide to form a strong bond to the osmium, the osmium must be electron rich enough to participate in  $\pi$ -backbonding with the CO  $\pi^*$ -orbitals. The osmium center is already in the +4 oxidation state, and  $\pi$ -donation to the CO ligand will further remove electron density from the osmium, so the HBA-B ligand isomerizes, coordinating in the better donating *cis- $\alpha$*  form, to offset the withdrawal of electron density by the  $\pi$ -acid ligand. The same thing happens when a phosphine ligand is replaced with an isocyanide ligand. The effect of coordination of the new ligand to make the osmium less electron rich is compensated by better donation from a new PAC ligand coordination geometry.

Additional support for this hypothesis is generated from the electrochemical behavior of  $\text{trans-Os}(\eta^4\text{-CHBA-DCB})(t\text{-Bupy})_2$ .<sup>16</sup> The cyclic voltammogram (Figure 3.5(A)) shows two reversible one-electron reductions and one reversible one-electron oxidation, representing the Os(III/II), Os(IV/III), and Os(V/IV) couples. If a bulk electrolysis is done at a potential more positive than the Os(V/IV) couple, the osmium species is completely converted to the osmium(V) cation. Figure 3.5(B) shows a CV of the solution following the electrolysis to osmium(V). The CV shows the three reversible waves due to the presence of

**Figure 3.5.** Cyclic voltammograms of  $\text{Os}(\eta^4\text{-CHBA-DCB})(t\text{-Bupy})_2$ . Recorded on 4.1 mM complex in  $\text{CH}_2\text{Cl}_2/0.1\text{ M TBAP}$  with a  $0.03\text{ cm}^2$  platinum electrode. Scan rate was  $200\text{ mV s}^{-1}$ .

(A) Osmium(IV).

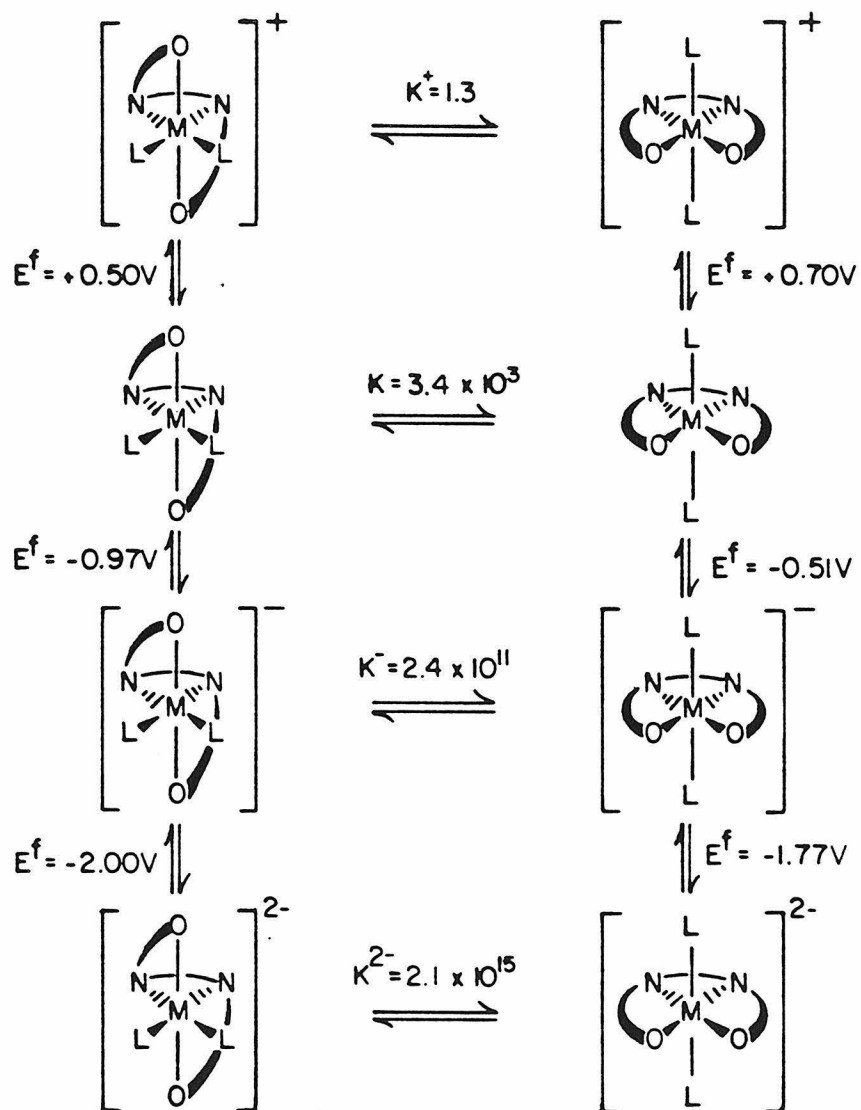
(B) Osmium(V).



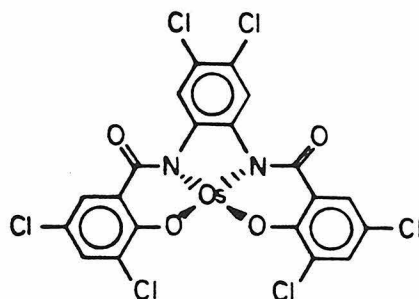
$[trans-Os(\eta^4-CHBA-DCB)(t-Bupy)_2]^+$ , and also has three new reversible redox couples. If the solution is bulk reduced back to osmium(IV), and a CV of the solution taken, the CV in Figure 3.5(A) is reproduced. It has been shown that following the electrolysis to osmium(V), the solution contains an equilibrium mixture of  $[trans-Os(\eta^4-CHBA-DCB)(t-Bupy)_2]^+$  and  $[cis-\alpha-Os(\eta^4-CHBA-DCB)(t-Bupy)_2]^+$ . The three reversible waves for the cis- $\alpha$  isomer are all present in the CV and come at lower potentials than the corresponding waves for the trans isomer. This fits with the suggestion that the PAC ligand in a cis- $\alpha$  complex is a better donor than the PAC ligand in a trans complex. What happens in the electrochemical experiment is as follows:  $trans-Os(\eta^4-CHBA-DCB)(t-Bupy)_2$  is oxidized by one electron forming the osmium(V) cation. Depletion of the electron density at the osmium center makes the more donating cis- $\alpha$  conformation more favorable energetically, and the CHBA-DCB ligand isomerizes to the cis- $\alpha$  coordination geometry to give an equilibrium mixture (which is approximately 1:1) of the trans and cis- $\alpha$  isomers. Knowing the equilibrium constant of the trans to cis- $\alpha$  equilibrium at the osmium(V) cation stage, and the three reduction potentials for each isomer, the equilibrium constants for the isomerization can be calculated for the other osmium oxidation states.<sup>20</sup> Scheme 3.3 shows the isomers at the different oxidation states and the equilibrium constants for the isomerizations. When the osmium center is electron rich at the osmium(II) stage, the trans isomer is highly favored. As the oxidation state increases, the osmium center becomes less electron rich and the cis- $\alpha$  isomer is increasingly favored. Changing the electron density at the metal center



**Scheme 3.3.** Thermodynamic relationships between cis and trans isomers of different oxidation states of Os( $\eta^4$ -CHBA-DCB)(*t*-Bupy)<sub>2</sub>.



≡



electrochemically can cause ligand isomerization to match its donating capability with what is best suited for the metal center.

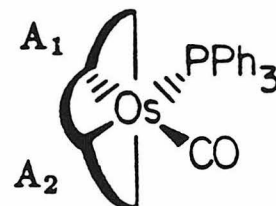
None of the osmium-(HBA-B) complexes demonstrates this electrochemical behavior. Bulk oxidations of *trans*-Os( $\eta^4$ -HBA-B)(PPh<sub>3</sub>)<sub>2</sub>, *trans*-Os( $\eta^4$ -HBA-B)(PPh<sub>3</sub>)(py), and *cis*- $\beta$ -Os( $\eta^4$ -HBA-B)(dppe) do not cause any isomerization. Perhaps this is because the HBA-B ligand is a better donor than the CHBA-DCB ligand, so isomerization is not required. Bulk reductions of *cis*- $\alpha$ -Os( $\eta^4$ -HBA-B)(PPh<sub>3</sub>)(CO) and *cis*- $\alpha$ -Os( $\eta^4$ -HBA-B)(PPh<sub>3</sub>)(*t*-BuNC)<sup>21</sup> do not cause any isomerization to isomers containing a less donating PAC ligand.

A nonplanar amide is expected to be both a better  $\sigma$ -donor and a better  $\pi$ -donor than a planar amide. Indeed, we have shown that nonplanar amides are better donors than planar amides. It would be interesting to know if this is due mainly to better  $\sigma$ -donation or to better  $\pi$ -donation. Table 3.5 lists the angular parameters for the two nonplanar amides of the carbonyl complex 10. Both amides are quite nonplanar as indicated by the high  $\bar{\tau}$  values. Both amides also show just a small amount of distortion toward a pyramidal amide carbon atom ( $\chi_C$ ). The amide trans to the triphenylphosphine ligand has a high  $\chi_N$  value indicating considerable pyramidalization at the amide nitrogen. The amide trans to the carbon monoxide ligand, however, has almost no pyramidalization. The high degree of pyramidalization at amide 2 indicates localization of the nitrogen  $p$ - $\pi$  electrons in the nitrogen  $p$ - $\pi$  orbital. The very low value of  $\chi_N$  for amide 1 indicates that although the amide C-N bond is greatly twisted, the nitrogen  $p$ - $\pi$  electrons are not localized on the amide nitrogen. Donation of these  $\pi$ -electrons to

**Table 3.5.** Angular parameters for the two amide ligands of *cis*- $\alpha$ -Os( $\eta^4$ -HBA-B)(PPh<sub>3</sub>)(CO) (10).

Angular Parameters for 10.

	<u>A</u> <sub>1</sub>	<u>A</u> <sub>2</sub>
$\chi_C$	6(2)°	6(2)°
$\chi_N$	-6(2)°	-33(2)°
$\bar{\tau}$	46(2)°	73(2)°



the osmium center would explain the low  $\chi_N$  value for amide 1. It is interesting that the amide trans to the strong  $\pi$ -acceptor (CO) ligand (amide 1) is participating in  $\pi$ -donation to the osmium center while the amide trans to the phosphine ligand (amide 2) localizes the amide nitrogen  $\pi$ -electrons largely on the nitrogen. We believe that this is evidence for  $\pi$ -donation from a nonplanar amide to the metal center. Although we cannot conclude whether a  $\sigma$ - or  $\pi$ -effect is the major contributor to the increased donation, this is evidence that increased  $\pi$ -donation is present.<sup>2 2</sup>

Calculation of the angular parameters for the two amides of the PAC ligand in  $\text{Os}(\eta^3\text{-(H)HBA-B})(\text{PPh}_3)(\text{phen})$  (15) shows that one of the amides is quite planar, while the other exhibits a high degree of nonplanarity. Figure 3.6 shows the ORTEP of 15 indicating the angular parameters for the two amides. The amide between the coordinated phenol and the phenylene bridge is reasonably planar, having no unusual angular parameters. The N-amido ligand attached to the uncoordinated phenol is distinctly nonplanar with a  $\bar{\tau}$  value of  $-40^\circ$  and a  $\chi_N$  value of  $-49^\circ$ . Only five monodentate metallo-N-amido groups derived from parent mono-N-substituted amides have  $\bar{\tau}$  values of greater magnitude. The  $\chi_N$  value is the largest in magnitude discovered to date. The  $\chi_C$  value of  $-10^\circ$  is also unusual, with only two other cases having  $|\chi_C|$  values as great as  $10^\circ$ . The osmium(III) center should not require a nonplanar amide for increased donation. The cause of the nonplanarity of the amide appears to be a steric clash between the entire carboxyphenol N-substituent and the bidentate phenanthroline ligand. The dihedral angle between the best planes of the carboxyphenol arm

**Figure 3.6.** ORTEP view of  $\text{Os}(\eta^3\text{-(H)HBA-B})(\text{PPh}_3)(\text{phen})$  (**15**) showing the angular parameters for the two amide ligands.





and the phenanthroline is  $12^\circ$ . Distances between the atoms of the carboxyphenol arm and the plane of the phenanthroline ligand vary from 2.70 Å to 3.50 Å. The shorter contacts are within Van der Waals distances.<sup>2 3</sup> Compound 15 represents the third class of inorganic compounds with nonplanar N-amido ligands, where the primary cause of the nonplanarity is a steric effect.

## Conclusions

An exciting result of the formation of cis- $\alpha$  osmium PAC ligand complexes is the discovery of nonplanar amide ligands. Using the angular parameters defined by Dunitz and Winkler, we have been able to compare the planarity of all the structurally characterized N-amido ligands. Clearly the amides of the PAC ligands of some of the complexes discussed here are unusual in their degree of nonplanarity and can be called the first nonplanar amide ligands.

So far we have observed three classes of nonplanar amide ligands. The first class is caused by structural constraints of the metal's coordination sphere. Complexes that are forced to adopt cis geometries to accommodate a bidentate auxiliary ligand such as bipy or dppe characterize this class. The second cause of nonplanar amide ligands is electronic perturbation of the metal center. Depleting the metal center of electron density can cause the formation of the more highly donating nonplanar amides to minimize this depletion. The formation of cis- $\alpha$  complexes upon coordination of a strong electron withdrawing ligand such as CO or RNC, and isomerization to a cis- $\alpha$  geometry upon electrochemical oxidation demonstrates this class. The third class of nonplanar amide includes those that are the result of steric pressure imparted on the R groups attached to the amide ligand. The osmium(III) complex  $\text{Os}(\eta^3\text{-HBA-B})(\text{PPh}_3)(\text{phen})$  is the example of this final class.

Certainly the most interesting type of nonplanar amide ligand is that caused by the electronic requirement of the metal. In these

cases all coordination geometries are available to the complexes, and the amides have a "choice" to be planar or nonplanar. The amides "choose" the geometry that will give them the donor properties most suited for the metal center. Since the nonplanar amides are better donors than the planar amides, the PAC ligands will adapt themselves to meet the electronic requirements of the metal, coordinating in a cis geometry forming nonplanar amides when strong donation is required, and coordinating in a trans geometry through planar amides when the stronger donating power is not needed.

The discovery of the isomerization possibilities of the tetradentate PAC ligands and the formation of nonplanar amide ligand fragments has important consequences in considering the design of PAC ligands. If N-amido PAC ligands are being designed to produce highly oxidizing inorganic complexes it will be important to design the PAC ligands such that spontaneous formation of nonplanar N-amido ligands cannot occur to reduce the oxidizing power of the metal center. Building more rigidity into the PAC ligand backbone would be a way to prevent nonplanar amide formation.

## Experimental

The syntheses of the osmium(HBA-B) complexes discussed in this chapter can be found in the experimental section of Chapter 2. That experimental section also includes the details of the structure determinations for compounds 10 and 15. The osmium complexes of PAC ligands besides the HBA-B ligand were made by other members of the group. Experimental details concerning these complexes can be found in the references listed where these complexes appear in the text.

The structural data for the coordinated amides were obtained through the Cambridge database which covers the literature through 1985. The programs available with the Cambridge files used were: CONNSER for searching the data for entries with the specified connectivity giving amide ligands, BIBSER for retrieving the bibliographical information for these entries, RETRIEVE for collecting the crystallographic data for each structure, and GEOM 78 for calculating the torsion angles  $\omega_1$ ,  $\omega_2$ , and  $\omega_3$  for each entry.

References

1. Keech, J.T. Ph.D. Dissertation, California Institute of Technology, Pasadena, California, 1987.
2. Anson, F.C.; Christie, J.A.; Collins, T.J.; Coots, R.J.; Furutani, T.; Gipson, S.L.; Keech, J.T.; Krafft, T.E.; Santarsiero, B.D.; Spies, G.H. *J. Am. Chem. Soc.* **1984**, *106*, 4460-72.
3. Collins, T.J.; Coots, R.J.; Furutani, T.T.; Keech, J.T.; Peake, G.T.; Santarsiero, B.D. *J. Am. Chem. Soc.* **1986**, *108*, 5333-9.
4. Stewart, W.E.; Siddall, T.H., III. *Chem. Rev.* **1970**, *70*, 517-51.
5. For the definitions of the coordination geometries see Figure 2.1.
6. Costain, C.C.; Dowling, J.M. *J. Chem. Phys.* **1960**, *32*, 158-65.
7. (a) Winkler, F.K.; Dunitz, J.D. *Acta Crystallogr., Sect. B* **1975**, *B31*, 264-7. (b) Winkler, F.K.; Dunitz, J.D. *Acta Crystallogr., Sect. B* **1975**, *B31*, 276-8. (c) Winkler, F.K.; Dunitz, J.D. *Acta Crystallogr., Sect. B* **1975**, *B31*, 281-3. (d) Winkler, F.K.; Dunitz, J.D. *Acta Crystallogr., Sect. B* **1975**, *B31*, 283-6. (e) Smolíková, J.; Tichý, M.; Bláha, K. *Collect. Czech. Chem. Commun.* **1976**, *41*, 413-29. (f) Kálal, P.; Bláha, K.; Langer, V. *Acta Crystallogr., Sect. C* **1984**, *C40*, 1242-5. (g) Hossain, M.B.; Baker, J.R.; van der Helm, D. *Acta Crystallogr., Sect. B* **1981**, *B37*, 575-9. (h) Barnes, C.L.; McGuffey, F.A.; van der Helm, D. *Acta Crystallogr., Sect. C* **1985**, *C41*, 92-5. (i) Paquette, L.A.; Kakihana, T.; Hansen, J.F.; Philips, J.C. *J.*

- Am. Chem. Soc.* 1971, 93, 152–61. (j) Blackburn, G.M.; Plackett, J.D. *J. Chem. Soc., Perkin Trans. 2* 1972, 1366–71.
8. (a) Sweet, R.M.; Dahl, L.F. *J. Am. Chem. Soc.* 1970, 92, 5489–507. (b) Woodward, R.B. "Recent Advances in the Chemistry of  $\beta$ -Lactam Antibiotics"; Elks, J.; Ed.; Chemical Society: London, 1977; pp 167–80. (c) Butler, A.R.; Freeman, K.A.; Wright, D.E. *Ibid.*; pp 299–303. (d) Proctor, P.; Gensmantel, N.P.; Page, M.I. *J. Chem. Soc., Perkin Trans. 2* 1982, 1185–92. (e) Page, M.I. *Acc. Chem. Res.* 1984, 17, 144–51.
9. (a) Smolíková, J.; Koblicová, Z.; Bláha, K. *Collect. Czech. Chem. Commun.* 1973, 38, 532–47. (b) Bláha, K.; Budesínský, M.; Koblicová, Z.; Malon, P.; Tichý, M. Baker, J.R.; Hossain, M.B.; van der Helm, D. *Ibid.* 1982, 47, 1000–19. (c) Ealick, S.E.; van der Helm, D. *Acta Crystallogr., Sect. B* 1975, B31, 2676–80. (d) Ealick, S.E.; Washecheck, D.M.; van der Helm, D. *Ibid.* 1976, B32, 895–900. (e) Ealick, S.E.; van der Helm, D. *Ibid.* 1977, B33, 76–80.
10. (a) Pracejus, H. *Chem. Ber.* 1959, 92, 988–98. (b) Pracejus, H. *Ibid.* 1965, 98, 2897–2905. (c) Pracejus, H.; Kehlen, M.; Kehlen, H.; Matschiner, H. *Tetrahedron* 1965, 21, 2257–70. (d) Hall, H.K., Jr.; Shaw, R.G., Jr.; Deutschmann, A. *J. Org. Chem.* 1980, 45, 3722–4. (e) Hall, H.K., Jr.; El-Shekeil, A. *Ibid.* 1980, 45, 5325–8. (f) Hall, H.K., Jr.; El-Shekeil, A. *Chem. Rev.* 1983, 83, 549–55. (g) Buchanan, G.L. *J. Chem. Soc., Perkin Trans. 1* 1984, 2669–70. (h) Coqueret, X.; Bourelle-Wargnier, F.; Chucho, J. *J. Org. Chem.* 1985, 50, 910–12.

11. (a) Dunitz, J.D.; Winkler, F.K. *J. Mol. Biol.* 1971, 59, 169-82, and references therein. (b) Dunitz, J.D.; Winkler, F.K. *Acta Crystallogr., Sect. B* 1975, B31, 251-63. (c) Warshel, A.; Leviyy, M.; Lifson, S. *J. Mol. Spectrosc.* 1970, 33, 84-99.
12. Definitions of amide nonplanarity parameters (ref. 11):  $\tau = (\omega_1 + \omega_2)/2$ , with the necessary condition  $|\omega_1 - \omega_2| < \pi$ . When this condition is not obeyed  $\tau = ((\omega_1 + \omega_2)/2) \bmod 2\pi$ . For  $-90^\circ < \tau < 90^\circ$  the amide is cisoid along the principal chain, and for  $-180^\circ < \tau < -90^\circ$  or  $90^\circ < \tau < 180^\circ$  the amide is transoid along the principal chain;  $\chi_N = (\omega_2 - \omega_3 + \pi) \bmod 2\pi$ ;  $\chi_C = (\omega_1 - \omega_3 + \pi) \bmod 2\pi$ . Amide torsion angles are as follows:  $\omega_1 = \text{C-C-N-C}$ ;  $\omega_2 = \text{O-C-N-Os}$ ;  $\omega_3 = \text{O-C-N-C}$ . Torsion angles have been numbered to coincide with those used previously for organic secondary amides with Os replacing H in  $\omega_2$  and are consistent with the recommendations of the IUPAC-IUB Commission on Biochemical Nomenclature; *J. Mol. Biol.* 1970, 50, 1-17.
13. The complete listing of references for the structures giving points in Figure 3.4 can be found in reference 3. The *cis*-diammineplatinum  $\alpha$ -pyrrolidonato complex,  $[\text{Pt}_4(\text{NH}_3)_8(\text{C}_4\text{H}_6\text{NO})_4](\text{NO}_3)_{5.48} \cdot 3\text{H}_2\text{O}$ , which is an apparent mixture of two tetranuclear species of different oxidation levels, shows several abnormally large  $\chi_C$  (21, 25, 26, 30, -36, 45,  $-45^\circ$ , there are two distinct molecules per unit cell) and  $\chi_N$  (35, -39,  $-48^\circ$ ) parameters which are difficult to rationalize. This structure contains other abnormal bond parameters. For instance, C-C single bond distances vary from 1.36-1.90 Å. The points derived from this work by

Matsumoto, Takahashi, and Fuwa are not included in Figure 3.4 (Matsumoto, D; Takahashi, H; Fuwa, K. *J. Am. Chem. Soc.* 1984, 106, 2049–54). The related pyrrolidonato, mixed-valence, tetranuclear species,  $[\text{Pt}_4(\text{NH}_3)_8(\text{C}_6\text{H}_6\text{NO})_4](\text{NO}_3)_6 \cdot \text{H}_2\text{O}$ , has been the subject of two reports by Matsumoto and Fuwa, and Matsumoto, Takahashi, and Fuwa (Matsumoto, K.; Fuwa, K. *J. Am. Chem. Soc.* 1982, 104, 897–8, Matsumoto, K.; Takahashi, J.; Fuwa, K. *Inorg. Chem.* 1983, 22, 4086–90). In the former a trihydrate is claimed for which several  $\alpha_{\text{C}}$  values ( $-24$ ,  $39^\circ$ ) are extremely large. In the latter, a dihydrate is claimed where one  $\alpha_{\text{C}}$  value is unreasonable ( $-74^\circ$ ), and another is at least inexplicably large ( $-28^\circ$ ). Presumably some atomic coordinates are inaccurate. The authors noted difficulties with this determination. The points for these structures are also excluded from Figure 3.4.

14. (a) Barner, C.J.; Collins, T.J.; Mapes, B.E.; Santarsiero, B.D. *Inorg. Chem.* in press. (b) Christie, J.A.; Collins, T.J.; Krafft, T.E.; Santarsiero, B.D.; Spies, B.J. *J. Chem. Soc., Chem. Commun.* 1984, 198–9. (c) Collins, T.J.; Santarsiero, B.D.; Spies, G.H. *J. Chem. Soc., Chem. Commun.* 1983, 681–2. (d) Anson, F.D.; Collins, T.J.; Coots, R.J.; Gipson, S.L.; Richmond, T.G. *J. Am. Chem. Soc.* 1984, 106, 5037–8. (e) Collins, T.J.; Richmond, T.G.; Santarsiero, B.D.; Treco, B.G.R.T. *J. Am. Chem. Soc.* 1986, 108, 2088–90.
15. (a) Ramachandran, B.N.; Lakshminarayanan, A.V.; Kolaskar, A.S. *Biochim. Biophys. Acta* 1973, 303, 8–13. (b) Kolaskar, A.S.; Lakshminarayanan, A.V.; Sarathy, K.P.; Sasisekharan, V. *Biopoly-*



- mers 1975, 14, 1081-94.
16. Anson, F.C.; Collins, T.J.; Gipson, S.L.; Keech, J.T.; Krafft, T.E.; Peake, G.T. *J. Am. Chem. Soc.* 1986, 108, 6593-605.
  17. Complexes of HBA-B have not been found to give more than one isomer of the same compound.
  18. (a) Anson, F.C.; Collins, T.J.; Gipson, S.L.; Krafft, T.E. unpublished results. (b) Krafft, T.E. Ph.D. Dissertation, California Institute of Technology, Pasadena, California, 1985.
  19. Lee, S.C. unpublished results.
  20. Since  $\Delta G = -RT \ln K$  for the equilibria between trans and cis- $\alpha$  isomers of a particular oxidation state, and  $\Delta G = -FE^f$  for different oxidation states of the same isomer, measuring the equilibrium constant at the cation stage and measuring the formal potentials of the redox couples allows one to calculate the equilibrium constants at the other oxidation states.
  21. These electrolyses tests were carried out by Stephen Gipson.
  22. It is true that amide 2 has a more severe twist angle about the C-N bond than amide 1, which arguably would lead to a larger  $\chi_N$  value for amide 2. We feel that the moderately larger  $\bar{\tau}$  value of amide 2 does not account for the very different  $\chi_N$  values of the two amides.
  23. These distances can be compared with layered trimesic acid (benzene-1,3,5-tricarboxylic acid) structures where the inter-layer distances are 3.31 and 3.32 Å. Herbstein, F.H.; Marsh, R.E. *Acta Crystallogr., Sect. B* 1977, B33, 2358-67. The inter-sheet separation in  $\beta$ -graphite is 3.35 Å. Pauling, L. *Proc.*

*Natl. Acad. Sci. U.S.A.* 1966, 56, 1646-52.

**Chapter 4**

Synthesis and Characterization of Osmium Complexes of  
3,5-dichloro-2-hydroxybenzamide (H<sub>2</sub>CHBA)

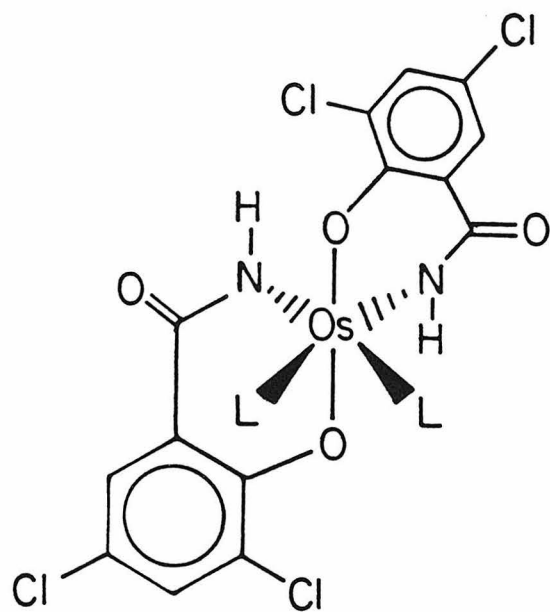
## Introduction

This chapter reports the results of some syntheses of osmium complexes of the ligand 3,5-dichloro-2-hydroxybenzamide ( $H_2CHBA$ ). This ligand coordinates as a bidentate dianionic ligand through a deprotonated phenol group and a deprotonated amide. To explain why osmium compounds of this ligand are interesting to us, it is necessary to review some previous results obtained in our group.

As stated in Chapter 1, the electro-oxidation of *trans*-Os(CHBA-Et)(py)<sub>2</sub> ( $H_4CHBA-Et \equiv 1,2$ -bis(3,5-dichloro-2-hydroxybenzamido)ethane [Figure 1.1]) in the presence of alcohol-caused ligand decomposition through a complex sequence of oxidation and hydrolysis steps of the PAC ligand's ethylene bridge. A large number of the intermediates were isolated and characterized to give remarkable knowledge of the decomposition sequence.<sup>1,2</sup> This decomposition sequence is shown in detail in Scheme 1.1. The final product isolated from the decomposition sequence was *cis*- $\alpha$ -Os( $\eta^2$ -CHBA)<sub>2</sub>(py)<sub>2</sub> (21) shown in Figure 4.1. The oxidation and hydrolysis reactions cleave the ethylene bridge and remove the two carbon atoms to give two bidentate ligands containing primary amide groups. Also during the decomposition, isomerization occurs to give the *cis*- $\alpha$  isomer of 21. Further electrochemical experiments with 21 showed that a solution of 21 with added primary or secondary alcohol would effect the catalytic electrochemical oxidation of the alcohol.<sup>2,3</sup>

Interest in the catalytic properties of this compound, 21,

**Figure 4.1.** Structure of *cis*- $\alpha$ -Os( $\eta^2$ -CHBA)<sub>2</sub>(py)<sub>2</sub> (21).



(L = py)

**21**

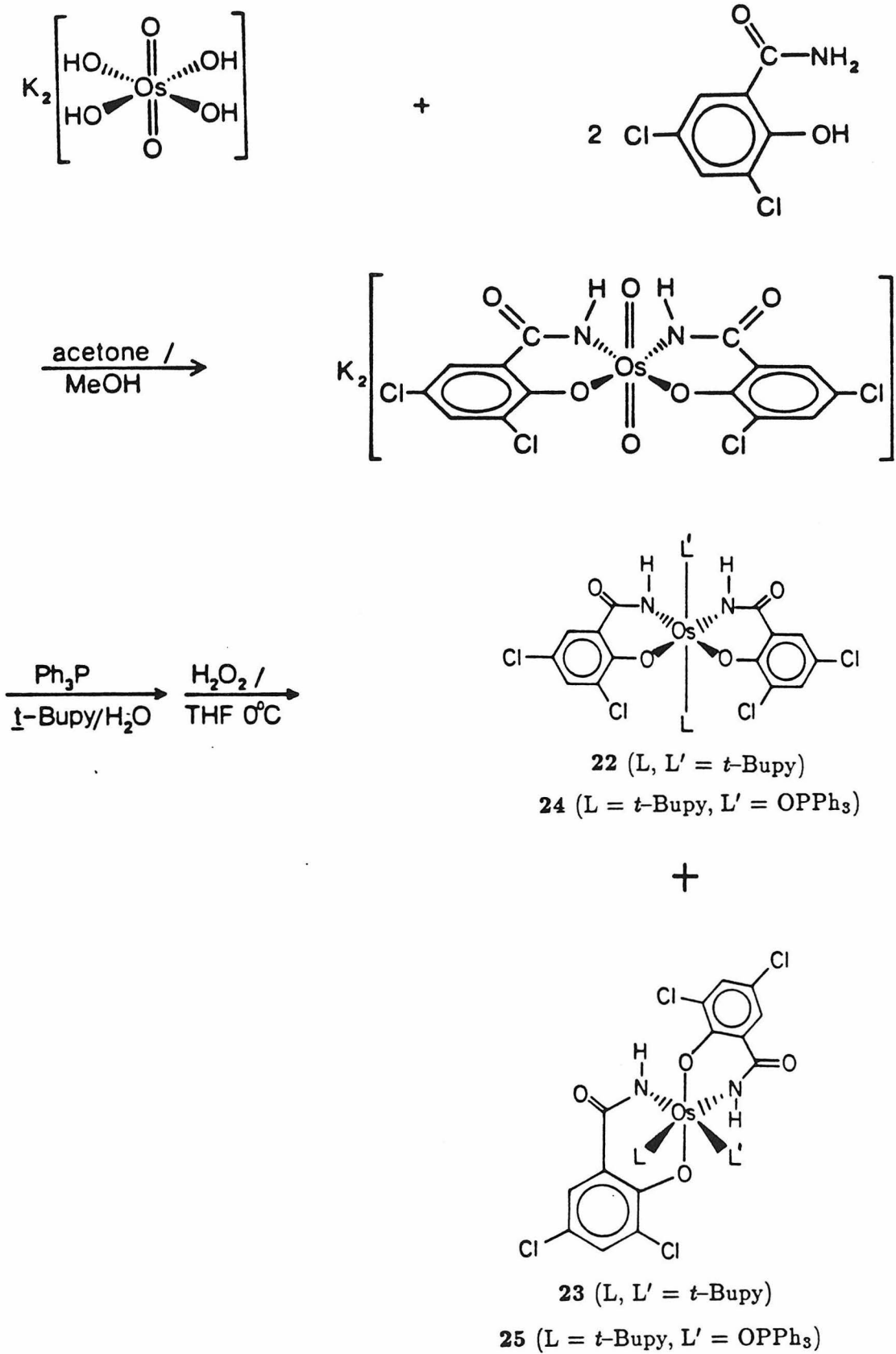
prompted attempts at alternative syntheses of osmium compounds containing two CHBA ligands and two pyridine-type ligands. A synthetic method analogous to that used for osmium with tetradentate PAC ligands was developed.  $K_2[Os(OH)_4(O)_2]$  reacted with two equivalents of  $H_2CHBA$  to give the trans-dioxo osmium(VI) complex,  $K_2[Os(\eta^2-CHBA)_2(O)_2]$ . This compound was reduced to osmium(III) with triphenyl phosphine in 4-*t*-butylpyridine and then oxidized with hydrogen peroxide to give a mixture of osmium(IV) complexes, which included *trans*- $Os(\eta^2-CHBA)_2(t-Bupy)_2$  (22), *cis- $\alpha$* - $Os(\eta^2-CHBA)_2(t-Bupy)_2$  (23), *trans*- $Os(\eta^2-CHBA)_2(t-Bupy)(OPPh_3)$  (24), and *cis*- $Os(\eta^2-CHBA)_2(t-Bupy)(OPPh_3)$  (25). (Scheme 4.1.)<sup>2</sup> Each of these compounds was found to exhibit electro-catalytic activity with alcohols.

Detailed studies of the electrochemical catalysis were carried out that gave a good deal of information about the catalysis. The oxidation reactions with primary or secondary alcohols gave the corresponding aldehydes or ketones. Selectivity was very good. No further oxidation was observed, and it was shown that the osmium complexes would not electro-oxidize aldehydes or ketones. A variety of alcohols could be oxidized, and all four complexes, 22, 23, 24, and 25 exhibited catalytic activity. Although the oxidation reactions were very selective, the catalysts were not long-lived, and the "best" oxidations gave turnover numbers of about 200.

Decomposition of the osmium catalysts begins with the passage of current. Evidence obtained suggests that decomposition is due to dissociation of a monodentate ligand (loss of *t*-butylpyridine or triphenylphosphine oxide) at the osmium(V) state. Electrochemical oxida-

**Scheme 4.1.** Synthesis of  $\text{Os}(\eta^2\text{-CHBA})_2(\text{L})_2$  complexes.





tion of the osmium species leads to two competing reactions: oxidation of alcohol and decomposition of the active catalyst. The decomposition of the catalyst is fast enough that the catalysts are short-lived.

Since catalyst decomposition is believed to involve loss of the monodentate pyridine or phosphine oxide ligand, replacing the two monodentate auxiliary ligands with a bidentate ligand (for example bipy or dppe) should slow ligand dissociation and improve catalyst lifetimes. The goal is to synthesize a complex analogous to **21** with one bipyridine ligand replacing two pyridine ligands. This has proved to be a difficult synthetic problem.

## Results and Discussion

As shown in Scheme 4.1, a fair amount of synthetic chemistry of  $\text{Os}(\eta^2\text{-CHBA})_2$  species had already been developed, and the species *cis*- $\alpha\text{-Os}(\eta^2\text{-CHBA})_2(t\text{-Bupy})_2$  (**23**) had been prepared. The simplest strategy to make a bipyridine compound was a ligand exchange reaction with **23**, replacing the two *t*-butylpyridine ligands with a bipy ligand.

*cis*- $\alpha\text{-Os}(\eta^2\text{-CHBA})_2(t\text{-Bupy})_2$  (**23**) does not react with bipyridine in either the Os(III) or Os(IV) oxidation states. The reactions have been tried with both neutral **23**, and with anionic Os(III) **23** produced by reduction of the Os(VI) dioxo with triphenylphosphine in the presence of *t*-butylpyridine. In both cases the pyridine ligands are not labile and ligand exchange reactions are not observed. Increasing the temperature of the reactions leads to decomposition of the complexes before any ligand exchange is observed.

The second approach to making the desired bipyridine product is to reduce the osmium(VI) dioxo,  $\text{K}_2[\text{Os}(\eta^2\text{-CHBA})_2(\text{O})_2]$ , with triphenylphosphine in the presence of bipyridine rather than pyridine. This approach has also been unsuccessful. Reduction of the dioxo in the presence of bipyridine leads to a mixture of uncharacterizable products.

Our experience with PAC ligand complexes of osmium has shown that osmium(IV) phosphine complexes are quite reactive to replacement of phosphine ligands by other donor ligands.<sup>4</sup> For example, *trans*- $\text{Os}(\eta^4\text{-HBA-B})(\text{PPh}_3)_2$  and *trans*- $\text{Os}(\eta^4\text{-CHBA-DCB})(\text{PPh}_3)_2$  react readily with phosphines, pyridines, and bipyridine. If a complex such as  $\text{Os}(\eta^2\text{-$

CHBA)<sub>2</sub>(PPh<sub>3</sub>)<sub>2</sub> were made, it might be susceptible to ligand exchange, and exchange two phosphine ligands for a dppe or bipy ligand.

The osmium(IV) bis triphenylphosphine complexes containing the tetradentate PAC ligands are prepared by reducing the osmium(VI) dioxos with a large excess of triphenylphosphine. Acid is needed to allow the reaction to proceed. Reaction of K<sub>2</sub>[*trans*-Os(η<sup>2</sup>-CHBA)<sub>2</sub>(O)<sub>2</sub>] with triphenylphosphine and acid, with no pyridines present, gives many products, none of which have been characterized.

Using a more reducing phosphine, we have been able to reduce the dioxo species with water as the only acid present. Dissolving K<sub>2</sub>-[*trans*-Os(η<sup>2</sup>-CHBA)<sub>2</sub>(O)<sub>2</sub>] in a THF/ethanol/water mixture and adding excess tri-*n*-butylphosphine gives an immediate color change from light orange to deep red. The deep red color is usually indicative of the osmium(III) oxidation state. Oxidation with solid K<sub>2</sub>S<sub>2</sub>O<sub>8</sub> gives a purple solution that contains a mixture of products. After successive column chromatography and preparative thin-layer chromatography, the two major products of the reaction, a blue species and a red species, can be isolated. Both compounds are paramagnetic with room temperature μ<sub>eff</sub> of ~0.9 BM, but both give well-resolved <sup>1</sup>H NMR spectra. The <sup>1</sup>H NMR spectra of the blue and red species are quite similar, both indicating the presence of two CHBA ligands and two PBu<sub>3</sub> ligands per osmium. The mass spectrum<sup>5</sup> of the blue species shows a molecular ion peak at 1004 mass units, suggesting the formulation Os(η<sup>2</sup>-CHBA)<sub>2</sub>-(PBu<sub>3</sub>)<sub>2</sub>, which has a molecular weight of 1002.9.<sup>6</sup> The NMR spectrum indicates a symmetry element present in the molecule, requiring the *trans* or *cis-α* geometry. The two possibilities cannot be distin-

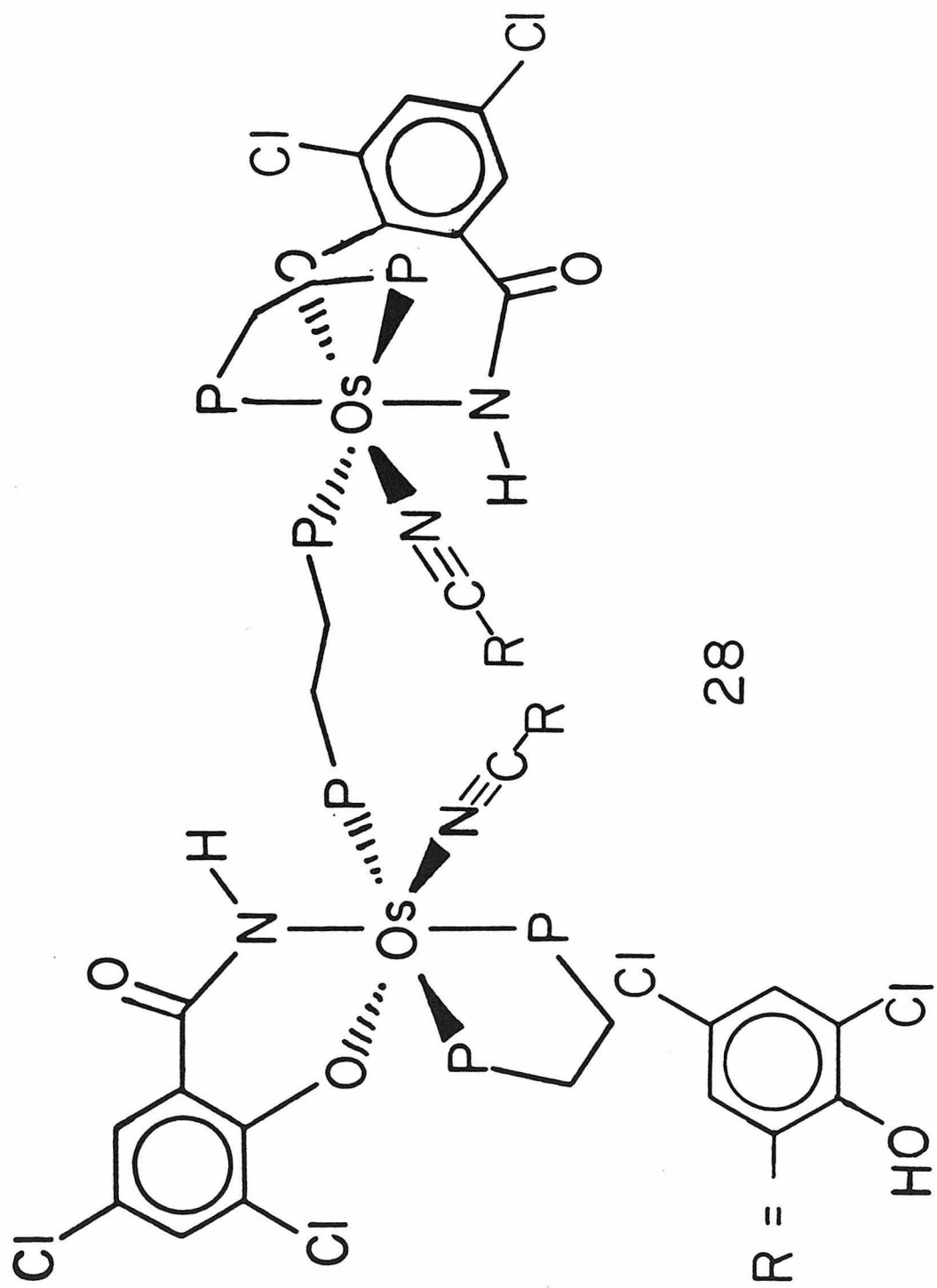
guished by the spectroscopic evidence, but we feel that *cis* tri-*n*-butylphosphine ligands would be unfavorable, and we formulate the blue compound as *trans*-Os( $\eta^2$ -CHBA)<sub>2</sub>(PBU<sub>3</sub>)<sub>2</sub> (26). The mass spectrum of the red compound shows a molecular ion at 1035 mass units, which is consistent with the formulation of Os( $\eta^2$ -CHBA)<sub>2</sub>(OPBU<sub>3</sub>)<sub>2</sub> (M.W. = 1034.9). Again, the <sup>1</sup>H NMR spectrum suggests the geometry is *trans* or *cis- $\alpha$* . We favor the formulation of the red species as *trans*-Os( $\eta^2$ -CHBA)<sub>2</sub>(OPBU<sub>3</sub>)<sub>2</sub> (27) for the same reason that we formulate 26 as the *trans* isomer.

The PBU<sub>3</sub> and OPBU<sub>3</sub> ligands are not as labile as we had hoped, although we would expect them to be less labile than PPh<sub>3</sub> ligands. Complex 27 shows no evidence of ligand exchange, and 26 gives a limited substitution chemistry. The blue 26 reacts with *t*-butylpyridine to give the bis pyridine species, Os( $\eta^2$ -CHBA)<sub>2</sub>(*t*-Bupy)<sub>2</sub>, but does not react at all with bipyridine. Triphenylphosphine also does not react, but 26 reacts with dppe in refluxing toluene to give a mixture of compounds. The only species isolated is a bright yellow compound, 28, obtained in low yield after chromatography of the reaction mixture. The yellow material is diamagnetic. Its <sup>1</sup>H NMR spectrum shows a multitude of resonances between 6.3 and 7.6 ppm that make the spectrum unassignable. The <sup>1</sup>H NMR spectrum also shows broad resonances in the 1.5 to 3.0 ppm range indicative of dppe bridge resonances. The cyclic voltammogram of a dichloromethane solution of 28 shows two reversible oxidations at +0.06 and +0.28 V vs. Fc<sup>+</sup>/Fc, and an irreversible oxidation at +0.77 V vs. Fc<sup>+</sup>/Fc. The small separation (220 mV) of the potentials of the redox couples suggests that 28 might be a dimer.

The fact that only oxidations are observed, and that **28** is diamagnetic, suggests that the oxidation state of the osmium is Os(II). A mass spectrum of **28** shows a molecular ion peak at 2359 mass units, confirming the dimer formulation. (A solution molecular weight determination also supports this.) The IR spectrum shows a moderate N-H stretch at  $3200\text{ cm}^{-1}$ , and a strong amide carbonyl stretch at  $1650\text{ cm}^{-1}$ . It also shows a moderate peak at  $2190\text{ cm}^{-1}$ .

Crystals of **28** were grown from a dichloromethane/ethanol solution and an X-ray diffraction study was carried out.<sup>7</sup> The complex crystallizes in the space group  $P2_1/n$ . The structure of the dimeric molecule is shown in Figure 4.2. The molecule consists of two octahedral osmium(II) centers linked by a dppe ligand. Each osmium also coordinates one bidentate dppe ligand, one bidentate CHBA ligand, and one monodentate 3,5-dichloro-2-hydroxybenzotrile ligand. The benzotrile ligand is formed from dehydration of a CHBA ligand amide group. The phenol groups of these ligands are protonated and are not coordinated. For this structure, data collection was stopped before a complete second shell of data was collected, due to decomposition of the crystal. A disorder of a solvent molecule of crystallization is also present. The shortage of data for such a large molecule, combined with the disorder problem, makes good refinement of the data difficult. The structure of the molecule is determined, but due to the poor refinement, reliable bond distances and angles are not available. Since the discussion of **28** does not rely on bond distances or angles in this complex, these data are not reported here. It is possible that modeling of the disorder, or constrained refinement would

**Figure 4.2.** Structure of  $[\text{Os}(\text{dppe})(\eta^2\text{-CHBA})(\eta^1\text{-CHBN})]_2\text{-}(\text{dppe})$  (**28**).





lead to more accurate structural parameters.<sup>8</sup>

Complex **28** is formulated as  $[\text{Os(II)(dppe)(}\eta^2\text{-CHBA)(}\eta^1\text{-CHBN)]_2\text{-}$   
(dppe) (CHBN  $\equiv$  3,5-dichloro-2-hydroxybenzotrile). The osmium(II) formulation fits with the magnetic properties and the  $^1\text{H}$  NMR spectrum. The calculated molecular weight of **28** is 2359.7, in agreement with the mass spectral data. In the course of the reaction the  $\text{PBu}_3$  ligands have been lost, and dppe ligands coordinate, and also the osmium is reduced to the Os(II) state, perhaps by excess phosphines in the reaction mixture. An interesting aspect of this reaction is the formation of the nitrile ligands. Partial dissociation of one of the CHBA ligands on each metal has occurred and the amide has been dehydrated to a nitrile ligand. (The nitrile ligands explain the band at  $2190\text{ cm}^{-1}$  in the IR spectrum.) Dehydration of a primary amide to give the corresponding nitrile is not uncommon,<sup>9</sup> but usually a dehydrating agent is required. The reverse reaction, partial hydrolysis of a nitrile to produce an amide, is known to be effected by transition metal species.<sup>10</sup>

Osmium complexes of CHBA, with bidentate auxiliary ligands have not been made, but some new osmium(IV) complexes containing two CHBA ligands have been, namely *trans*- $\text{Os}(\eta^2\text{-CHBA})_2(\text{PBu}_3)_2$  (**26**), and *trans*- $\text{Os}(\eta^2\text{-CHBA})_2(\text{OPBu}_3)_2$  (**27**). Since these complexes are similar to the complexes known to be electrochemical catalysts, **26** and **27** have been tested for catalysis. In the cases of catalysts **22–25**, a cyclic voltammogram of a solution of the catalyst, with added 1 M benzyl alcohol, shows an anodic wave indicating a catalytic oxidation. Similar experiments with **26** and **27** have been carried out.

From the previous catalytic studies it is postulated that the active catalytic species is the monoprotinated form of  $\text{Os}(\eta^2\text{-CHBA})_2(\text{L})_2$ . A good way of testing a complex for catalytic electro-oxidation is to add a strong acid and 1 M benzyl alcohol to the osmium complex solution and record the cyclic voltammogram, scanning to a potential high enough to oxidize the osmium complex. If catalytic oxidation is occurring, a large anodic wave should be observed.

The cyclic voltammogram of a dichloromethane solution of *trans*- $\text{Os}(\eta^2\text{-CHBA})_2(\text{PBU}_3)_2$  (26) is shown in Figure 4.3(A). The Os(IV/III) couple is at  $-0.73$  V vs.  $\text{Fc}^+/\text{Fc}$ . The CV also shows an irreversible oxidation at  $+0.54$  V vs.  $\text{Fc}^+/\text{Fc}$ . Figure 4.3(B) shows a CV of the same solution after a large excess of  $\text{HClO}_4$  is added. In the protonated species, the Os(IV/III) couple is shifted to  $+0.26$  V. If benzyl alcohol is added to give a concentration of 1 M, the CV shown in Figure 4.3(C) is the result. We still observe the Os(IV/III) couple, and there is a peak at  $+0.8$  V vs.  $\text{Fc}^+/\text{Fc}$ . It is difficult to say what the new peak at  $+0.8$  V is due to, but it seems there is no catalytic oxidation of benzyl alcohol.

The CV of a dichloromethane solution of *trans*- $\text{Os}(\eta^2\text{-CHBA})_2(\text{OPBu}_3)_2$  (27) is shown in Figure 4.4(A). The  $\text{OPBu}_3$  ligands are better donors than the  $\text{PBU}_3$  ligands, and the Os(IV/III) couple is observed at  $-1.25$  V vs.  $\text{Fc}^+/\text{Fc}$ . An irreversible oxidation is seen at  $+0.50$  V. Adding excess  $\text{HClO}_4$  shifts the Os(IV/III) couple to  $-0.28$  V vs.  $\text{Fc}^+/\text{Fc}$ . (Figure 4.4(B).) There is still an irreversible oxidation at about  $+0.8$  V. Adding benzyl alcohol to give a concentration of 1 M gives the CV shown in Figure 4.4(C). At about  $+0.8$  V a large anodic

**Figure 4.3** Cyclic voltammograms of *trans*-Os( $\eta^2$ -CHBA)<sub>2</sub>-(PBU<sub>3</sub>)<sub>2</sub> (**26**).

Recorded in CH<sub>2</sub>Cl<sub>2</sub>/0.1 M TBAP containing 1 mM **26**, using a BPG working electrode (0.17 cm<sup>2</sup>). Scan rate = 200 mV s<sup>-1</sup>. Scale is referenced in volts vs. the Fc<sup>+</sup>/Fc couple.

(A) only **26**.

(B) **26** with excess HClO<sub>4</sub>.

(C) **26** plus HClO<sub>4</sub> plus 1 M benzyl alcohol.

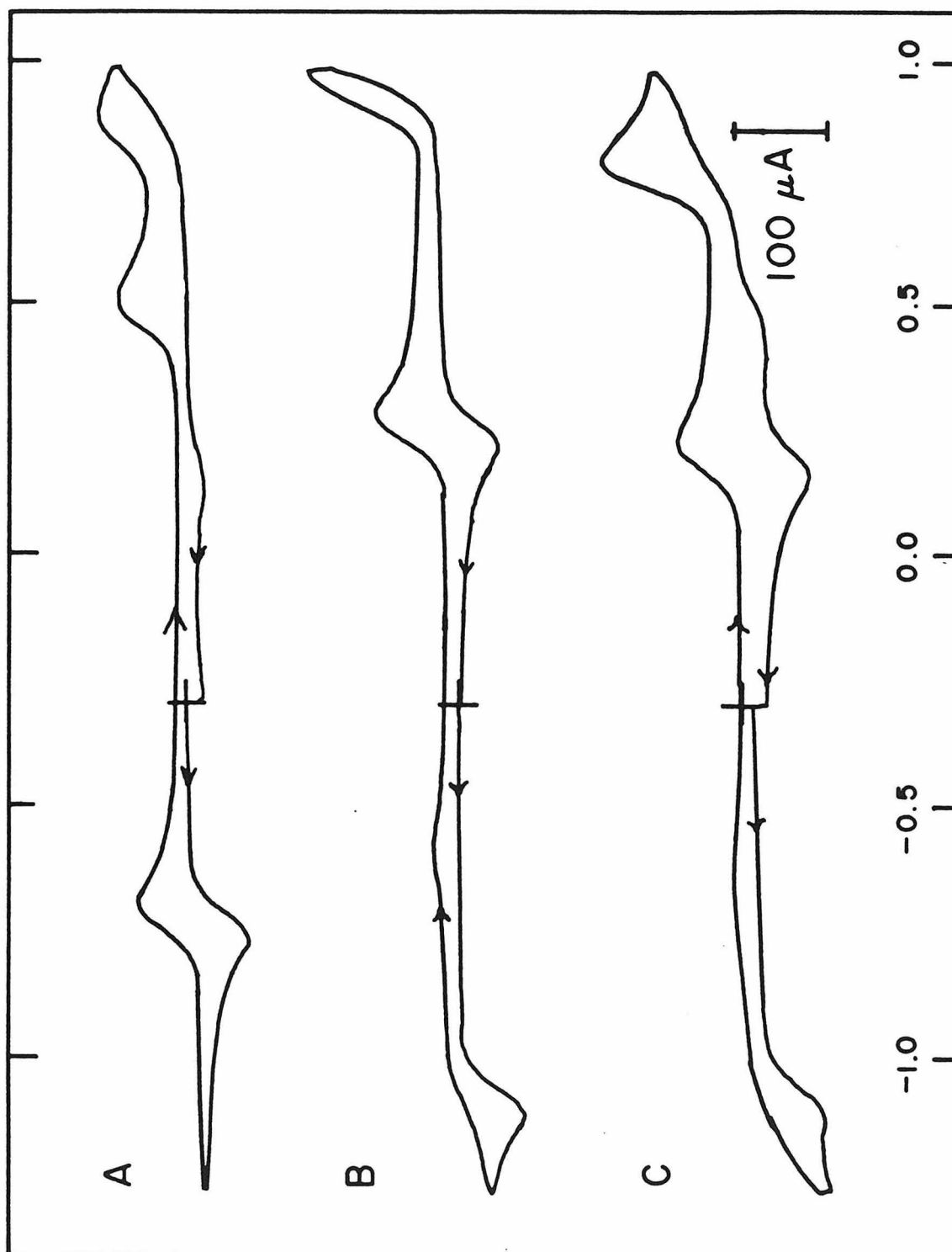


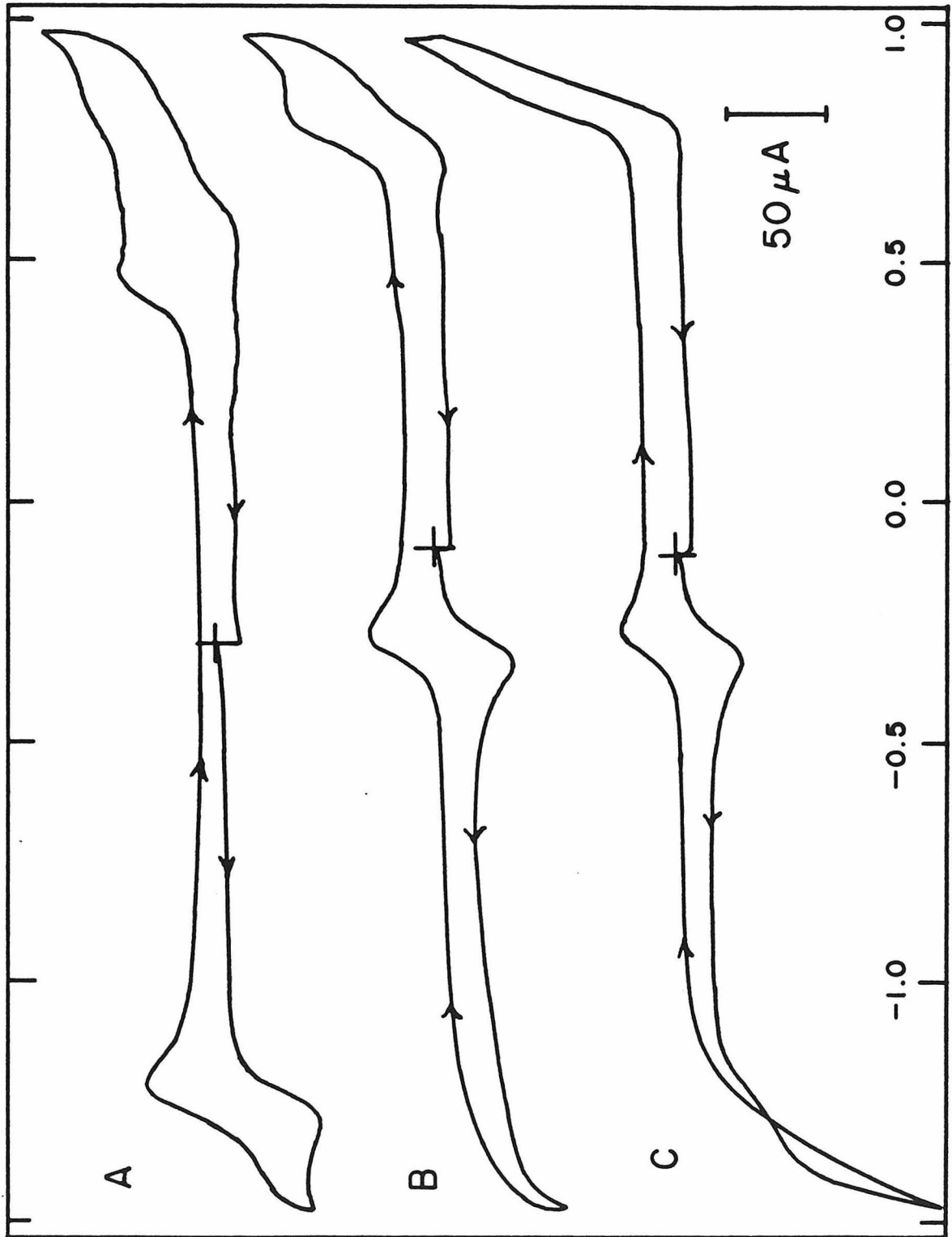
**Figure 4.4.** Cyclic voltammograms of *trans*-Os( $\eta^2$ -CHBA)<sub>2</sub>(OPBu<sub>3</sub>)<sub>2</sub> (27). Recorded in CH<sub>2</sub>Cl<sub>2</sub>/0.1 M TBAP containing 1 mM 27, using a BPG working electrode (0.17 cm<sup>2</sup>). Scan rate = 200 mv s<sup>-1</sup>.

Scale is in volts vs. the Fc<sup>+</sup>/Fc couple.

(A) 27.

(B) 27 plus excess HClO<sub>4</sub>.

(C) 27 plus excess HClO<sub>4</sub> plus 1 M benzyl alcohol.



current begins to flow. Compared to some of the catalytic waves observed previously,<sup>1-3</sup> it is small, but nonetheless it appears to be a catalytic wave.

Of the catalysts studied previously, 22-25, some were better catalysts than others, and gave larger catalytic waves in the CV than the others.<sup>1-3</sup> The CV's of some of the catalysts show catalytic oxidation waves that are almost imperceptible. In order to determine if compounds 26 and 27 are really catalysts for the electro-oxidation of alcohols, and to get an idea of how good they are, a series of experiments must be done. Electrolyses experiments measuring the charge consumed, analysis of organic products, control electrolyses with aldehydes and ketones, experiments varying catalyst concentration, alcohol, alcohol concentration, *et cetera*, are some of these experiments. A thorough study of these complexes has not yet been undertaken.

It is interesting that *trans*-Os( $\eta^2$ -CHBA)<sub>2</sub>(PBU<sub>3</sub>)<sub>2</sub> (26) does not appear to be an electro-catalyst. The redox potentials of this complex might not be at the proper potentials to give catalysis. It is possible that the Os(V/IV) couple of the protonated 26 is at a high enough potential that oxidation to Os(V) does not occur in the CV experiment. An unfavorable steric interaction between the bulky PBU<sub>3</sub> ligands and alcohol substrate might also be a factor. In *trans*-Os( $\eta^2$ -CHBA)<sub>2</sub>(OPBU<sub>3</sub>)<sub>2</sub> (27), the redox potentials are lower and might allow oxidation to Os(V) starting a catalytic cycle. The OPBU<sub>3</sub> ligands would also allow more room around the metal than the PBU<sub>3</sub> ligands, which might be why 27 appears to be a catalyst and 26 does not. Question as these cannot be answered without a detailed study.

## Conclusions

This project had the goal of preparing an  $\text{Os}(\eta^2\text{-CHBA})_2(\text{bipy})$  complex. What should be thermodynamically stable proved to be synthetically difficult to obtain. In the process of working toward the target molecule, some interesting compounds were prepared and we gained knowledge of these ligand systems, but the goal was not realized.

Several reasons the target molecule is difficult to synthesize can be expressed. We have seen that ligand exchange reactions of the osmium(IV) species are not facile. The simple pyridine exchange reactions are not facile. In the case of the complex with  $\text{PBu}_3$  ligands, which does show some ligand exchange reactivity, we also observe no exchange with bipyridine. We have not observed isomerization in a reaction of these osmium(IV) species,  $\text{Os}(\eta^2\text{-CHBA})(\text{L})_2$ , converting a trans complex to a cis complex, or vice versa. Production of cis complexes only occurs in reductions from Os(VI) to Os(IV), or in the electrochemical decomposition sequence. It may well be that not only ligand exchange, but also trans to cis isomerization, is very slow in these complexes. If trans to cis isomerization is not favorable, it will be difficult to make a bipyridine product starting with a trans Os(IV) species. Perhaps a more promising route to the desired complexes starts with the osmium(VI) dioxo,  $\text{K}_2[\text{Os}(\eta^2\text{-CHBA})_2(\text{O})_2]$ , and reduces it with dppe or dmpe. Experiments along these lines have also been tried, but the results are not promising.



## Experimental

**Materials.** Acetone (Mallinckrodt), chlorine (Matheson), diethyl ether (Baker), ethanol (U.S. Industrial), hexanes (Aldrich), and toluene (Aldrich), were reagent grade and were used as received, unless otherwise noted. Dichloromethane (Baker) and tetrahydrofuran (Baker) were distilled from calcium hydride prior to use. 2,2'-bipyridine (99%, Aldrich), 1,2-bis(diphenylphosphino)ethane (97%, Aldrich), osmium tetroxide (99.8%, Alfa), potassium persulfate (Baker), pyridine (Baker), tri-*n*-butylphosphine (Aldrich) (98.5%, MCB), and triphenylphosphine (99%, Aldrich) were all used as received. Silica gel used in column chromatography was 60-200 mesh (Davison). Preparative TLC plates were silica gel (GF 2000, Analtech).

**Physical Measurements.**  $^1\text{H}$  NMR spectra were recorded at 399.7822 MHz on a JEOL GX-400 spectrometer.  $^1\text{H}$  chemical shifts are reported in ppm( $\delta$ ) vs.  $\text{Me}_4\text{Si}$  with the solvent ( $\text{CDCl}_3$ ,  $\delta$  7.24) as internal standard. Infrared spectra were recorded on a Beckman IR 4240 spectrometer. Magnetic moments were obtained on a Cahn Faraday magnetic susceptibility balance equipped with a permanent magnet. The magnetic balance was calibrated using  $\text{HgCo}(\text{SCN})_4$ . Mass spectra were obtained from the Southern California Regional Mass Spectral facility at the University of California, Riverside. Elemental analyses were obtained at the Caltech analytical facility. Solvents of crystallization were quantified by  $^1\text{H}$  NMR spectroscopy of the authentic samples submitted

for elemental analyses.

**Electrochemical Procedures.** Dichloromethane (Mallinckrodt) used in cyclic voltammetric experiments was reagent grade and was further purified by distillation from calcium hydride. TBAP supporting electrolyte (Southwestern Analytical Chemicals) was dried, recrystallized twice from acetone/diethyl ether, and then dried under vacuum. The TBAP concentration in all solutions was 0.1 M. BPG electrodes (Union Carbide Co., Chicago) used for cyclic voltammetry were cut and mounted as previously described. (See Chapter 2, ref. 33.) The reference electrode was a saturated KCl silver/silver chloride electrode (Ag/AgCl). All potentials are quoted with respect to the formal potential of the ferrocinium/ferrocene couple which, under these conditions, we have consistently measured as +0.48 V vs. SCE, or ca. +0.70 V vs. NHE.

Cyclic voltammetry was performed with a Princeton Applied Research Model 173/179 potentiostat/digital coulometer equipped with positive feedback IR-compensation and a Model 175 universal programmer. Current-voltage curves were recorded on a Houston Instruments Model 2000 X-Y recorder.

**X-ray Data Collection and Structure Determination of 28.** A crystal of  $[\text{Os}(\text{dppe})(\eta^2\text{-CHBA})(\eta^1\text{-CHBN})]_2(\text{dppe})$  (28) was obtained from a dichloromethane/ethanol solution. Intensity data were collected on an Enraf-Nonius CAD4 diffractometer with graphite monochromator using  $\text{Mo K}_\alpha$  radiation ( $\lambda = 0.7107 \text{ \AA}$ ). Intensity measurements were recorded for

all reflections in one quadrant ( $2\theta < 30^\circ$ ). Only partial data collection was completed for  $30^\circ < 2\theta < 40^\circ$  due to decomposition of the crystal. A total of 16,358 reflections were measured and averaged over 2/m symmetry to yield 7757 total averaged reflections. The positions of the osmium atoms were derived from a Patterson map. Subsequent Fourier and difference maps revealed all remaining nonhydrogen atoms. Refinement was carried out by full-matrix least-squares methods, minimizing  $\sum w(F_o^2 - F_c^2)^2$  for all nonhydrogen atoms, with isotropic thermal parameters for all atoms. A disorder in the solvent molecule of crystallization prevented final refinement. Cell constants and collection data are given in Table 4.1.

**Syntheses.** All reactions were carried out in air unless otherwise noted. 3,5-dichloro-2-hydroxybenzamide ( $H_2CHBA$ ) was obtained by chlorination of salicylamide with  $Cl_2$  gas.<sup>2</sup>  $K_2[trans-Os(\eta^2-CHBA)_2(O)_2]$  was prepared according to a method previously developed.<sup>1 1</sup>

$trans-Os(\eta^2-CHBA)_2(PBu_3)_2$  (26) and  $trans-Os(\eta^2-CHBA)_2(OPBu_3)_2$  (27).  $K_2[trans-Os(\eta^2-CHBA)_2(O)_2]$  (400mg; 0.56 mmol) was dissolved in a THF/ethanol/water mixture (60 mL/40 mL/3 mL). Tri-*n*-butylphosphine (1.5 mL; 6.0 mmol) was added and the mixture was stirred at room temperature (1 h).  $K_2S_2O_8$  (15 g) was added and the heterogeneous mixture was stirred at room temperature (8–24 h). The mixture was filtered through silica gel washing the purple solution through with THF. Water (10 mL) was added and the THF was removed on a rotary evaporator. The residue was extracted with diethyl ether, and the ether solution was washed with a saturated sodium chloride solution and dried

**Table 4.1.** Collection data and cell constants for the crystal structure determination of **28**.

Formula	$\text{C}_{106}\text{H}_{84}\text{N}_4\text{Cl}_8\text{O}_6\text{Os}_2\text{P}_6$
Formula Weight	2359.7
Unit-cell Constants	$a = 18.306(2)\text{\AA}$ , $b = 22.630(3)\text{\AA}$ , $c = 25.288(4)\text{\AA}$ , $\beta = 103.226(12)^\circ$ $V = 10197\text{\AA}^3$
Z	4
Space group	$\text{P}2_1/n$
$\mu(\text{MoK}\alpha)$	$30.4\text{ cm}^{-1}$
Scan type and speed	$\theta - 2\theta$ ; $4^\circ\text{ min}^{-1}$
Scan range	$1^\circ$ below $\text{K}\alpha_1$ to $1^\circ$ above $\text{K}\alpha_2$
Background counting	stationary counts for one half of scan time at each end of scan
Collection range (partial shell)	$\pm h, \pm k, \pm l$ ; $2\theta < 30^\circ$ $\pm h, \pm k, \pm l$ ; $30^\circ < 2\theta < 40^\circ$
No. of reflections measured	16358
No. of unique data, $m$	7757
No. of data with $I > 0$	6895
No. of data with $I > 3\sigma(I)$	5885
$R^a$ (for $I > 0$ )	0.136
$R$ (for $I > 3\sigma(I)$ )	0.120
Goodness of fit <sup>b</sup>	4.57

$$^a R = \sum ||F_o| - |F_c|| / \sum |F_o|$$

$$^b \text{Goodness of fit} = [w(F_o^2 - F_c^2)^2 / (m - p)]^{1/2}$$

over  $\text{MgSO}_4$ . After filtration, the ether was removed on a rotary evaporator and the residue was dissolved in a small amount of dichloromethane. The solution was chromatographed on a silica gel column, eluting excess tri-*n*-butylphosphine with dichloromethane. When blue products started to come off the column, elution with 5/1 dichloromethane/acetone was begun, the blue eluent collected, and later the red eluent collected separately. Eluting with acetone removed any remaining red product from the column. The compounds were further purified by several preparative TLC's (silica gel, 2000 microns, 5/1  $\text{CH}_2\text{Cl}_2$ /acetone).

The blue 26 was crystallized from ethanol/water, and the red 27 was crystallized from dichloromethane/hexanes. Yields were variable depending on the reaction time with persulfate. Longer reaction times increased the yield of 27 and decreased the yield of 26.

26. Yield: 90–163 mg (16–29%). Anal. Calcd for  $\text{C}_{38}\text{H}_{60}\text{N}_2\text{Cl}_4\text{O}_4\text{OsP}_2$ : C, 45.51; H, 6.03; N, 2.79. Found: C, 45.43; H, 5.97; N, 2.72.  $^1\text{H}$  NMR ( $\text{CDCl}_3$ ):  $\delta$  25.54 (s, 2H) CHBA(NH); 9.65 (d, 2H,  $J=3\text{Hz}$ ) CHBA; 8.44 (d, 2H,  $J=3\text{Hz}$ ) CHBA; 1.54 (broad s, 12H)  $\text{PBu}_3$ ; 1.19 (q, 12H,  $J=7\text{Hz}$ )  $\text{PBu}_3$ ; 0.84 (t, 18H,  $J=7\text{Hz}$ )  $\text{PBu}_3$ ;  $-0.65$  (broad s, 12H)  $\text{PBu}_3$ . IR (Nujol):  $3260\text{ cm}^{-1}$  (m),  $\nu(\text{NH})$ ;  $1615\text{ cm}^{-1}$  (s),  $\nu(\text{amide})$ .

27. Yield: 15–67 mg (3–11%). Anal. Calcd for  $\text{C}_{38}\text{H}_{60}\text{N}_2\text{Cl}_4\text{O}_6\text{OsP}_2$ : C, 44.10; H, 5.84; N, 2.71. Found: C, 43.82; H, 5.79; N, 2.71.  $^1\text{H}$  NMR ( $\text{CDCl}_3$ ):  $\delta$  21.17 (s, 2H) CHBA(NH); 9.77 (d, 2H,  $J=3\text{Hz}$ ) CHBA; 8.62 (d, 2H,  $J=3\text{Hz}$ ) CHBA; 1.89 (m, 12H)  $\text{OPBu}_3$ ; 1.43 (q, 12H,  $J=7\text{Hz}$ )  $\text{OPBu}_3$ ; 0.90 (t, 18H,  $J=7\text{Hz}$ )  $\text{OPBu}_3$ ; 0.69 (broad s, 12H)  $\text{OPBu}_3$ . IR (Nujol):  $3260\text{ cm}^{-1}$  (m),  $\nu(\text{NH})$ ;  $1620\text{ cm}^{-1}$  (s),  $\nu(\text{amide})$ .

$[\text{Os}(\text{dppe})(\eta^2\text{-CHBA})(\eta^1\text{-CHBN})_2(\text{dppe})]$  (28). *trans*-Os( $\eta^2\text{-CHBA}$ )<sub>2</sub>-  
 (PBU<sub>3</sub>)<sub>2</sub> (100 mg;  $1.0 \times 10^{-5}$  mol) and 1,2-bis(diphenylphosphino)ethane  
 (dppe) (280 mg; 0.70 mmol) were dissolved in toluene (35 mL) and  
 heated at reflux, under a nitrogen atmosphere (2h). The toluene was  
 removed on a rotary evaporator, and the residue was dissolved in a  
 small amount of dichloromethane. The solution was chromatographed on  
 a silica gel column, eluting with dichloromethane to remove excess  
 dppe, and then with 5/1 dichloromethane/acetone to collect brown and  
 yellow bands. The products were evaporated to dryness on a rotary  
 evaporator and the residue was dissolved in a small amount of di-  
 chloromethane. Preparative TLC (silica gel, 2000 microns) with 30/1  
 dichloromethane/acetone allowed the separation of a bright yellow  
 band. The yellow product was washed from the silica gel with THF and  
 crystallized from dichloromethane/ethanol. Yield: 43 mg (37%).  
 Anal. Calcd for C<sub>106</sub>H<sub>84</sub>N<sub>4</sub>Cl<sub>8</sub>O<sub>6</sub>Os<sub>2</sub>P<sub>6</sub>•0.25(CH<sub>2</sub>Cl<sub>2</sub>): C, 53.60; H, 3.58;  
 N, 2.35. Found: C, 53.37; H, 3.50; N, 2.40. <sup>1</sup>H NMR (CDCl<sub>3</sub>):  $\delta$  9.00  
 (s, 2H) CHBA(NH); 6.3–7.7 (m, 64H) aromatic; 5.59(m, 4H) aromatic;  
 1.4–3.2 (broad singlets, 12H) dppe, –CH<sub>2</sub>–. IR (Nujol): 3200 cm<sup>-1</sup>  
 (m),  $\nu$ (NH); 2190 cm<sup>-1</sup> (m),  $\nu$ (C≡N); 1620 cm<sup>-1</sup> (s),  $\nu$ (amide).

References

1. Anson, F.C.; Collins, T.J.; Coots, R.J.; Gipson, S.L.; Krafft, T.E.; *Inorg. Chem.* submitted.
2. Krafft, T.E. Ph.D. Dissertation, California Institute of Technology, Pasadena, California, 1985.
3. (a) Anson, F.C.; Collins, T.J.; Gipson, S.L.; Krafft, T.E. *Inorg. Chem.* submitted. (b) Gipson, S.L. Ph.D. Dissertation, California Institute of Technology, Pasadena, California, 1986.
4. (a) Anson, F.C.; Christie, J.A.; Collins, T.J.; Coots, R.J.; Furutani, T.T.; Gipson, S.L.; Keech, J.T.; Krafft, T.E.; Santarsiero, B.D.; Spies, G.H.; *J. Am. Chem. Soc.* **1984**, *106*, 4460-72. (b) See Chapter 2 of this thesis.
5. The mass spectra reported here were obtained at the Southern California Regional Mass Spectral Facility at the University of California, Riverside. The spectra were obtained using a Fast Atom Bombardment (FAB) method.
6. It is common in FAB mass spectra for protonation of the molecule to occur, and to observe the molecular ion at one mass unit greater than the molecular weight. Dr. Rich Kondrat, University of California, Riverside, personal communication.
7. The X-ray study was carried out by Sonny C. Lee and Bernard D. Santarsiero. Thanks go to them for their efforts.
8. B.D. Santarsiero, personal communication.
9. (a) Yokoyama, M.; Yoshida, S.; Imamoto, T. *Synthesis* **1982**, 591-2. (b) Barger, T.M.; Riley, C.M. *Synth. Commun.* **1980**, *10*,



- 479-87. (c) Olah, G.A.; Vankar, Y.D.; Garcia-Luna, A. *Synthesis* 1979, 227-8. (d) Harrison, C.R.; Hodge, P.; Rogers, W.J. *Synthesis* 1977, 41-3. (e) Campagna, F.; Carotti, A.; Casini, G. *Tetrahedron Lett.* 1977, 1813-16. (f) Hendrickson, J.B.; Schwartzman, S.M. *Tetrahedron Lett.* 1975, 277-80. (g) Relles, H.M.; Schluenz, R.W. *J. Am. Chem. Soc.* 1974, 96, 6469-75. (h) Graham, J.C.; Marr, D.H. *Can. J. Chem.* 1972, 50, 3857-60. (i) Monson, R.S.; Priest, D.N. *Can. J. Chem.* 1971, 49, 2897-8. (j) Dennis, W.E. *J. Org. Chem.* 1970, 35, 3253-5. (k) Norris, J.F.; Klemka, A.J. *J. Am. Chem. Soc.* 1940, 62, 1432-5.
10. (a) Ravindranathan, M.; Kalyanam, N.; Sivaram, S. *J. Org. Chem.* 1982, 479, 4812-13. (b) Paraskewas, S. *Synthesis* 1974, 574-5. (c) Watanabe, K.; Sakai, K. *Bull. Chem. Soc. Jpn.* 1966, 39, 8-14. (d) Watanabe, K. *Bull. Chem. Soc. Jpn.* 1964, 37, 1325-9.
11. Malin, J.M. *Inorg. Syn.* 1980, 20, 61-3.

## Chapter 5

### Synthesis of Osmium Complexes Containing 2-(2-hydroxyphenyl)imidazole Ligands

## Introduction

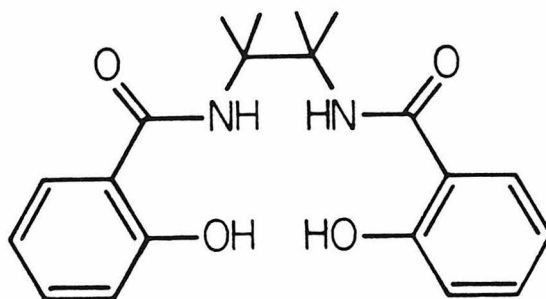
In the course of developing methods for coordinating PAC ligands to transition metals, a fusion reaction of  $(\text{NH}_4)_2[\text{OsCl}_6]$  with the PAC ligand  $\text{H}_4\text{HBA-DMB}$  ( $\text{H}_4\text{HBA-DMB} \equiv 2,3\text{-bis}(2\text{-hydroxybenzamido})\text{-}2,3\text{-dimethylbutane}$ ) (Figure 5.1) was tried. Fusion of finely-ground  $(\text{NH}_4)_2[\text{OsCl}_6]$  with two equivalents of  $\text{H}_4\text{HBA-DMB}$  at  $320\text{--}330^\circ\text{C}$  resulted in a black residue. An osmium complex was isolated from this residue and crystals of the complex suitable for an X-ray structure were grown.<sup>1</sup> The structure of the complex, *trans*- $\text{OsCl}_2(\eta^2\text{-}2\text{-(2-phenoxy)-}4,4,5,5\text{-tetramethylimidazoline})_2$  (29) is shown in Figure 5.2. The complex is a neutral osmium(IV) species coordinating two chloride ligands and two bidentate imidazoline-phenoxide ligands. At the high temperatures of the fusion reaction the  $\text{H}_4\text{HBA-DMB}$  molecule had decomposed forming the imidazoline ring and eliminating one of the hydroxybenzamide units.

We became interested in osmium compounds with this type of chelating ligand, and were interested in comparing the properties and oxidation chemistry associated with this type of complex, with osmium complexes of the tetradentate tetraanionic PAC ligands. Imidazole and imidazoline ligands can coordinate as neutral two-electron donor ligands or, when deprotonated, as anionic two-electron donor ligands. Bidentate imidazole-phenoxide ligands similar to those in 29 were especially interesting to us. These ligands, coordinated as dianions, have a resonance mechanism available to reduce the oxidation state of

the metal center (Scheme 5.1). This might enable these ligands to stabilize highly oxidized metal centers. In light of the versatile coordination chemistry available to these ligands, we thought that osmium complexes of these ligands would have interesting oxidation properties.

The goals of the project were to make bidentate imidazole and imidazoline ligands containing phenoxide groups. After the ligands had been prepared the coordination chemistry and the oxidation chemistry would be investigated.

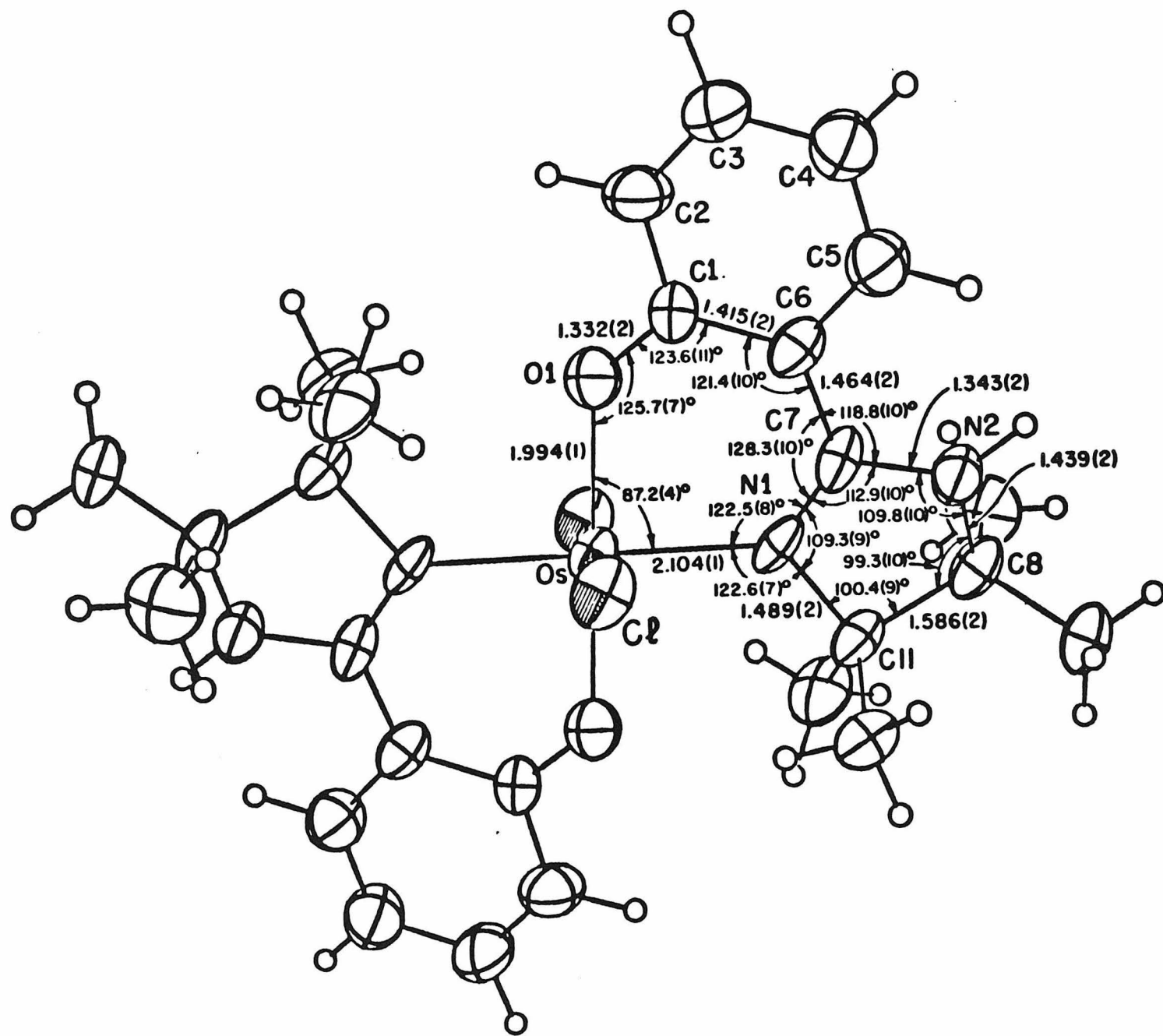
**Figure 5.1.** The PAC ligand  $H_4HBA$ -DMB.



2,3-bis(2-hydroxybenzamido)-2,3-dimethylbutane

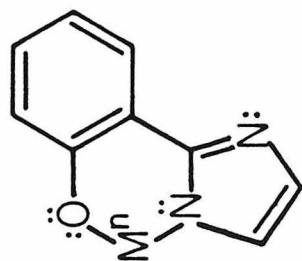
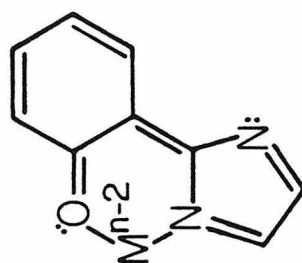
(H<sub>4</sub>HBA-DMB)

**Figure 5.2.** Structure of  $\text{OsCl}_2(\eta^2\text{-}2\text{-}(2\text{-phenoxy})\text{-}4,4,5,5\text{-tetramethylimidazoline})_2$ .





**Scheme 5.1.** Resonance of coordinated phenoxide-imidazole ligands.



## Results and Discussion

Several ligands with the desired features have been prepared. The prototype ligand, 2-(2-hydroxyphenyl)imidazole, is reported in the literature.<sup>2</sup> Its synthesis is shown in Scheme 5.2. This synthesis gives two potential ligands, 2-(2-hydroxyphenyl)imidazoline (30), and 2-(2-hydroxyphenyl)imidazole (31). This synthetic strategy has been used to prepare the additional compound, 2-(5-*t*-butyl-2-hydroxyphenyl)imidazoline (32), and a fourth ligand, 2-(2-hydroxyphenyl)-5,6-dimethylbenzimidazole (33), is available from Aldrich. (Figure 5.3.)

These ligands all react with  $K_2[Os(OH)(O)_2]$  in similar ways to give neutral osmium(VI) trans-dioxo complexes (Scheme 5.3). Mixing methanol solutions of  $K_2[Os(OH)_4(O)_2]$  and the bidentate ligand (2 eq) results in precipitation of the product as orange crystals.<sup>3</sup>

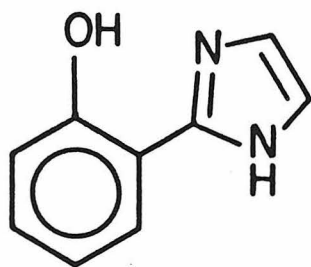
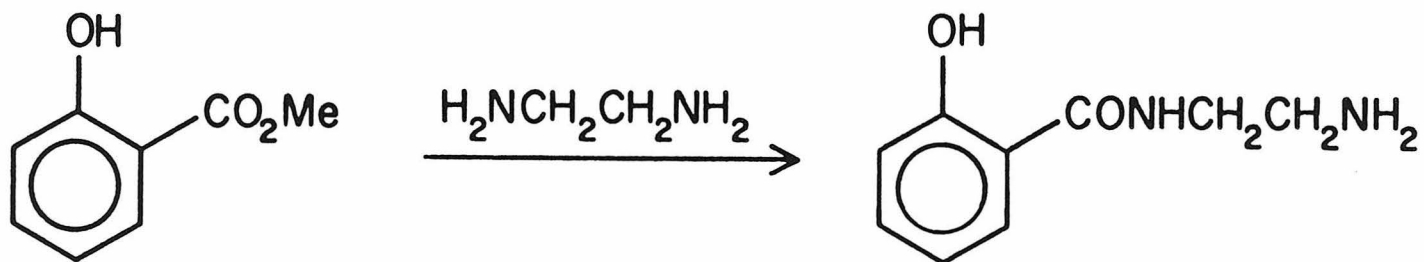
The IR spectra of these complexes all show strong bands in the 840–850  $cm^{-1}$  range, indicative of osmium trans-dioxo asymmetric stretches.<sup>4</sup> Labeling the oxo groups of 37 with  $^{18}O$  shifts the 840  $cm^{-1}$  band to 804  $cm^{-1}$  confirming the assignment. The IR spectra also show strong bands in the 3200–3400  $cm^{-1}$  range, indicative of N–H stretching modes. These data lead to the formulation of the osmium products as neutral osmium(VI) trans-dioxo complexes containing two bidentate, monoanionic chelating ligands, as shown in Scheme 5.3.

The only complex that exhibits any solubility is 37. The  $^1H$  NMR spectrum of this complex indicates that a symmetry element relates the two bidentate ligands, supporting the proposed structure.<sup>5</sup>

The poor solubility of the osmium complexes prohibits further re-

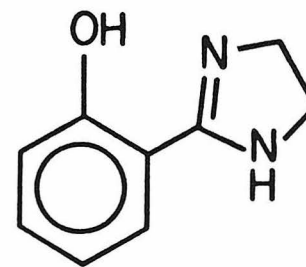
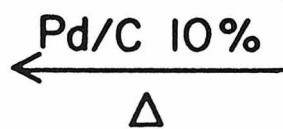
actions of these compounds. Attempts at making analogous ligands with attached *t*-butyl groups to improve the solubility of the complexes were unsuccessful.

**Scheme 5.2.** Synthesis of 2-(2-hydroxyphenyl)imidazole (31).



31

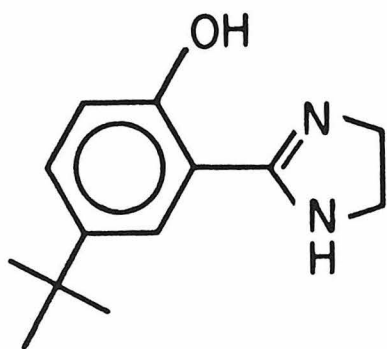
2-(2-hydroxyphenyl)imidazole



30

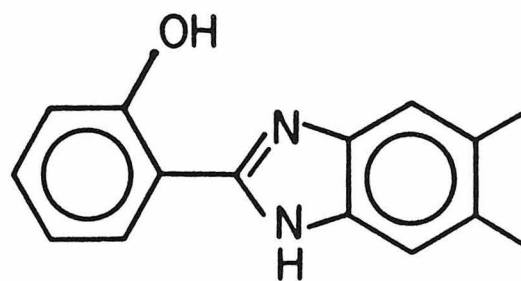
2-(2-hydroxyphenyl)imidazoline

**Figure 5.3.** The two ligands 2-(5-*t*-butyl-2-hydroxyphenyl)-imidazoline (32) and 2-(2-hydroxyphenyl)-5,6-dimethylbenzimidazole (33).



**32**

2-(5-*t*-butyl-2-hydroxyphenyl)imidazoline

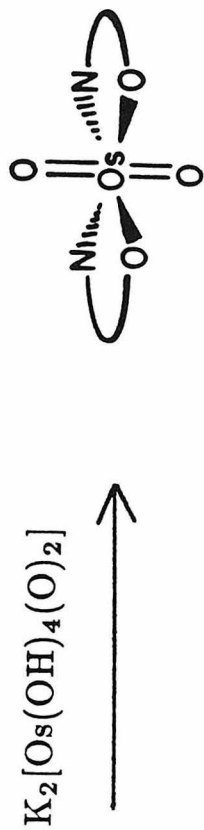


**33**

2-(2-hydroxyphenyl)-5,6-dimethylbenzimidazole



**Scheme 5.3.** Synthesis of osmium complexes of 2-(2-hydroxyphenyl)imidazole ligands.



30 , 31, 32 or 33

ligands coordinate as  
monoanions

## Conclusions

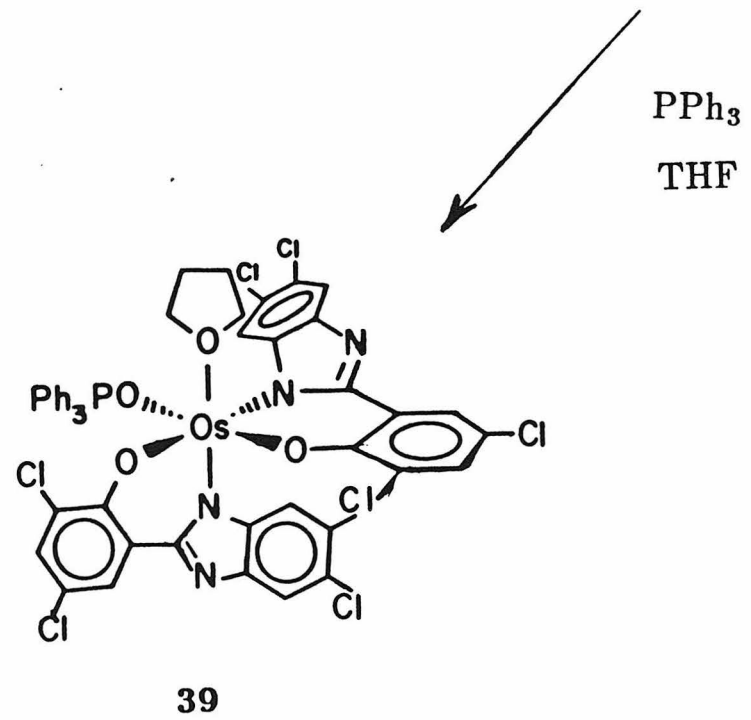
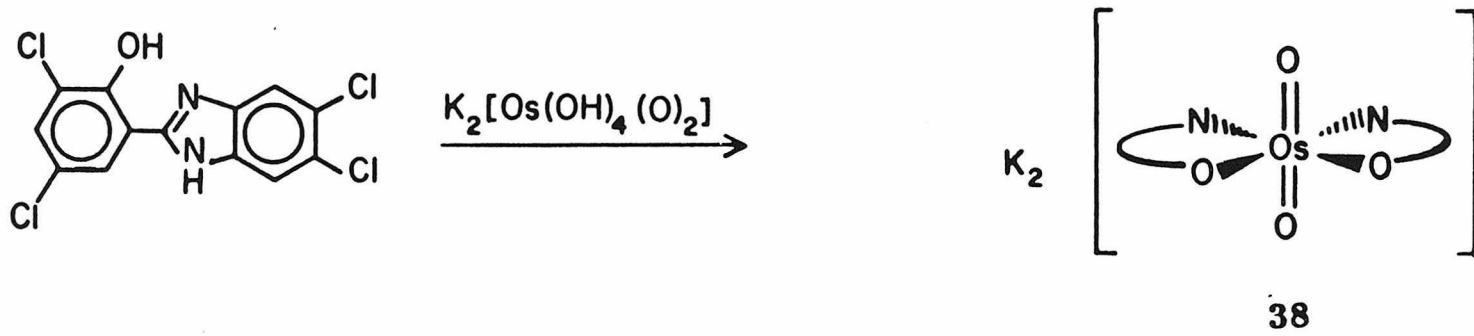
It appears that coordination of the bidentate imidazole-phenoxide ligands to osmium is easily achieved. The ligands coordinate as monoanions through a deprotonated phenol and a nitrogen atom of the imidazole or imidazoline ring. Further reactions of these complexes and investigation of their high oxidation state chemistry would be interesting, but solubility problems preclude such studies with the complexes available.

Since the time work on this project was discontinued, other ligands of this type have become available, and a limited investigation of their coordination chemistry has been carried out.<sup>6</sup> For example, 2-(3,5-dichloro-2-hydroxyphenyl)-5,6-dichlorobenzimidazole has been prepared, and reacts with  $K_2[Os(OH)_4(O)_2]$  as shown in Scheme 5.4. It is interesting that this ligand is found to coordinate as a dianion, giving the osmium(VI) trans-dioxo dianion (38), in contrast to what is observed for the ligands discussed above. Reaction of 38 with one equivalent of triphenylphosphine in THF produces a complex, 39, in low (<30%) yield. An X-ray crystal structure determination<sup>7</sup> of 39 shows it to have the structure shown in Scheme 5.4. The complex is a neutral osmium(IV) complex with the bidentate ligands coordinated as dianions, and triphenylphosphine oxide and tetrahydrofuran auxiliary ligands.

Perhaps with the availability of new 2-(2-hydroxyphenyl)benzimidazole ligands, and a synthetic route to octahedral osmium(IV) complexes coordinating the bidentate ligands as dianions, the oxidation

chemistry of these complexes, and the donor properties of these ligands can be investigated in detail.

**Scheme 5.4.** Osmium complexes with 2-(3,5-dichloro-2-hydroxyphenyl)-5,6-dichlorobenzimidazole ligands.



## Experimental

**Materials.** Benzene (thiophene free, Aldrich), diethyl ether (Baker), diphenyl ether (MCB), ethanol (U.S. Industrial), hexanes (Aldrich), and methanol (Baker) were reagent grade and were used as received, unless otherwise noted. Dichloromethane (Baker) was distilled from calcium hydride prior to use. 2-(2-Hydroxyphenyl)-4,5-dimethylbenzimidazole (Aldrich, Alfred Bader), methyl salicylate (MCB), osmium tetroxide (99.8%, Alfa), and palladium on carbon (10%, Aldrich) were used as received. Ethylenediamine (MCB) was freshly distilled prior to use. Silica gel used in column chromatography was 60–200 mesh (Davison).

**Physical Measurements.**  $^1\text{H}$  NMR spectra were recorded at 90 MHz on a Varian EM-390 spectrometer.  $^1\text{H}$  chemical shifts are reported in ppm( $\delta$ ) vs.  $\text{Me}_4\text{Si}$  with the solvent ( $\text{CDCl}_3$ ,  $\delta$  7.24;  $\text{DMSO-d}_6$ ,  $\delta$  2.49) as internal standard. Infrared spectra were recorded on a Beckman IR 4240 spectrometer. Elemental analyses were obtained at the Caltech analytical facility. Solvents of crystallization were quantified by  $^1\text{H}$  NMR spectroscopy of the authentic samples submitted for elemental analyses.

**Syntheses.** All reactions were carried out in air unless otherwise noted.  $\text{K}_2[\text{Os}(\text{OH})_4(\text{O})_2]$ <sup>8</sup> and 2-acetyl-5-*t*-butylsalicylic acid<sup>9</sup> were prepared as described in the literature.

**Methyl-5-*t*-butylsalicylate.** 5-*t*-butylsalicylic acid (1.99 g; 10.2 mmol) was dissolved in methanol (28 mL). Concentrated H<sub>2</sub>SO<sub>4</sub> (1.0 mL) was added and the solution was heated at reflux (1 h). The mixture was cooled to room temperature and added to water (10 mL). The organic product was extracted into diethyl ether (10 mL). The ether solution was washed with water (7 mL) and portions (7 mL) of 5% NaHCO<sub>3</sub>(aq) until the washings were basic. A final wash with saturated NaCl(aq) was done and the ether solution was dried over MgSO<sub>4</sub>. The solvent was removed under vacuum to give a white solid. Yield: 1.51 g (71%). <sup>1</sup>H NMR (CDCl<sub>3</sub>): δ 7.8 (d, 1H, J=3Hz) H<sub>6</sub>; 7.6 (dd, 1H, J=9,3Hz) H<sub>4</sub>; 6.9 (d, 1H, J=9Hz) H<sub>3</sub>; 3.9 (s, 3H) CH<sub>3</sub>; 1.3 (s, 9H) *t*-butyl. IR (Nujol): 3200 cm<sup>-1</sup> (s), ν(OH); 1682 cm<sup>-1</sup> (s), ν(CO). M.P.: 39–41°.

**2-(2-hydroxyphenyl)imidazoline (30).** This imidazoline, and the imidazole following were prepared according to the procedure outlined in the literature.<sup>2</sup> The details of the procedure are included here because the report in the literature is not detailed. Methylsalicylate (8.5 mL; 65.6 mmol) was added to freshly distilled ethylenediamine (13.4 mL; 198 mmol) and the mixture was heated at reflux (12 h). The volatiles were removed on a rotary evaporator leaving a yellow oil. Diphenyl ether (100 mL) was added to the oil and the solution was heated at reflux (4 h) under a nitrogen atmosphere. The solution was allowed to cool and a solid precipitated. The solid was filtered and washed with a large quantity of diethyl ether. Recrystallization from ethanol/hexanes gave tan needles. Yield: 1.0 g



(9.4%). The  $^1\text{H}$  NMR spectrum and the IR spectrum match those reported.

**2-(2-hydroxyphenyl)imidazole (31).** 2-(2-hydroxyphenyl)imidazoline (1.8 g; 11.1 mmol) was dissolved in diphenyl ether (12 mL), and palladium on carbon (10%, 150 mg) was added. The mixture was stirred and heated at reflux (5 h) under a nitrogen atmosphere. The hot reaction mixture was filtered through a pad of celite and allowed to cool. The mixture was chromatographed on a silica gel column eluting first with benzene to remove the diphenyl ether, and then with diethyl ether. The ether solution was reduced to a few milliliters on a rotary evaporator and placed in an ice bath to precipitate white crystals. The imidazole was filtered and washed with hexanes. Yield: 1.27 g (71%). The  $^1\text{H}$  NMR and IR spectra match those reported.

**2-(5-*t*-butyl-2-hydroxyphenyl)imidazoline (32).** Methyl-5-*t*-butylsalicylate (1.99 g; 9.56 mmol) was added to freshly distilled ethylenediamine (20 mL; 296 mmol) and the mixture was heated at reflux (12 h). The excess ethylenediamine was removed under vacuum leaving a thick golden oil. The oil was washed with two portions (5 mL) of dichloromethane, and each was removed under vacuum. Diphenyl ether (20 mL) was added and the solution was heated at reflux (4.5 h) under a nitrogen atmosphere. The mixture was chromatographed on a silica gel column eluting with dichloromethane to remove diphenyl ether and other impurities, and then with ethanol to remove the product. Hexanes were added to the ethanol solution to give pale yellow crystals. The solid was filtered and washed with hexanes. Yield: 0.40 g (20%).  $^1\text{H}$  NMR ( $\text{CDCl}_3$ ):  $\delta$  8.2 (broad s, 1H) NH; 7.3 (m, 2H)  $\text{H}_4$ ,  $\text{H}_6$ ; 6.9 (d, 1H,  $J=9\text{Hz}$ )  $\text{H}_3$ ; 3.8 (s, 4H)  $-\text{CH}_2\text{CH}_2-$ ; 1.3 (s, 9H) *t*-butyl.

*trans*-Os(2-(2-phenoxy)imidazoline)<sub>2</sub>(O)<sub>2</sub> (34). K<sub>2</sub>[Os(OH)<sub>4</sub>(O)<sub>2</sub>] (100 mg; 0.27 mmol) was dissolved in methanol (30 mL) and the solution was filtered. 2-(2-hydroxyphenyl)imidazoline (92 mg; 0.57 mmol) was dissolved in methanol (10 mL) and the two methanol solutions were poured together and stirred once. After a few minutes orange crystals precipitated from solution. The product was filtered and washed with methanol. Yield: 113 mg (76%). Anal. Calcd for C<sub>18</sub>H<sub>18</sub>N<sub>4</sub>O<sub>4</sub>Os: C, 39.70; H, 3.33; N, 10.29. Found: C, 39.82; H, 3.45; N, 10.29. IR (Nujol): 3370 cm<sup>-1</sup> (s), ν(NH); 855 cm<sup>-1</sup> (s), ν<sub>as</sub>(OsO<sub>2</sub>).

*trans*-Os(2-(2-phenoxy)imidazole)<sub>2</sub>(O)<sub>2</sub> (35). K<sub>2</sub>[Os(OH)<sub>4</sub>(O)<sub>2</sub>] (50 mg; 0.14 mmol) was dissolved in methanol (30 mL). This solution was added to a solution of 2-(2-hydroxyphenyl)imidazole (47 mg; 0.29 mmol) in methanol (10 mL). The solution was allowed to sit until product crystals had settled out. The volume of the solution was reduced on a rotary evaporator and the orange product filtered and washed with methanol. Yield: 35 mg (48%). Anal. Calcd for C<sub>18</sub>H<sub>14</sub>N<sub>4</sub>O<sub>4</sub>Os: C, 39.99; H, 2.62; N, 10.37. Found: C, 39.91; H, 2.76; N, 10.25. IR (Nujol): 3200 cm<sup>-1</sup> (s), ν(NH); 820 cm<sup>-1</sup> (s), ν<sub>as</sub>(OsO<sub>2</sub>).

*trans*-Os(2-(5-*t*-butyl-2-phenoxy)imidazoline)<sub>2</sub>(O)<sub>2</sub> (36). K<sub>2</sub>[Os(OH)<sub>4</sub>(O)<sub>2</sub>] (100 mg; 0.27 mmol) was dissolved in methanol (25 mL). A solution of 2-(5-*t*-butyl-2-hydroxyphenyl)imidazoline (122 mg; 0.56 mmol) in methanol (10 mL) was added to the osmium solution. After a minute orange crystals settled out and were filtered, and washed with methanol. Yield: 112 mg (63%). Anal. Calcd for C<sub>26</sub>H<sub>34</sub>N<sub>4</sub>O<sub>4</sub>Os: C, 47.54; H, 5.23; N, 8.53. Found: C, 47.76; H, 5.17; N, 8.47. IR (Nujol): 3370 cm<sup>-1</sup> (s), ν(NH); 840 cm<sup>-1</sup> (s), ν<sub>as</sub>(OsO<sub>2</sub>).

*trans*-Os(2-(2-phenoxy)-5,6-dimethylbenzimidazole)<sub>2</sub>(O)<sub>2</sub> (37). K<sub>2</sub>-[Os(OH)<sub>4</sub>(O)<sub>2</sub>] (100 mg; 0.27 mmol) was dissolved in methanol (60 mL). This solution was added to a solution of 2-(2-hydroxyphenyl)-5,6-dimethylbenzimidazole (130 mg; 0.55 mmol) in methanol (15 mL) and stirred once. The volume of the solution was reduced on a rotary evaporator, and brown crystals were precipitated by slowly adding diethyl ether. The crystals were filtered and washed with a small amount of methanol, and diethyl ether. Yield: 132 mg (70%). Anal. Calcd for C<sub>30</sub>H<sub>26</sub>N<sub>4</sub>O<sub>4</sub>Os•(H<sub>2</sub>O): C, 50.27; H, 3.94; N, 7.81. Found: C, 50.24; H, 3.71; N, 7.80. <sup>1</sup>H NMR (DMSO-d<sub>6</sub>): δ 8.1 (d, 2H, J=8Hz) phenyl; 7.3 (t, 2H, J=8Hz) phenyl; 7.2 (s, 2H) phenyl; 6.9 (d, 2H, J=8Hz) phenyl; 6.7 (t, 2H, J=8Hz) phenyl; 6.3 (s, 2H) phenyl; 2.4 (s, 2H) NH; 2.2 (s, 6H) methyl; 1.7 (s, 6H) methyl. IR (Nujol): 840 cm<sup>-1</sup> (s), ν<sub>as</sub>(OsO<sub>2</sub>).

References

1. Christie, J.A.; Collins, T.J.; Santarsiero, B.D.; Spies, G.H. unpublished results.
2. Rogers, G.A.; Bruce, T.C. *J. Am. Chem. Soc.* 1974, 96, 2463-72.
3. The reaction with ligand 33 does not result in precipitation. The product is crystallized in the work-up. (See experimental.)
4. (a) Schröder, M. *Chem. Rev.* 1980, 80, 187-213. (b) Griffith, W.P.; Rossetti, R. *J. Chem. Soc., Dalton Trans.* 1972, 1449-53. (c) Griffith, W.P. *J. Chem. Soc. (A)* 1969, 211-18.
5. Though the spectroscopic properties require a trans arrangement of oxo groups, we cannot conclude whether the nitrogen atoms of the bidentate ligands are cis to each other or trans to each other.
6. Barner, C.J.; Collins, T.J. unpublished results.
7. Barner, C.J.; Collins, T.J.; Coots, R.J. unpublished results.
8. Malin, J.M. *Inorg. Syn.* 1980, 20, 61-3.
9. Meyer, J.; Bernhauer, K. *Monatshefte für Chemie* 1929, 53/54, 740.